L-BAND ORTHOGONAL-MODE CROSSED-SLOT ANTENNA AND VHF CROSSED-LOOP ANTENNA

Tryggvi Olsson
Brian P. Stapleton
The Boeing Company
P.O. Box 3707
Seattle, Washington   98124

AUGUST 1972

FINAL REPORT

Prepared for:

NATIONAL AERONAUTICS AND SPACE ADMINISTRATION
Communications Programs
Washington D.C.   20546

1. Report No. DOT-TSC-NASA-72-2	2. Government Accession No.	3. Recipient's Catalog No.
4. Title and Subtitle L-BAND ORTHOGONAL-MODE CROSSED-SLOT ANTENNA AND VHF CROSSED-LOOP ANTENNA		5. Report Date August 1972
		6. Performing Organization Code
7. Author(s) Tryggvi Olsson and Brian P. Stapleton		8. Performing Organization Report No. D6-60163
9. Performing Organization Name and Address The Boeing Company P.O. Box 3707 Seattle, Washingon 98124		10. Work Unit No. NA-05/OS-219 R-1021 and R-2525
		11. Contract or Grant No. DOT-TSC-130
		13. Type of Report and Period Covered
12. Sponsoring Agency Name and Address National Aeronautics and Space Admin. Communications Programs Washington, D.C. 20546		Contractor Final Report
		14. Sponsoring Agency Code
15. Supplementary Notes Key words Cont. Antenna, Aeronautical		

16. Abstract

A low-gain, circularly polarized, L-band antenna; a low-gain, lineraly polarized, L-band antenna; and a low-gain, circularly polarized, upper hemisphere, VHF satellite communications antenna intended for airborne applications are described in this report. The text includes impedance and antenna radiation pattern data, along with physical description of the construction of the antennas.

17. Key Words Balanced feed, Orthogonal mode, Circular polarization, Characteristic impedance, Aircraft Antennas Hemispherical Antennas	18. Distribution Statement DOCUMENT IS AVAILABLE TO THE PUBLIC THROUGH THE NATIONAL TECHNICAL INFORMATION SERVICE, SPRINGFIELD, VIRGINIA 22151.		
19. Security Classif. (of this report) Unclassified	20. Security Classif. (of this page) Unclassified	21. No. of Pages	22. Price

$\mathcal{I}$

SUMMARY

This report summarizes the work performed under contract number DOT-TSC-130. Two antennas were developed under this contract—an L-band orthogonal-mode crossed-slot antenna and a VHF crossed-loop antenna. The L-band antenna can be flush mounted on the top centerline of a commercial jet transport and provide adequate coverage over the upper hemisphere to communicate with a satellite. The L-band antenna developed has a peak gain of 4.5 dB with respect to a circular isotrope. The design goal was for an antenna gain greater or equal to - 2 dB below a circular isotrope at $10°$ above the horizon. The antenna chosen to fulfill this requirement is a crossed-slot iris backed by a cavity. The radiation beamwidth of such an iris has wide beamwidths in the two axes of interest. The radiation patterns given in this report indicate that, for a very high percentage of the intended coverage sector, the gain requirement is satisfied.

In addition, a low-gain antenna was developed under this contract to provide VHF satellite coverage over the upper hemisphere. The results obtained at L-band frequencies could then be compared with the VHF results to evaluate the merits of one frequency band over the other. The VHF antenna was intended to cover the upper hemisphere when installed at a suitable top centerline location on a commercial jet transport. The design goal was for an antenna gain of greater than or equal to -1 dB below a circular isotrope from $10°$ above the horizon to the zenith. To achieve such a requirement in a practical aircraft design, a crossed-loop radiator configuration was chosen. The antenna is furnished with an aerodynamically shaped fiberglass radome to which the crossed-loop antenna is fastened. A basic loop element provides a wide beamwidth in one plane, thus, arraying two loops perpendicular to one another provides wide beamwidths in two axes. The antenna is mounted external to the aircraft and has been qualification tested to handle 500 watts in the CW mode at a pressure altitude of 45,000 ft. A cavity-type antenna is impractical for a VHF antenna solution because of the physical size of the cavity required. Computer reduction of the antenna radiation patterns indicates an antenna directivity of greater than -1 dB for 80% of the specified coverage area.

ORTHOGONAL-MODE CROSSED-SLOT ANTENNA–CIRCULARLY POLARIZED

Introduction

The L-band orthogonal-mode crossed-slot antenna is intended for satellite communication in the 1540- to 1660-MHz frequency range and provides radiation pattern coverage of the upper hemisphere when installed on the top centerline of an airplane. The basic antenna consists of two orthogonal half-wavelength slots fed in balance and phase quadrature, thus providing a low-gain circularly polarized radiator.

The antenna, shown in figures 1 and 2, is flush mounted and weighs 2.9 lb. It has two output ports marked "R" and "L" for right- and left-hand circular polarization, respectively. The polarization can be selected remotely with an external coaxial switch. Two production antennas were furnished under this contract: one receiving antenna and one transmitting antenna with a power-handling capability of 500 watts in the CW mode at 45,000-ft altitude.

Requirements

The basic requirements are that a single flush-mounted antenna installed on the airplane top centerline shall provide upper hemispherical radiation pattern coverage with relatively small gain variations in this half space. The antenna shall provide right- or left-hand circular polarization selectable with a high degree of circularity over the widest possible space angle around zenith. Furthermore, there shall be a sharp cutoff at the horizon with a minimum of gain in the lower hemisphere to enhance multipath signal rejection. To meet these requirements a cavity-backed iris consisting of two orthogonal half-wavelength slots is selected as the basic antenna configuration (see fig. 3).

Theory of the Antenna

In the following description the crossed-slot iris is assumed to be located in a horizontal ground plane. The coordinate system for all pattern descriptions is shown in figure 4.

The principle of operation is illustrated in figure 5. Figures 5a and 5b show the idealized far field E-plane and H-plane patterns of the individual slots in the crossed-slot iris. Figure 5c shows the pattern of the crossed-slot iris which is obtained by superposition of the individual slot patterns. When the individual slot fields (symbolized by the electric field vectors $\bar{E}_a$ and $\bar{E}_b$ in fig. 5) are equal in magnitude and in phase quadrature, pure circular polarization (0 dB axial ratio) is obtained

in the direction $\theta = 0°$. As one moves off axis, the circularity becomes poorer due to the increased axial ratio between the E-plane and the H-plane fields, i.e., the ratio between the $\bar{E}_\theta$ and $\bar{E}_\phi$ field components, which are defined in figure 4. As the horizon is approached ($\theta = 90°$) the polarization becomes nearly linear as the vertical $\bar{E}_\theta$ component is dominant. A finite-size ground plane and a curved fuselage will alter the idealized pattern. Figures 12 and 13 show pitch and roll plane patterns obtained with the antenna installed in a 4- by 4-ft fuselage section and with circularly polarized illumination. The decrease in the radiation on the horizon is attributed to the finite size and the finite conductivity of the ground plane. Test results are treated in a later paragraph.

Mechanical Construction

The basic construction of the antenna is illustrated in figure 6. The 2024-T351 aluminum housing has a mounting flange conformed to the top fuselage of the Convair 880 airplane. The orthogonal slots are etched out on a 1/8-in.-thick, 2-oz copper-clad Teflon-loaded fiberglass plate mounted in the antenna aperture. The slots are fed in balance by capacitively-coupled copper strips bridging the slots, as shown in figure 7.

The dual coaxial feed cables of each individual slot are connected through T-connectors to the two output ports of the 90° ring hybrid circuit located at the bottom of the antenna cavity. The hybrid circuit is a tri-plate stripline design made of two 1/8-in.-thick, 2-oz copper clad Teflon-loaded fiberglass plates. The hybrid input ports, i.e., the antenna input ports, are terminated in two TNC stripline connectors (top launch type) mounted on the bottom of the antenna housing. The two input connectors are marked "R" and "L" for right- and left-hand circular polarization, respectively. The desired mode of polarization is then obtained from the properly marked output connector when the other connector is terminated in 50 ohms. The antenna cavity is filled with rigid, closed-cell foam (Emerson & Cuming, Inc., Eccofoam, type FPH), and a 1/16-in.-thick, 5-in.-diameter Teflon plate is bonded to the antenna aperture for moisture sealing.

One receiving antenna (serial number DOT-TSC-004) and one transmitting antenna (DOT-TSC-005) were furnished under this contract. The two antennas have nearly identical impedance, efficiency, and radiation pattern characteristics. However, the transmitting antenna is furnished with larger coaxial feed cables and a temperature-isolating layer of foam Teflon between the radiating aperture and the foam-filled cavity for rf power handling purposes. Thus, the transmitting antenna is designed to handle 500 watts of CW power at 45,000-ft altitude although this unit was not tested for power-handling capabilities..

Feed Network–Impedance Matching

Figure 8 shows schematically the antenna feed network and the external control circuit (coaxial transfer switch) which enables the remote selection of right- or left-hand circular polarization.

The individual slots are fed in balance as shown in figures 7 and 8. The balanced feed enables the individual slot impedances to track each other when both slots are fed. This impedance tracking is necessary to feed the slots in phase quadrature and with equal power division by means of a simple quadrature hybrid. If the slots are fed unbalanced, e.g., only one feed strip bridging each slot, there will be a considerable mutual coupling between the slots making impedance tracking of the individual slots impossible and requiring a very complex feed network.

The equivalent electrical network presented to each of the dual feed cables at the capacitively coupled feed strips (fig. 7) is shown in figure 9. The antenna inductance and radiation resistance (including loss resistance) are represented by L_A and R_A, respectively. These values are a function of the feed strip position, and both values approach zero if the feed strip is moved toward the end of the slot. C_F is the fringing capacitance between the strip and the slot edges. C_S is the stripline capacitance. The position, length, and width of the strip are dimensioned to present approximately 25 ohms to the feed cable at the band center frequency: 1600 MHz. The paired feed cables then transform this impedance and match it to 50 ohms within a 2:1 VSWR limit at the hybrid output ports (O′ and O″ in fig. 8). The measured values of mutual coupling between the slots and the antenna impedance at O′ and O″ are given in the "Electrical Data" section which follows.

When the impedances at O′ and O″ track each other the quadrature hybrid will provide equal power and a relative phase shift of 90 between the slots. Under these conditions the antenna will transmit (or receive) a purely circularly polarized field on the axis of the antenna aperture. When port R is connected to the transmitter and L is terminated in 50 ohms the field is right-hand circularly polarized. In the opposite configuration left-hand circular polarization will be transmitted.

The values of power division and relative phase shift between ports O′ and O″ of the hybrid are given in the next section. The maximum amplitude difference between O′ and O″ over the 1540- to 1660-MHz frequency range of the antenna is 0.25 dB. This amplitude unbalance will yield an axial ratio of 0.25 dB in the transmitted field when driven into the nearly identical antenna impedances. The maximum phase deviation from the ideal 90° at ports O′ and O″ is 0.5°. This phase error in itself will yield an axial ratio of 0.3 dB. However, even when the effects of these maximum errors are summed as a worst case the axial ratio of the on-axis radiated field is well within the specified 2-dB limit.

4

Electrical Data

The electrical performance data presented in this section are obtained from measurements on the production transmitting antenna, serial number DOT-TSC-005. These data are nearly identical to those measured on the receiving antenna, serial number DOT-TSC-004, and are therefore representative for both of the delivered production antennas.

All measurements were performed with the antenna installed in a curved 4- by 4-ft ground plane simulating a top fuselage section of the Convair 880 airplane, as shown in figure 10.

Impedance—Figure 11 is a Smith chart plot of the individual slot impedances referred to the hybrid output ports, O' and O" in figure 8. The measured impedances are within the specified 2:1 VSWR limit (50 ohm reference) over the 1540- to 1660-MHz frequency range.

The impedances of the slots are tracking each other very closely, which indicates a low level of mutual coupling. This is necessary in order to feed the slots with equal power division and phase quadrature from the built-in ring hybrid.

The impedance data were measured simultaneously, with both slots fed from the hybrid through equal length slotted lines and interconnecting cables. The data are obtained for the antenna operating in the right-hand circularly polarized mode. When the antenna operates in the left-hand circularly polarized mode identical data are obtained, although each plot now is referred to the opposite port.

Isolation—The isolation between the individual slots was measured at the ports O' and O", i.e., with the hybrid disconnected a reference power level was applied to one slot at O' and the power coupled to the other slot was monitored at O". The values are given in table 1.

TABLE 1.—ISOLATION BETWEEN SLOTS

Frequency, MHz	Isolation between slots, dB
1540	19
1600	20
1660	21

Hybrid Characteristics—The insertion loss, phase shift, and isolation between the ports of the hybrid are given in tables 2, 3, and 4, respectively. During the measurements unused ports were terminated in 50 ohms.

TABLE 2.—POWER DIVISION CHARACTERISTICS

Frequency, MHz	Insertion loss between ports, dB			
	R—O'	R—O"	L—O'	L—O"
1540	3.05	3.30	3.25	3.00
1600	3.05	3.05	3.05	3.05
1660	3.05	3.05	3.10	3.10

TABLE 3.—PHASE SHIFT CHARACTERISTICS

Frequency MHz	Phase shift between ports, deg	
	O'—O"	L—R
1540	89.9	90.3
1600	90.5	89.6
1660	90.5	89.6

TABLE 4.—ISOLATION CHARACTERISTICS

Frequency, MHz	Isolation between adjacent ports, dB	
	L—R	O'—O"
1540	16.5	16.5
1600	18.0	18.0
1660	19.0	19.0

Antenna Input VSWR—The VSWR at the antenna input ports, L and R, was measured on each port with the other port terminated in 50 ohms. The test results given in table 5 show that the VSWR is within the specified 2:1 limit over the 1540- to 1660-MHz frequency range.

TABLE 5.—ANTENNA INPUT VSWR

Frequency, MHz	Antenna input VSWR	
	Port R	Port L
1540	1.52	1.44
1600	1.05	1.23
1660	1.08	1.04

Radiation Patterns

Radiation pattern measurements were performed on the production antenna to determine pattern characteristics, directivity, and gain. With the antenna installed in the ground plane shown in figure 10, and assuming the antenna oriented as if it were installed on the airplane top fuselage centerline, the radiation patterns were measured in the following "cuts":

● Pitch (vertical plane through the longitudinal axis of the airplane)

● Roll (vertical plane normal to the longitudinal axis of the airplane)

In addition to the pattern measurements, the maximum directivity of the antenna in the zenith direction ($\theta = 0°$) was measured to be 5.1 dB. By comparative measurements between the antenna and a reference standard gain horn antenna, the maximum antenna gain was determined to be 4.5 dB. From the directivity and the gain values the antenna efficiency is determined to be 87%, which is above the required 80% minimum limit.

Figures 12 through 15 show polar diagram radiation patterns for both the right- and left-hand circularly polarized modes. As no significant pattern variations occur over the frequency band, only the patterns measured at 1540 MHz are submitted. The patterns are plotted in voltage with the maximum radiation level referred to the edge of the polar diagram (the "100" level).

To ease the pattern evaluation, the isotropic radiation level is shown as a circle on the polar diagram. The gain variations in the intended 160° usage sector around zenith ($0° \leqslant \theta \leqslant 80°$) can be determined from the polar diagram patterns. Thus, the patterns show that the gain is varying between 2.4 and 4.5 dB above isotropic level in a 90° cone around zenith ($0° \leqslant \theta \leqslant 45°$). A gain coverage equal to or higher than isotropic level (0 dB) will be obtained in a 140° cone around zenith ($0° \leqslant \theta \leqslant 70°$). At $\theta = 80°$, which is the limit of the usage sector, the average gain is 2 dB below isotropic level. It should be noted that these measured gain values are nearly identical to the original design goals. On and below the horizon ($\theta \geqslant 90°$) the radiation level decreases rapidly, which is highly desirable to reduce multipath signals from the sea. This decrease in signal level at angles near the horizon is more pronounced in the pitch plane due to the larger ground plane (fuselage) in this dimension, whereas in the roll plane "spillover" effects on the curved fuselage cause a relatively higher radiation level on and below the horizon.

Scale Model Pattern Study

The full-scale radiation pattern measurements discussed in the previous section were performed on a small fuselage section and served primarily as a qualification testing of the antenna. These patterns can only give a coarse performance evaluation of the antenna installation on an airplane.

To obtain detailed pattern characteristics, including the effects of the airframe, the most practical method is scale-model pattern measurements. Such patterns were obtained for two installation locations on the Convair 880 airplane:

- STA 820, top centerline

- STA 820, 35° to the right of top centerline

7

Due to the similarity between the Convair 880 and the Boeing 707 airframes, a 1/20th-scale model 707 airplane was used for the measurements. A 1/20th-scale model antenna was fabricated and installed at the equivalent locations on the 707 model airplane. All patterns are marked Convair 880, although the measurements were performed on a 707 airplane. As the production antenna operates at 1540 to 1660 MHz, the frequency used for the scale-model pattern measurements was 32 GHz.

Before its installation in the model airplane, the model antenna was installed on a 2.4- by 2.4-in. curved ground plane (a 1/20th-scale version of the ground plane shown in fig. 10) and radiation patterns in the pitch and the roll cuts for right-hand circular polarization were measured at the scale frequency (32 GHz). This was done to verify that the model antenna possesses the pattern characteristics of the production antenna. Figures 16 and 17 show these patterns, and it can be seen that they compare favorably to the full-scale patterns in figures 12 and 13. The lack of radiation below the horizon in the model patterns is caused by absorbent material behind and around the ground plane, which was applied to prevent reflections from the relatively large waveguide feed network. The results obtained with the antenna installed on the scale model airplane are discussed in the following paragraphs.

Polar Diagram Patterns—With the model antenna operating in the right-hand circularly polarized mode, patterns were obtained for both right- and left-hand circularly polarized illumination, i.e., main polarization and cross polarization, respectively.

Figures 18 through 23 show the patterns measured on the antenna installed at the top centerline location. The patterns in figures 24 through 29 are those of the side-mounted antenna. The patterns are plotted in voltage, with the maximum radiation level referred to the edge of the polar diagram (the "100" level). The patterns were measured in the principal planes:

- Pitch (vertical plane through the longitudinal axis)

- Roll (vertical plane normal to the longitudinal axis)

- Yaw (horizontal plane through the longitudinal axis)

The constant angle, the variable angle, and polarization of the rf field are indicated on each polar diagram.

Integration—The total energy radiated over the sphere (right- as well as left-hand polarized energy) was integrated to establish the directivity of the antenna when installed at the above-mentioned two locations on the scale-model airplane. The maximum directivity of the antenna is:

8

- 5.6 dB installed at STA 820 on top centerline

- 7.0 dB installed at STA 820 35° to the right of top centerline

The higher maximum directivity of the antenna mounted off the centerline is caused by wing structure interference, i.e., the patterns have larger and narrower lobes than those of the antenna mounted on the top centerline. The isotropic level is shown as a circle on the polar diagram patterns.

Radiation Distribution Plot—Radiation distribution plots were obtained with the model antenna installed and operating as described in the previous paragraph. These data for right- and left-hand circularly polarized illumination show the radiation levels over the full sphere in 2° increments, thus giving a detailed resolution of the radiation distribution. Figures 30 and 31 are the plots for the top-mounted antenna, and figures 32 and 33 are those for the side-mounted antenna. The maximum directivity, which is represented by the lowest number in the radiation distribution plot, is indicated on each of the plots. The interpretation of the radiation distribution plot is discussed in detail in the "VHF Crossed-Loop Antenna" section. Using the plot to determine the directivity in a given direction the gain at these coordinates can be determined by subtracting 0.6 dB from the directivity value found, since it was established that the production antenna has an efficiency of 86%.

Conclusions

The circularly polarized orthogonal-mode crossed-slot antenna is intended to serve as an upper hemisphere coverage antenna. From the radiation patterns and the distribution plots for the top centerline location it certainly accomplishes this by providing an antenna directivity equal to or better than isotropic for a very high percentage of the intended sector coverage, i.e., $\theta = 0°$ to $\theta = 80°$. In addition, the coverage below the horizon decreases rapidly below the 100° conic. This condition is highly desirable to prevent sea-reflected signals from entering into the receiver.

The radiation patterns at 35° to the right of top centerline show the influence of reflections. The roll pattern indicates lobing due to reflections from airplane surfaces, namely the right wing. This antenna is intended to have low gain and wide beamwidth. The wide beamwidth accounts for illumination of airplane surfaces, which in turn cause reflections as evidenced by lobing in the patterns. This antenna cannot be recommended for installation other than on the top centerline. The patterns on top centerline compare very favorably with those obtained for the production antenna when installed in the 4- by 4-ft ground plane shown in figure 10. The most noticeable difference is the effect of the vertical fin in the lower conic near 80°. No significant pattern improvement aft is anticipated by moving the top centerline antenna location either fore or aft.
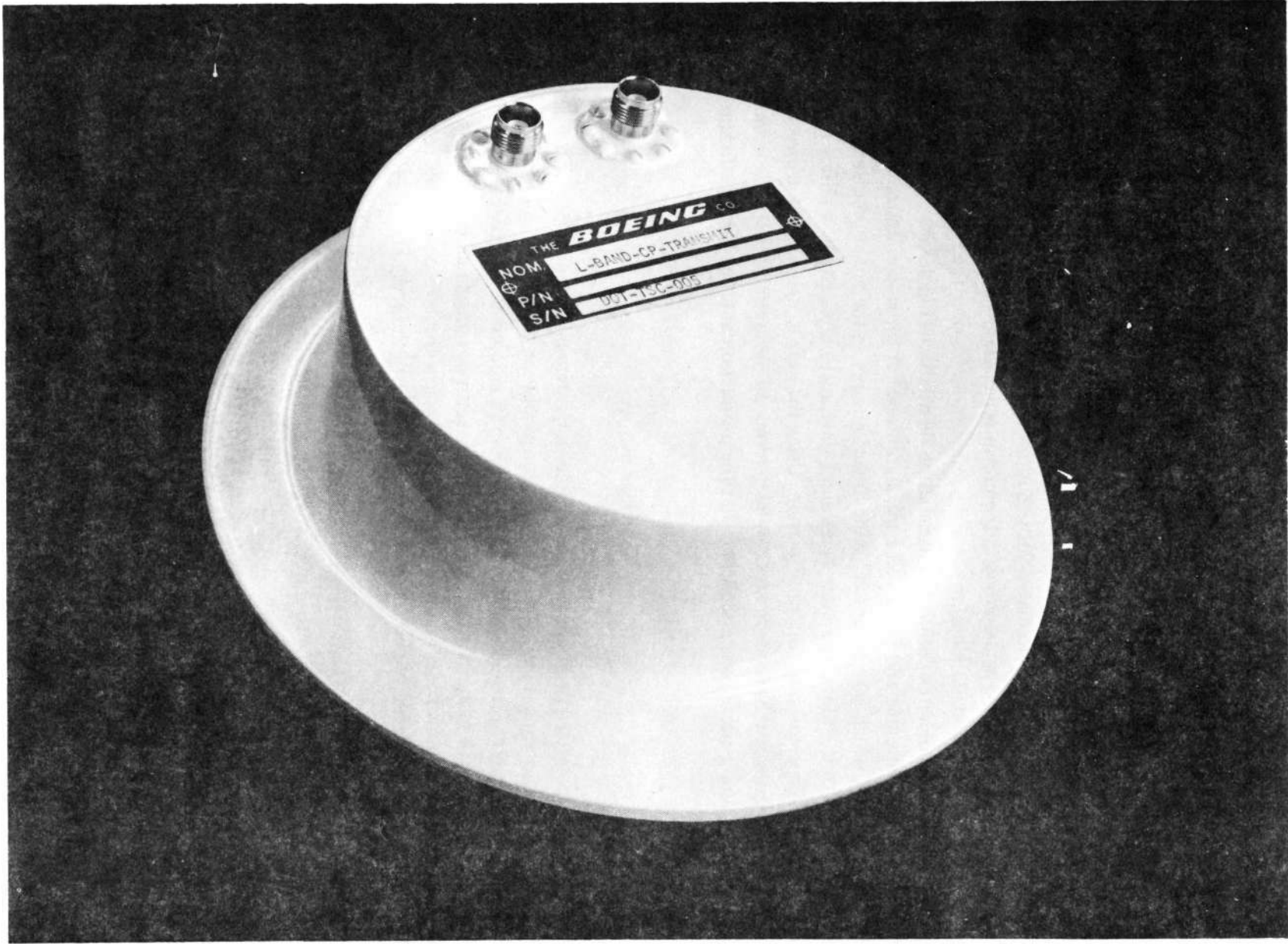
Figure 1.—Orthogonal-Mode Crossed-Slot Antenna—Bottom
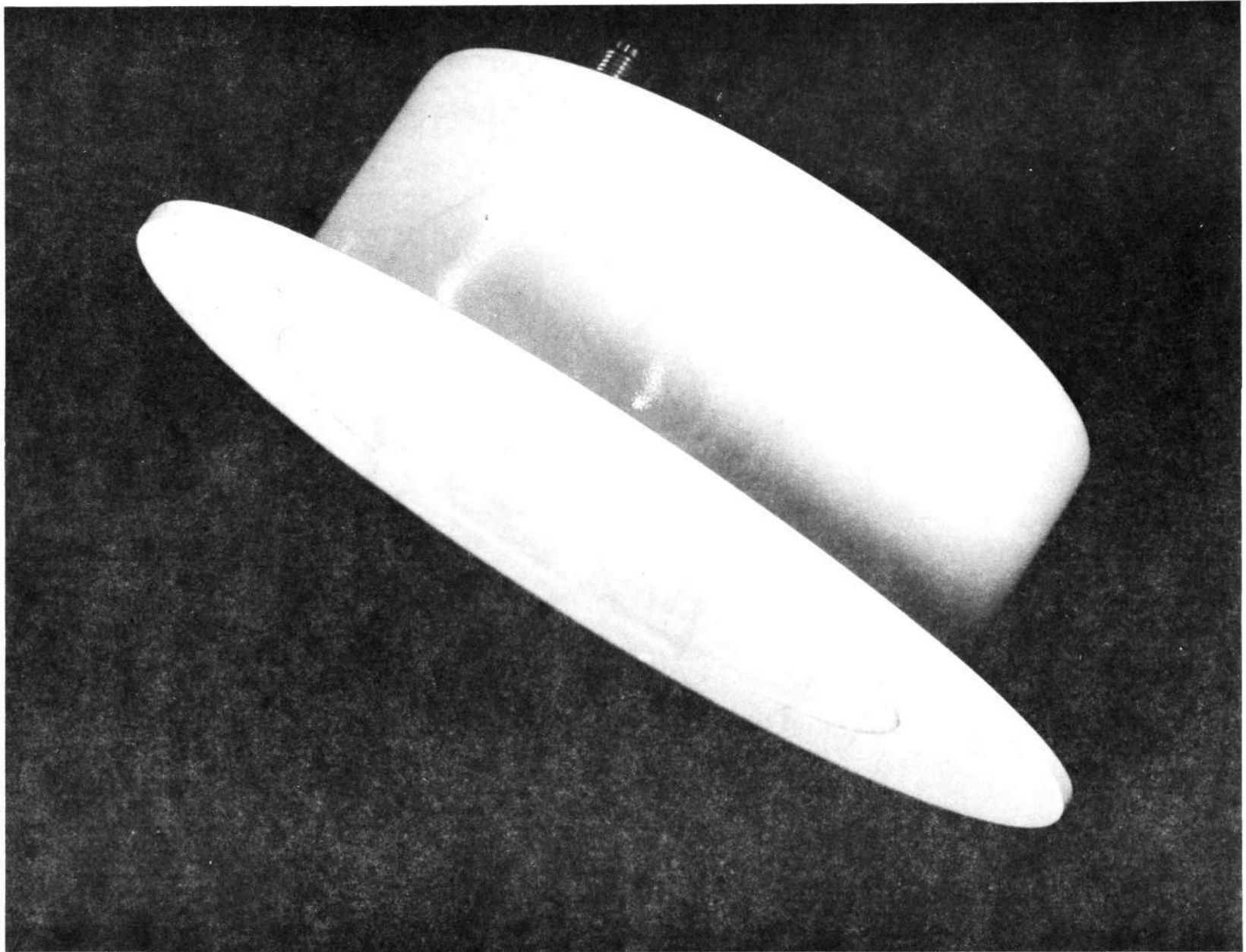
Figure 2.—Orthogonal-Mode Crossed-Slot Antenna—Top
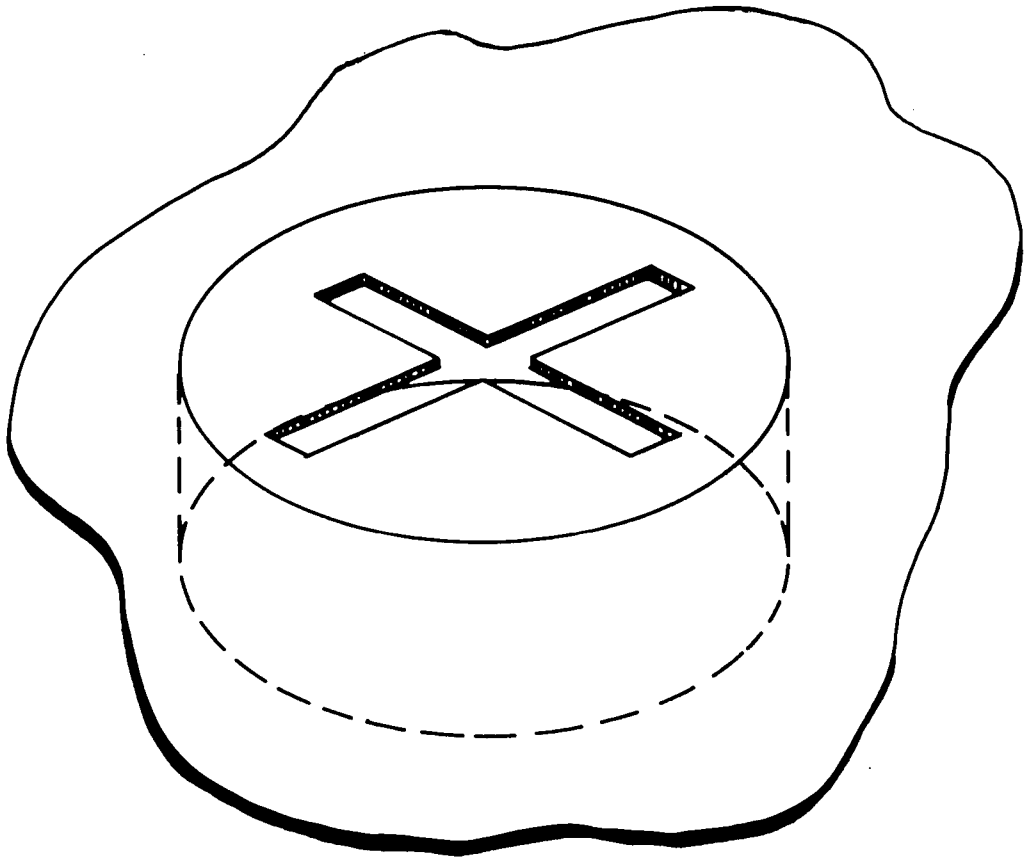
Figure 3.– Cavity-Backed Orthogonal Slots
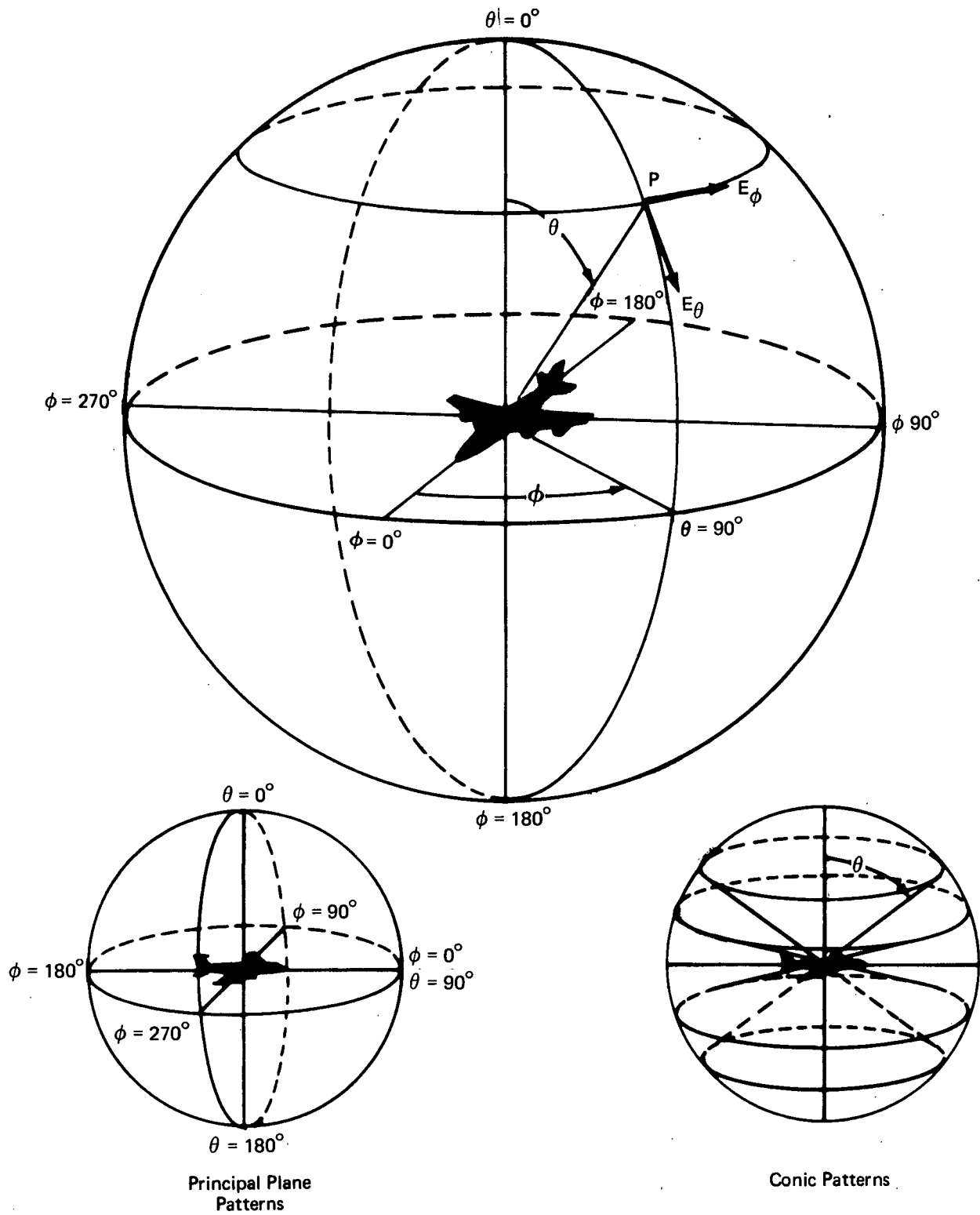
Figure 4.—Airplane Coordinate System

(a) Slot a
Idealized E-plane and H-plane far-field pattern

E-plane

H-plane

$\overline{E}_a$

(b) Slot b
Idealized E-plane and H-plane far-field pattern

$\overline{E}_b$

H-plane

E-plane

(c) Combined Slots
$|\overline{E}_a| = |\overline{E}_b|$ in the direction normal to the iris

$\overline{E}_b$

$\overline{E}_a$
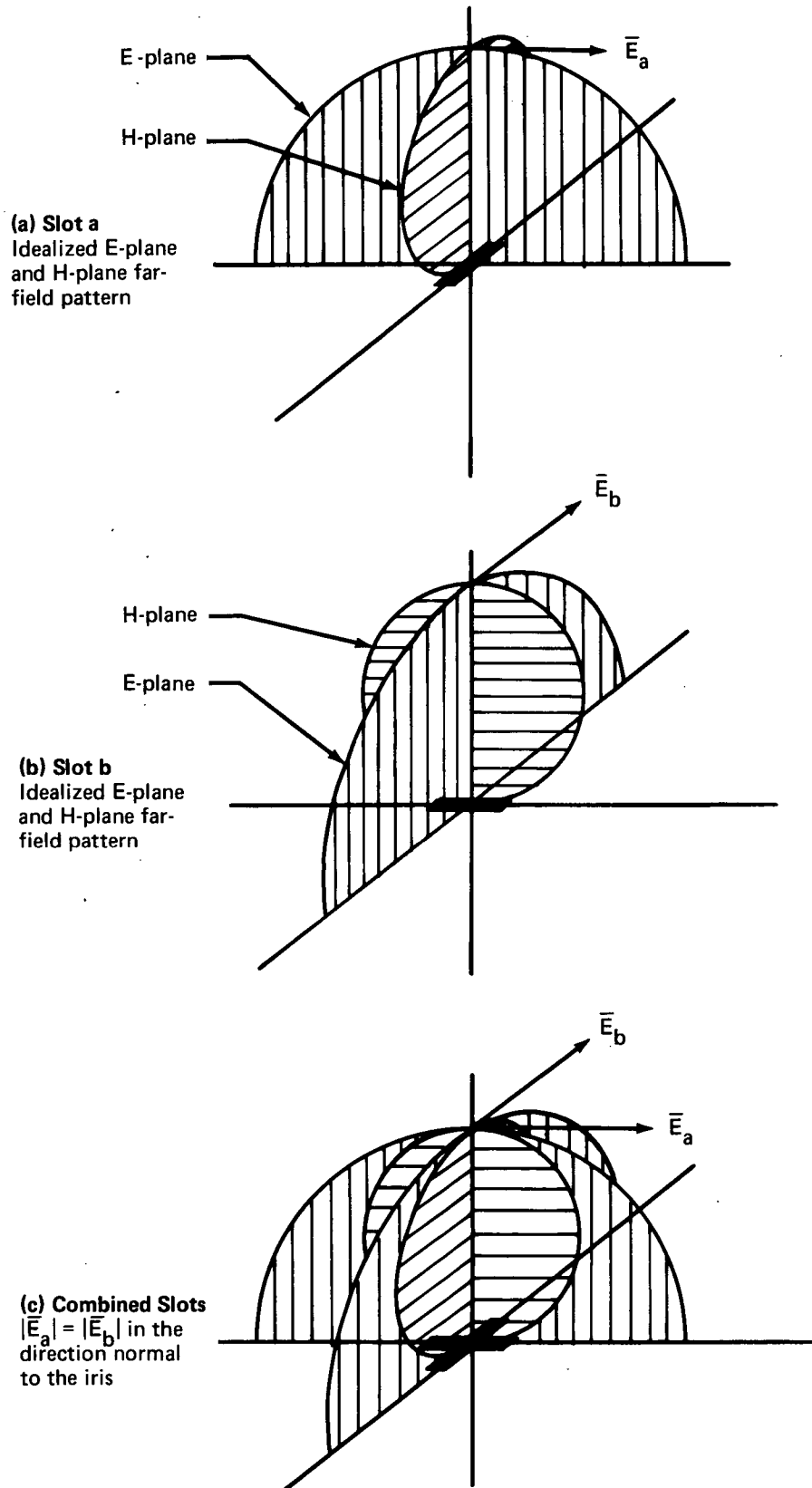
Figure 5.—Idealized E-Plane and H-Plane Far-Field Patterns From a Crossed-Slot Iris in a Horizontal Ground Plane

14

*1/8-in.-thick, 2-oz copper clad,
Teflon-loaded fiberglass
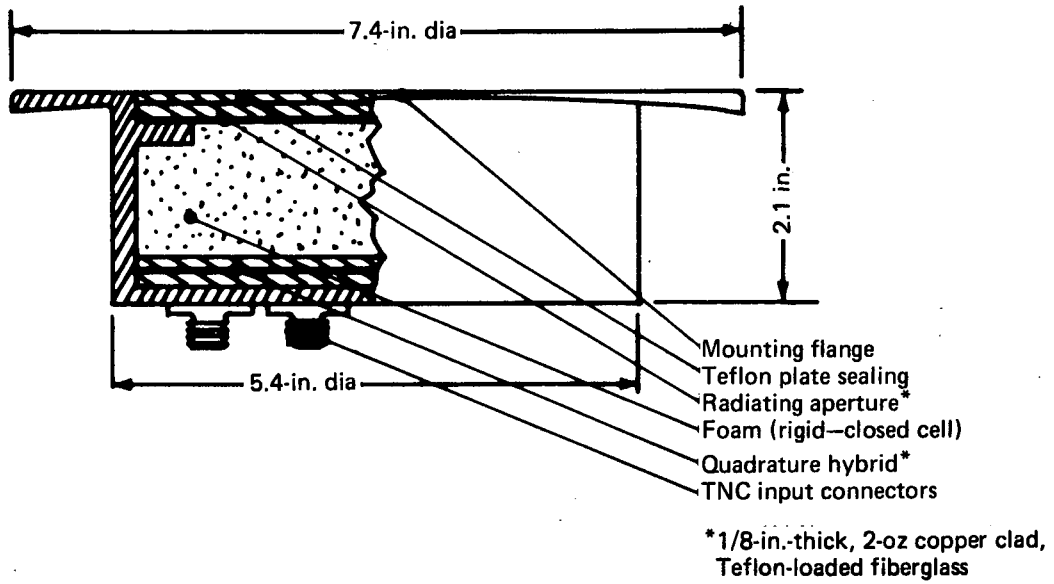
Figure 6.—Antenna Mechanical Construction
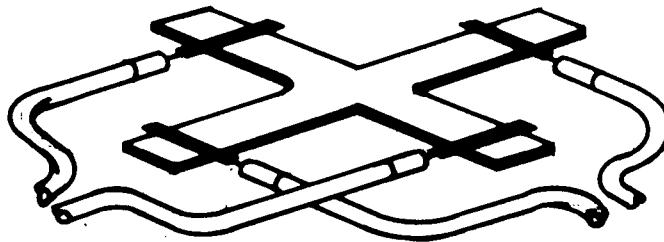
Figure 7.—Slot Feed Arrangement
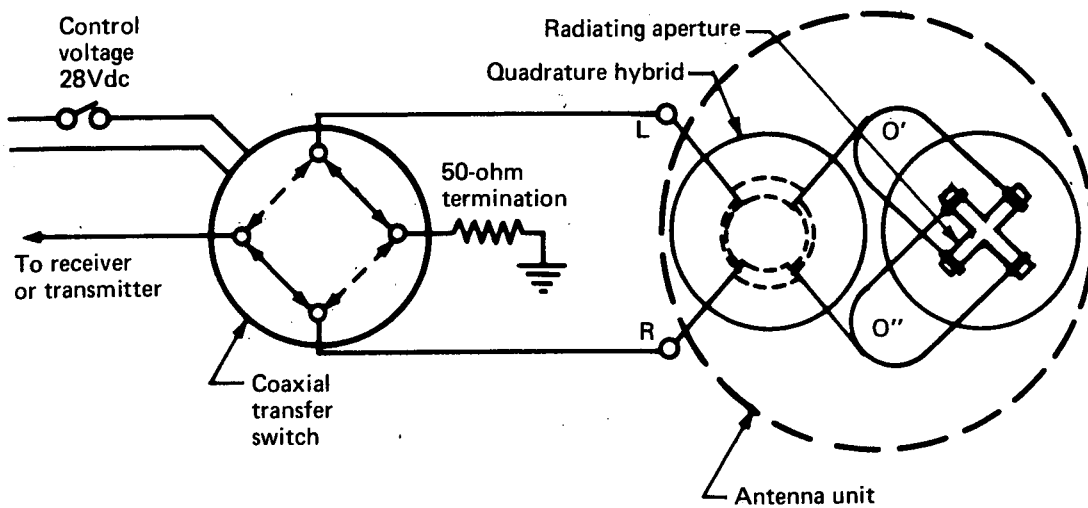
Figure 8.—Antenna Feed Network and External Control Circuit
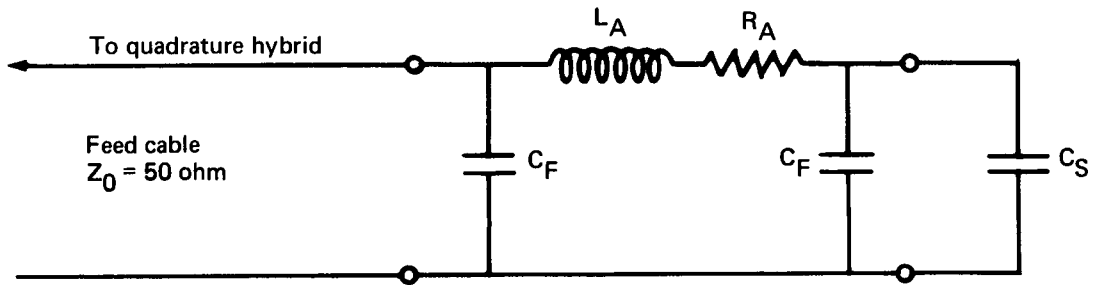
Figure 9.—Equivalent Network of Slot and Feed Strips
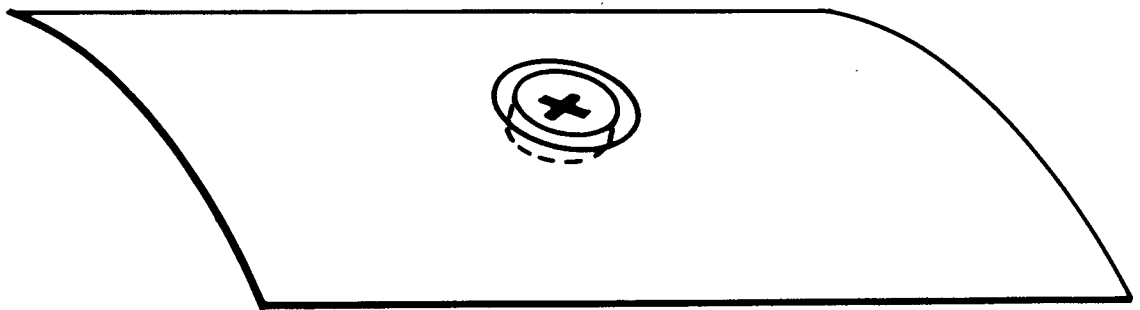
Figure 10.—Circularly Polarized Orthogonal-Mode Crossed Slot Antenna Mounted on Fuselage Section for Impedance and Pattern measurements

16
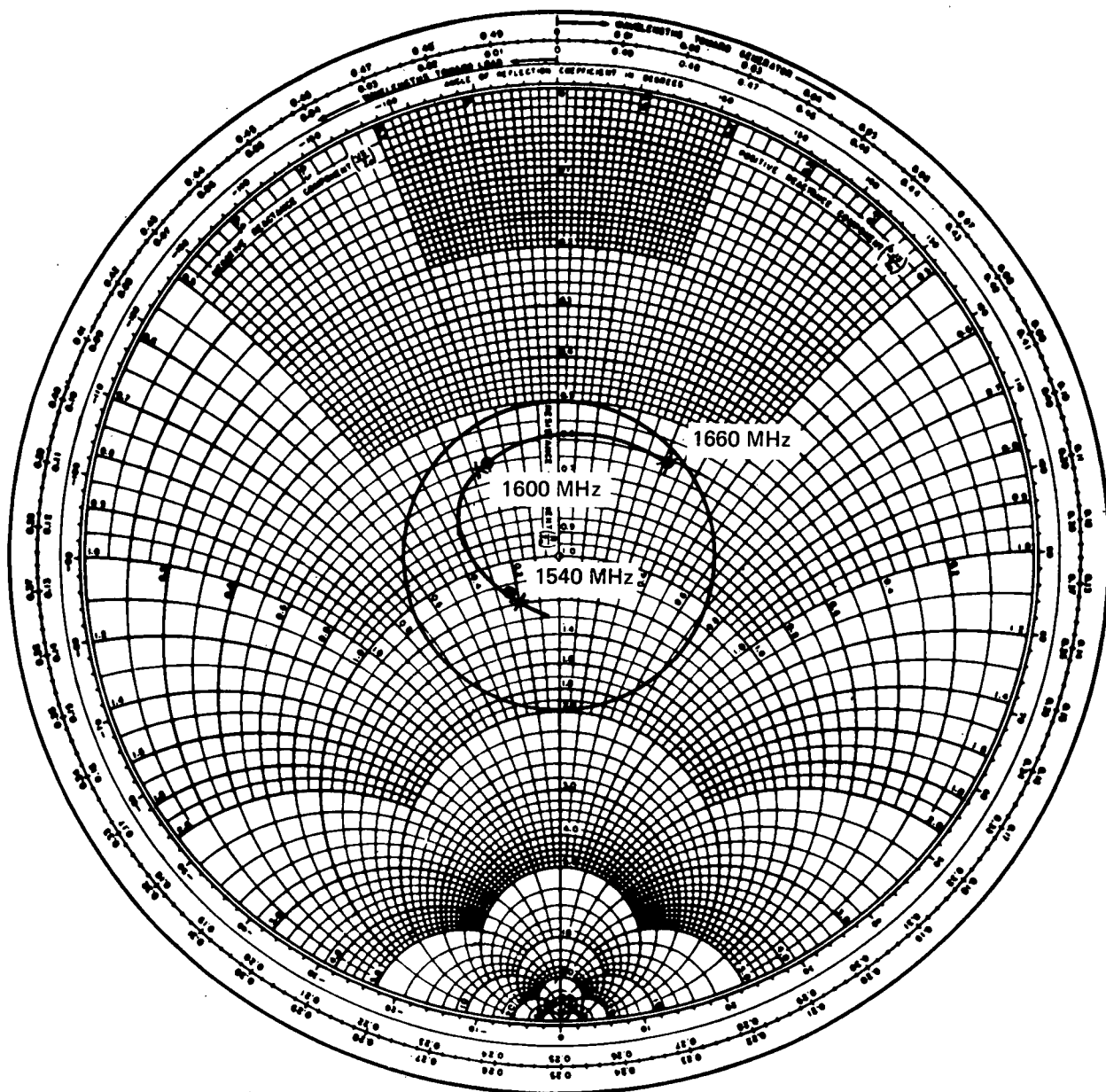
x = impedance at O'
● = impedance at O''
$Z_0 = 50$ ohms
Specification-required frequency: 1540-1660 MHz
VSWR < 2:1
Antenna S/N: DOT-TSC-005

Remarks: Antenna impedance is measured at O' and O'' with both slots fed with equal power and in phase quadrature (right or left hand circular polarization).

Figure 11.—Impedance Plot of Orthogonal-Mode Crossed-Slot Antenna, Circular Polarization
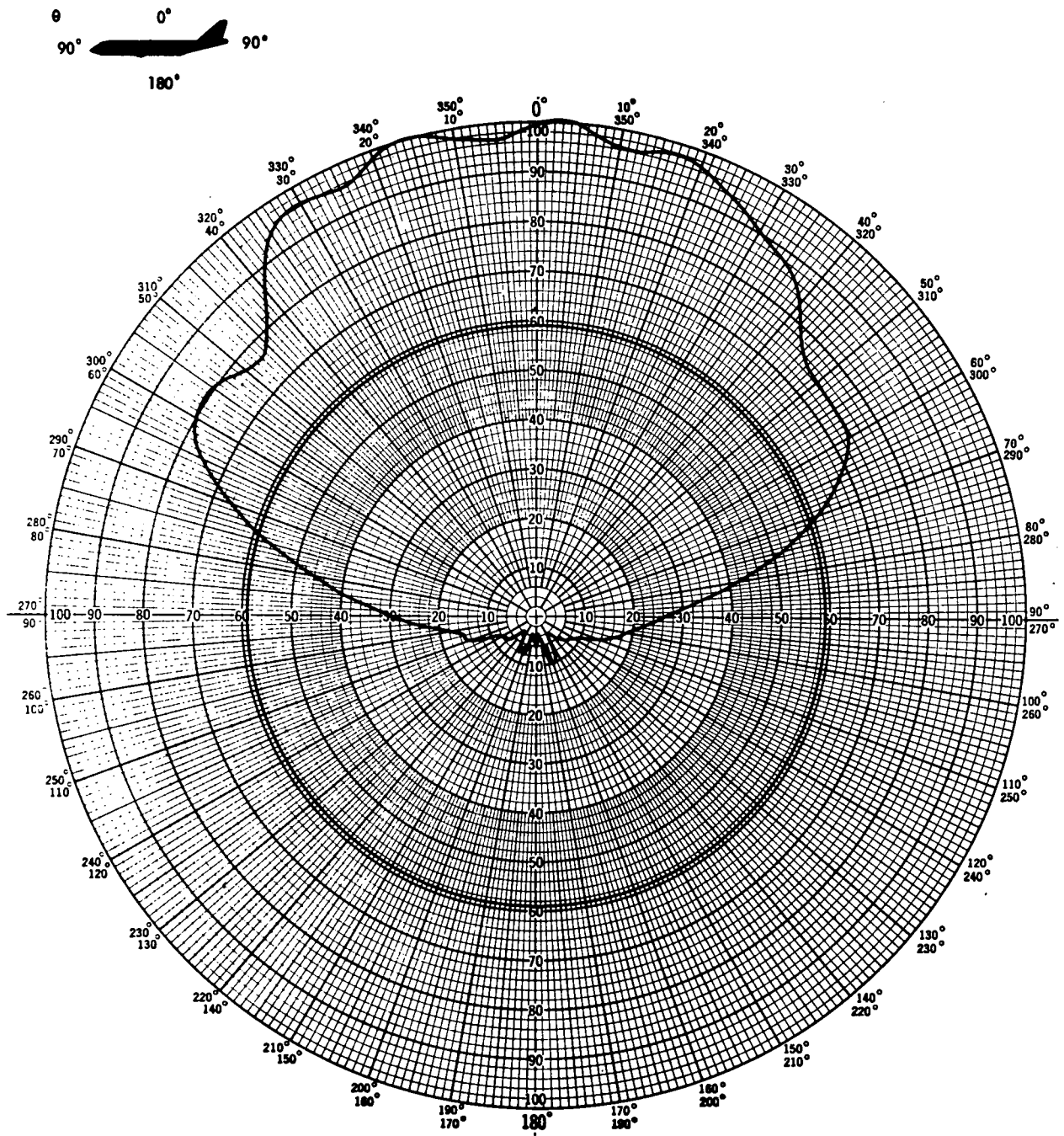
17

Maximum gain: 4.5 dB
Curve plotted in voltage
Variable angle θ
Constant angle $\phi = 0°$

Model scale: full
Frequency: 1540 MHz
Antenna location: 4-ft-square curved ground plane
Antenna S/N: DOT-TSC-005

Figure 12.—Orthogonal-Mode Crossed-Slot Antenna Pitch Plane Pattern, Right Hand Circular Polarization
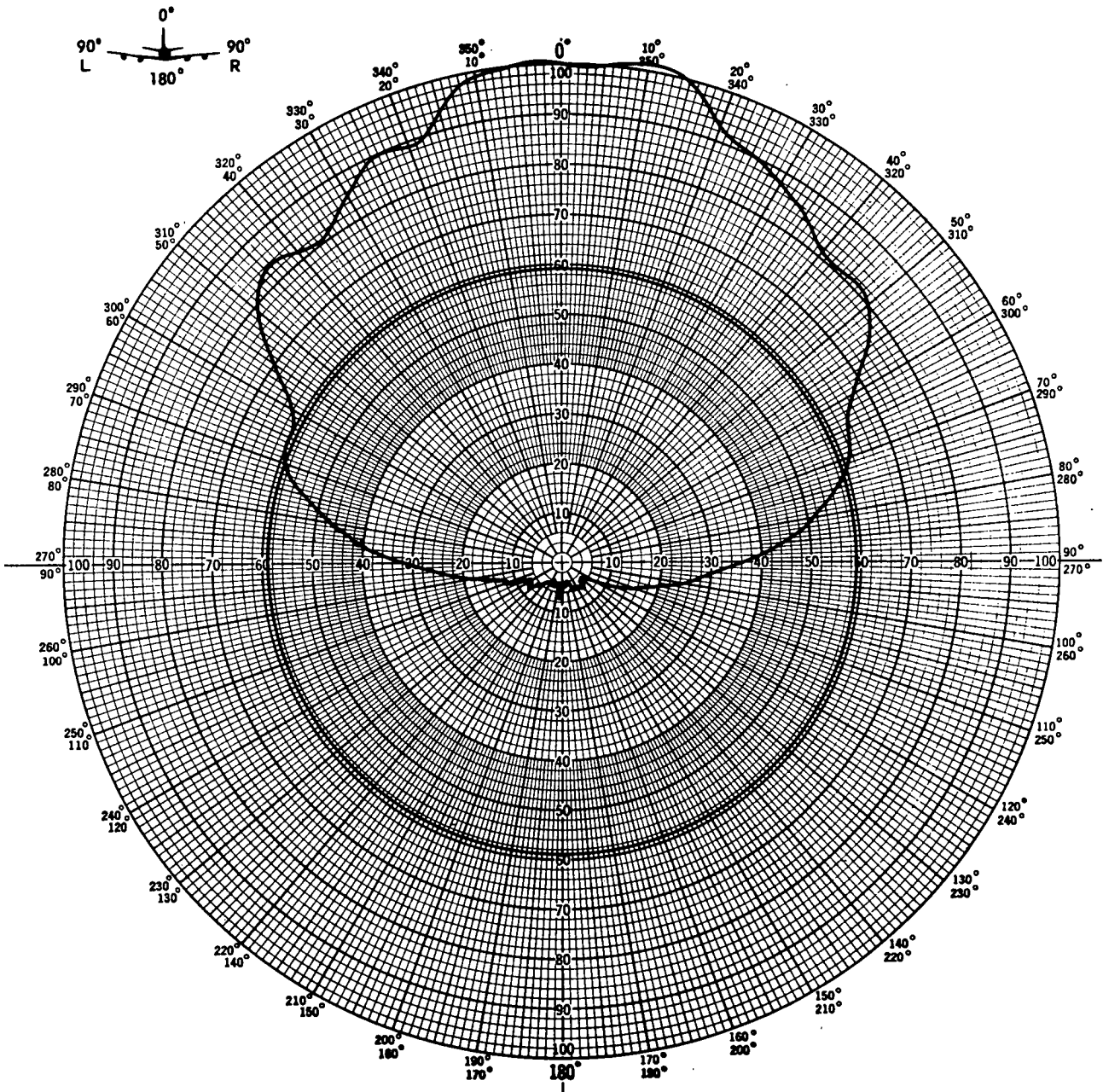
Maximum gain: 4.5 dB
Curve plotted in voltage
Variable angle θ
Constant angle $\phi = 90°$

Model scale: full
Frequency: 1540 MHz
Antenna location: 4-ft-square curved ground plane
Antenna S/N: DOT-TSC-005

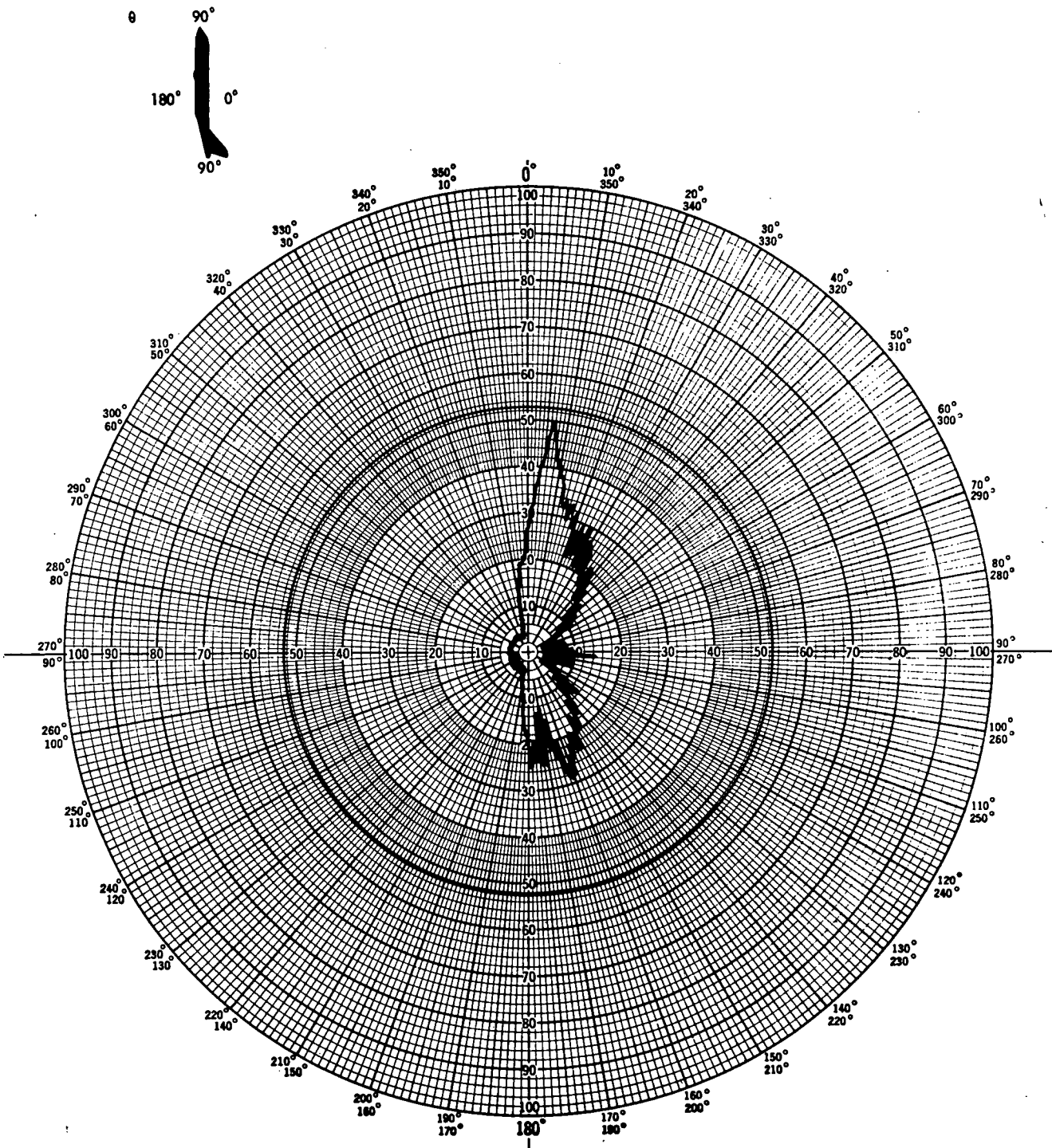*Figure 13. —Orthogonal-Mode Crossed-Slot Antenna Roll Plane Pattern,
Right Hand Circular Polarization*
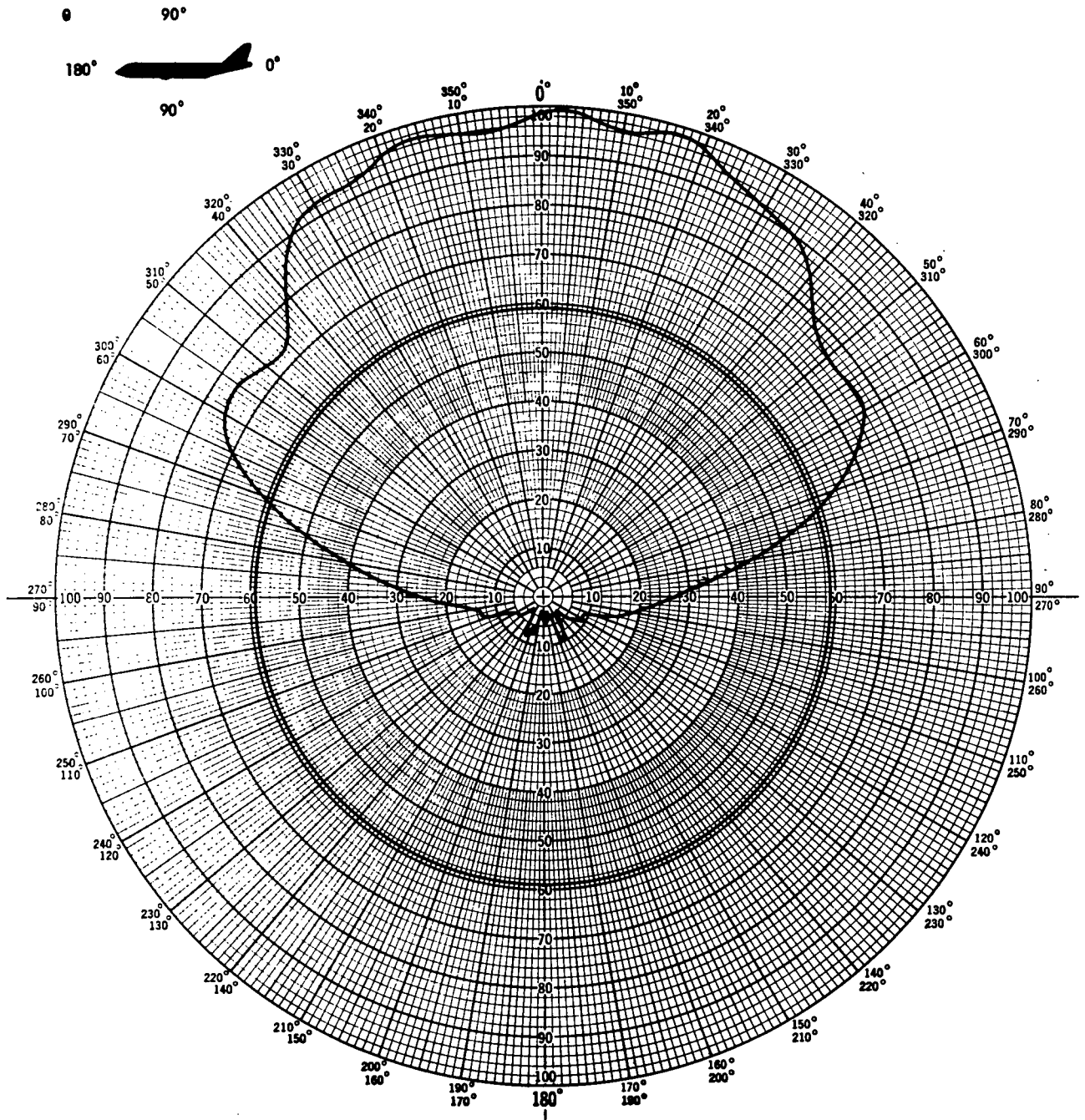
Maximum gain: 4.5 dB
Curve plotted in voltage
Variable angle θ
Constant angle $\phi = 0°$

Model scale: full
Frequency: 1540 MHz
Antenna location: 4-ft-square curved ground plane
Antenna S/N: DOT-TSC-005

Figure 14.—Orthogonal-Mode Crossed-Slot Antenna Pitch Plane Pattern,
Left Hand Circular Polarization
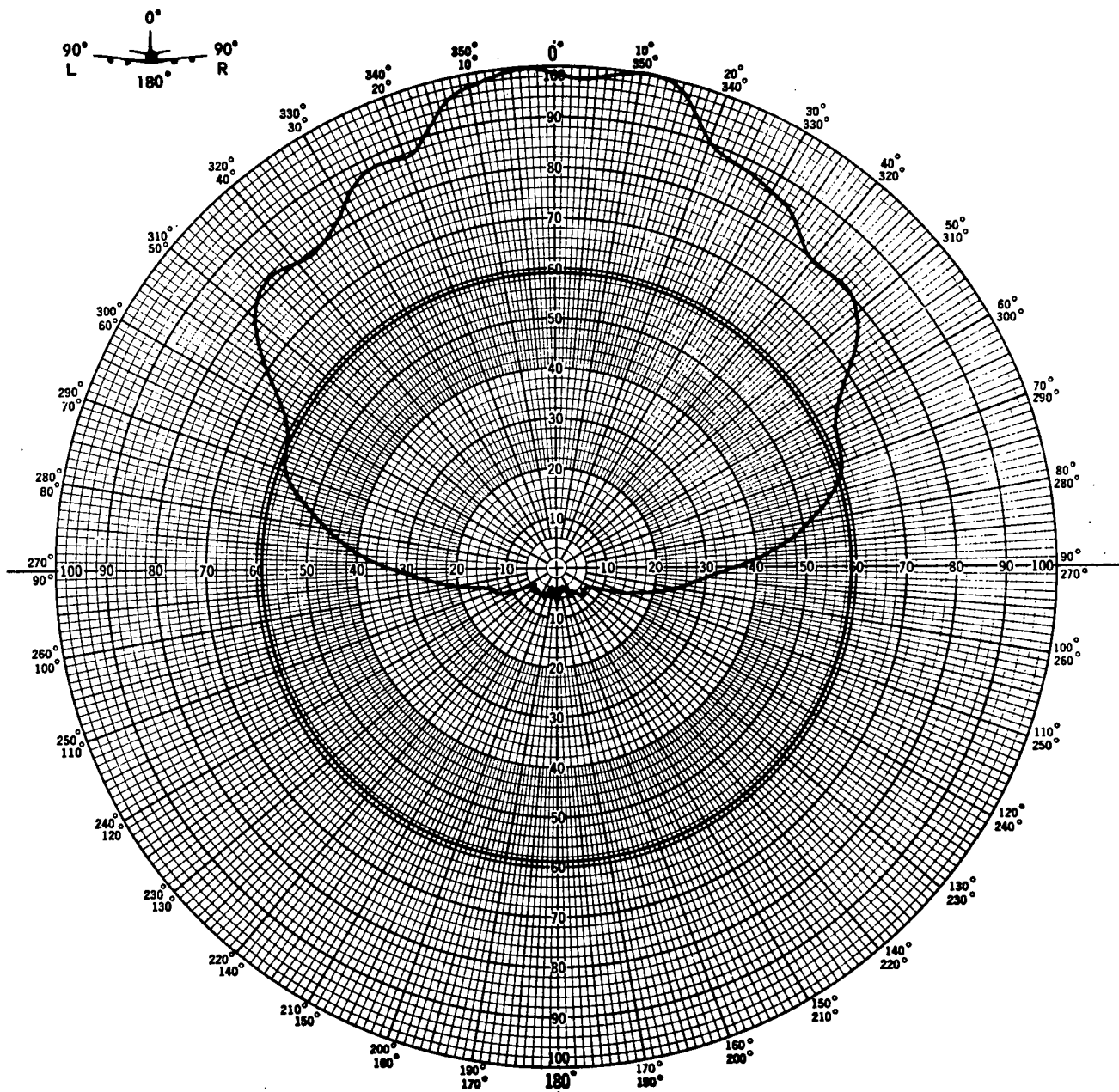
Maximum gain: 4.5 dB
Curve plotted in voltage
Variable angle θ
Constant angle $\phi = 90°$

Model scale: full
Frequency: 1540 MHz
Antenna location: 4-ft-square curved ground plane
Antenna S/N: DOT-TSC-005

Figure 15.—Orthogonal-Mode Crossed-Slot Antenna Roll Plane Pattern,
Left Hand Circular Polarization
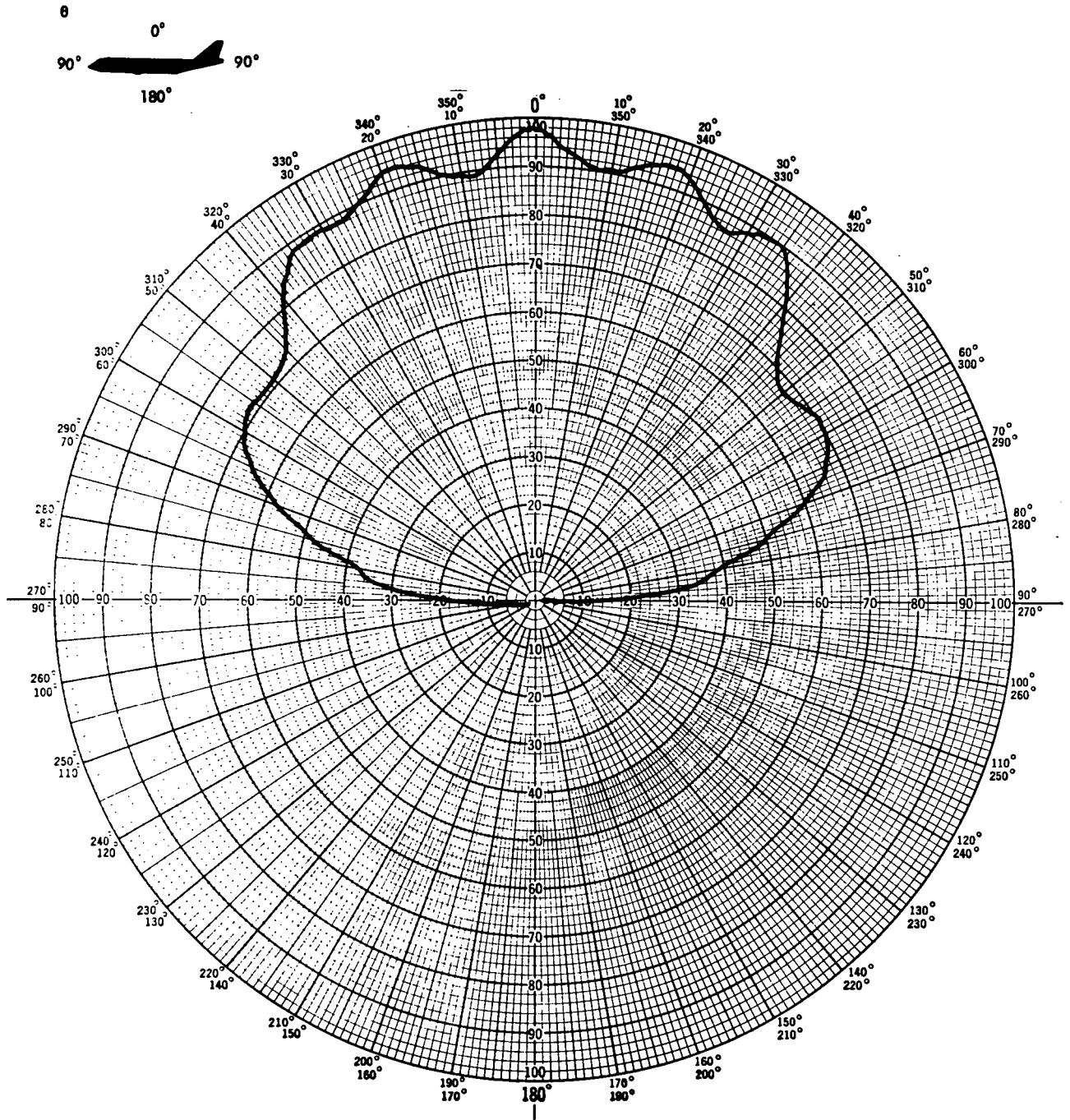
Curve plotted in voltage
Variable angle θ
Constant angle $\phi = 0°$

Model scale: 1/20
Full-scale frequency: 1540 MHz
Antenna location: 2.4-in.-square ground plane

Figure 16.—Orthogonal-Mode Crossed-Slot Antenna Pitch Plane Pattern on Model Ground Plane
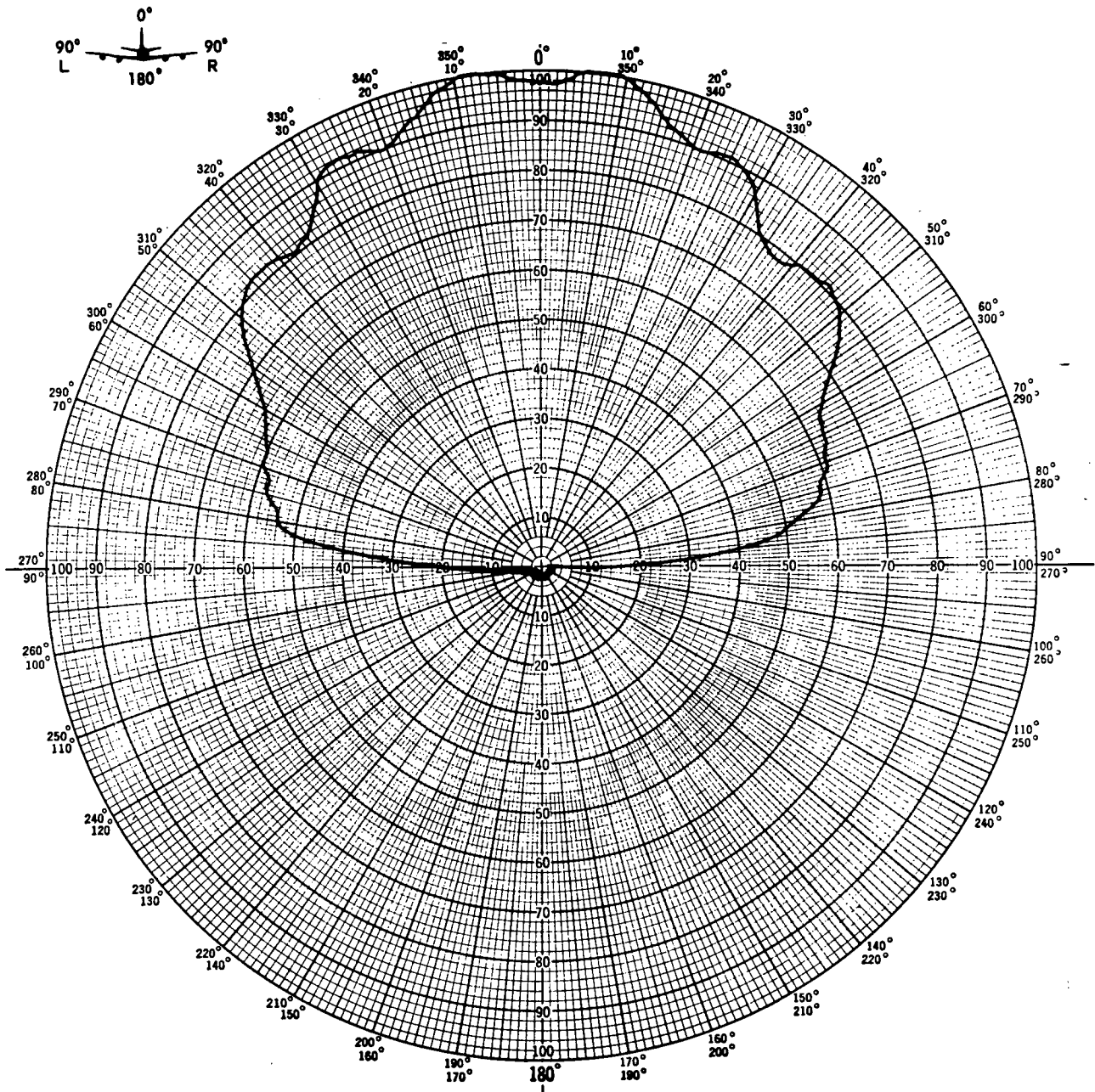
Curve plotted in voltage
Variable angle θ
Constant angle $\phi = 90°$

Model scale: 1/20
Full-scale frequency: 1540 MHz
Antenna location: 2.4-in.-square ground plane

Figure 17.—Orthogonal-Mode Crossed-Slot Antenna Roll Plane Pattern on Model Ground Plane
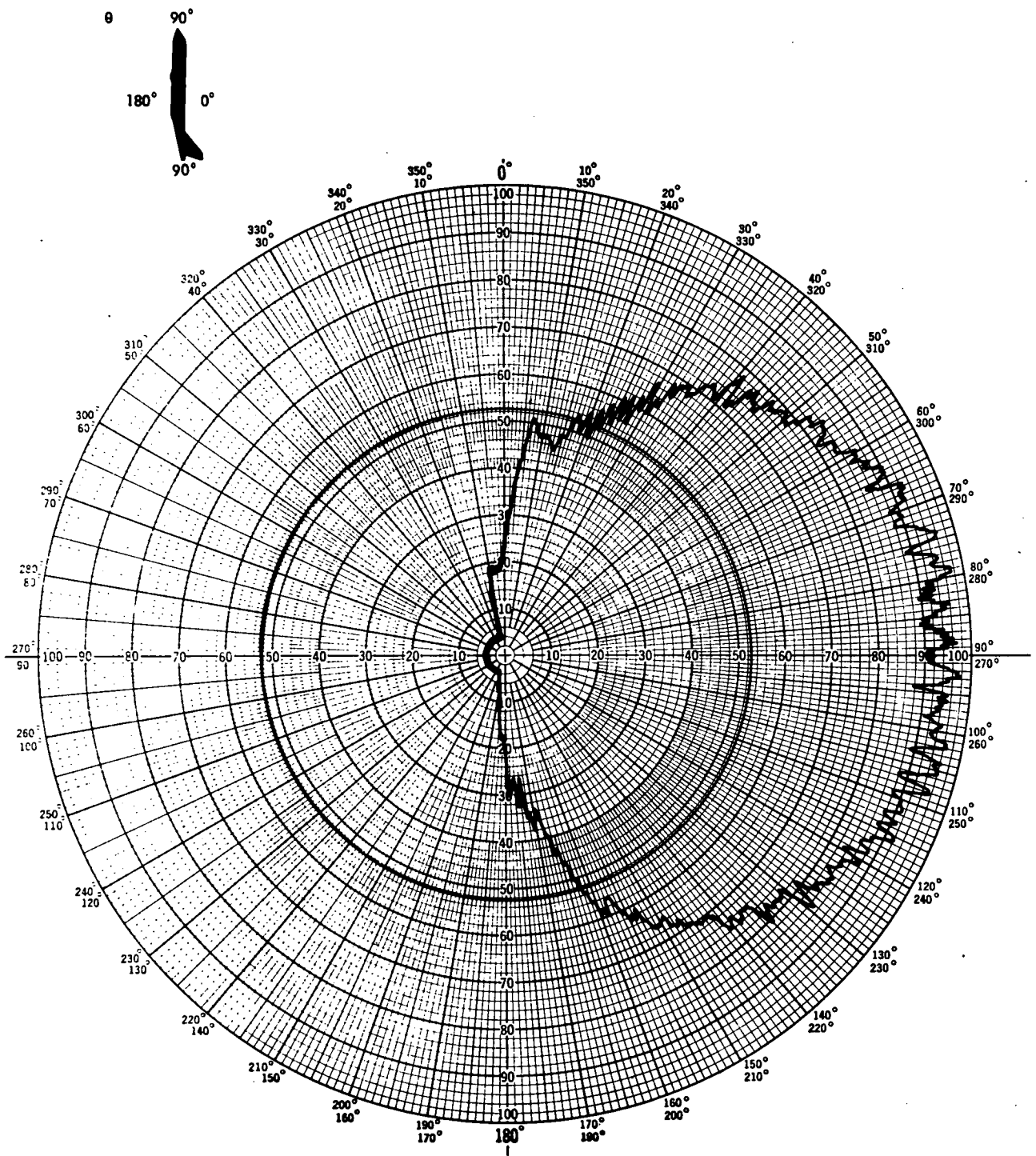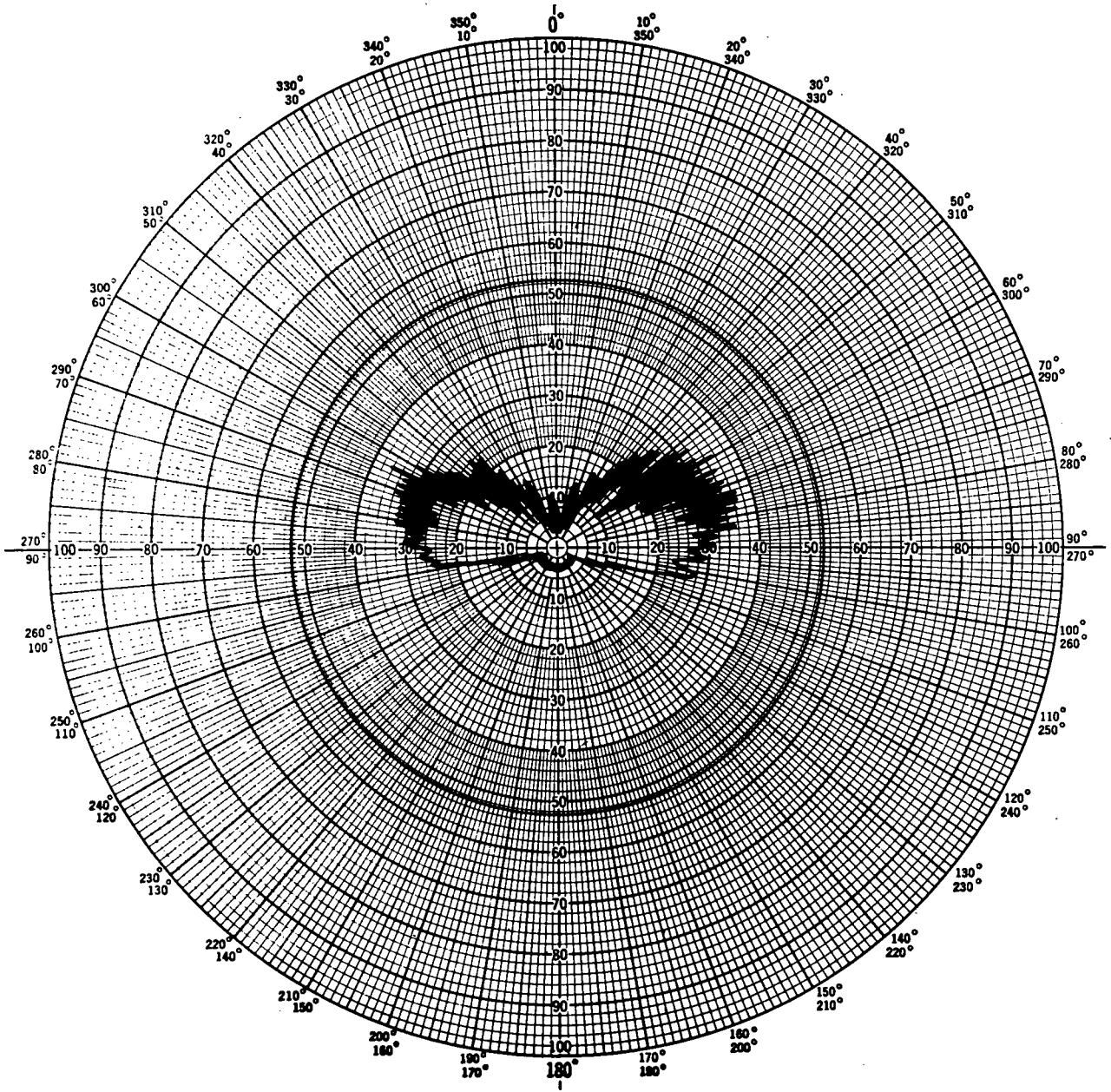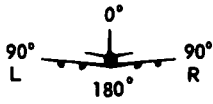
Maximum directivity: 5.6 dB
Curve plotted in voltage
Variable angle θ
Constant angle $\phi = 0°$

Model scale: 1/20
Full-scale frequency: 1600 MHz
Convair 880 airplane
Antenna location: top centerline at STA 820

Figure 18.—Orthogonal-Mode Crossed-Slot Antenna Pitch Plane Pattern,
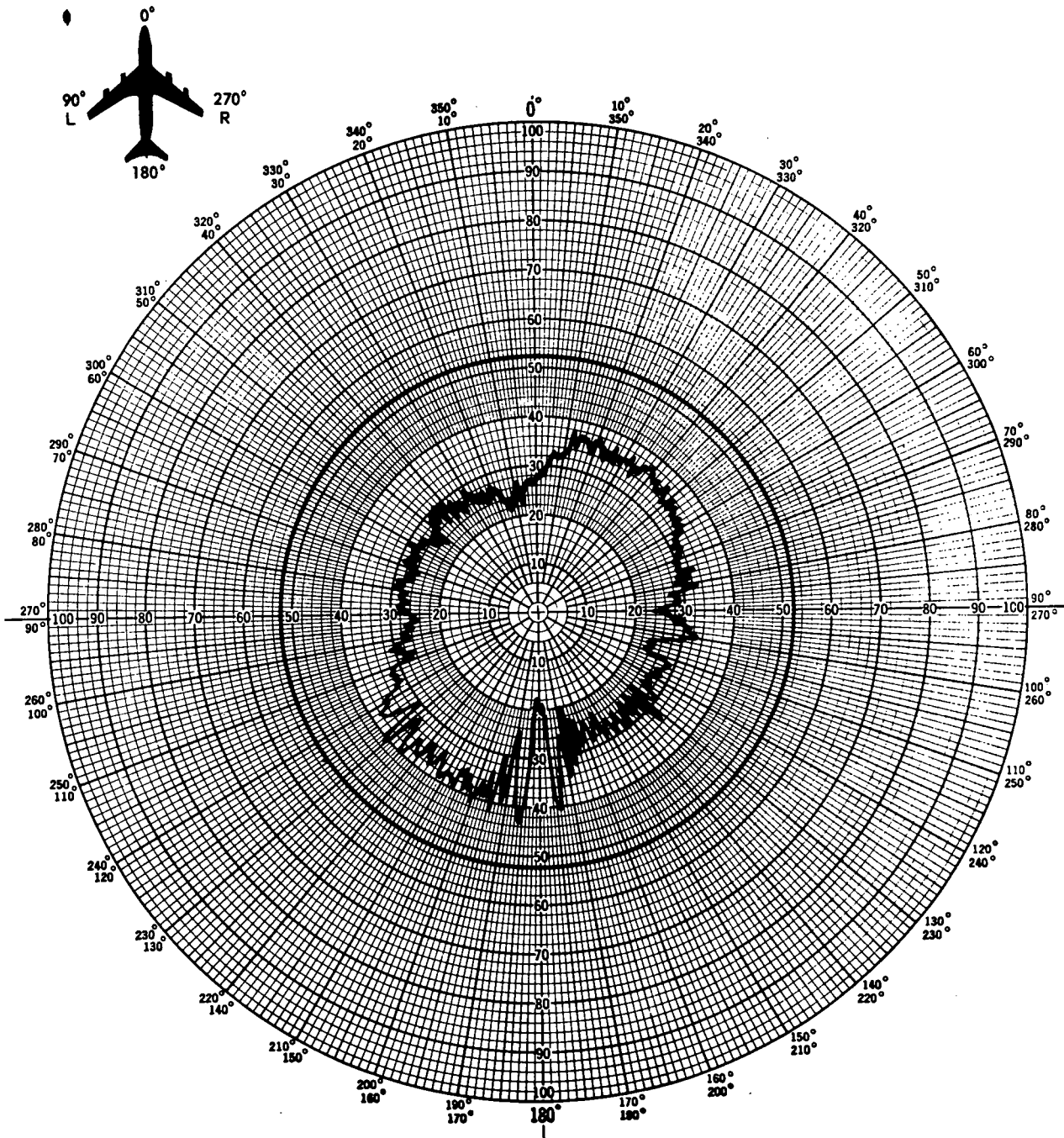*Right Hand Circular (Principal) Polarization*
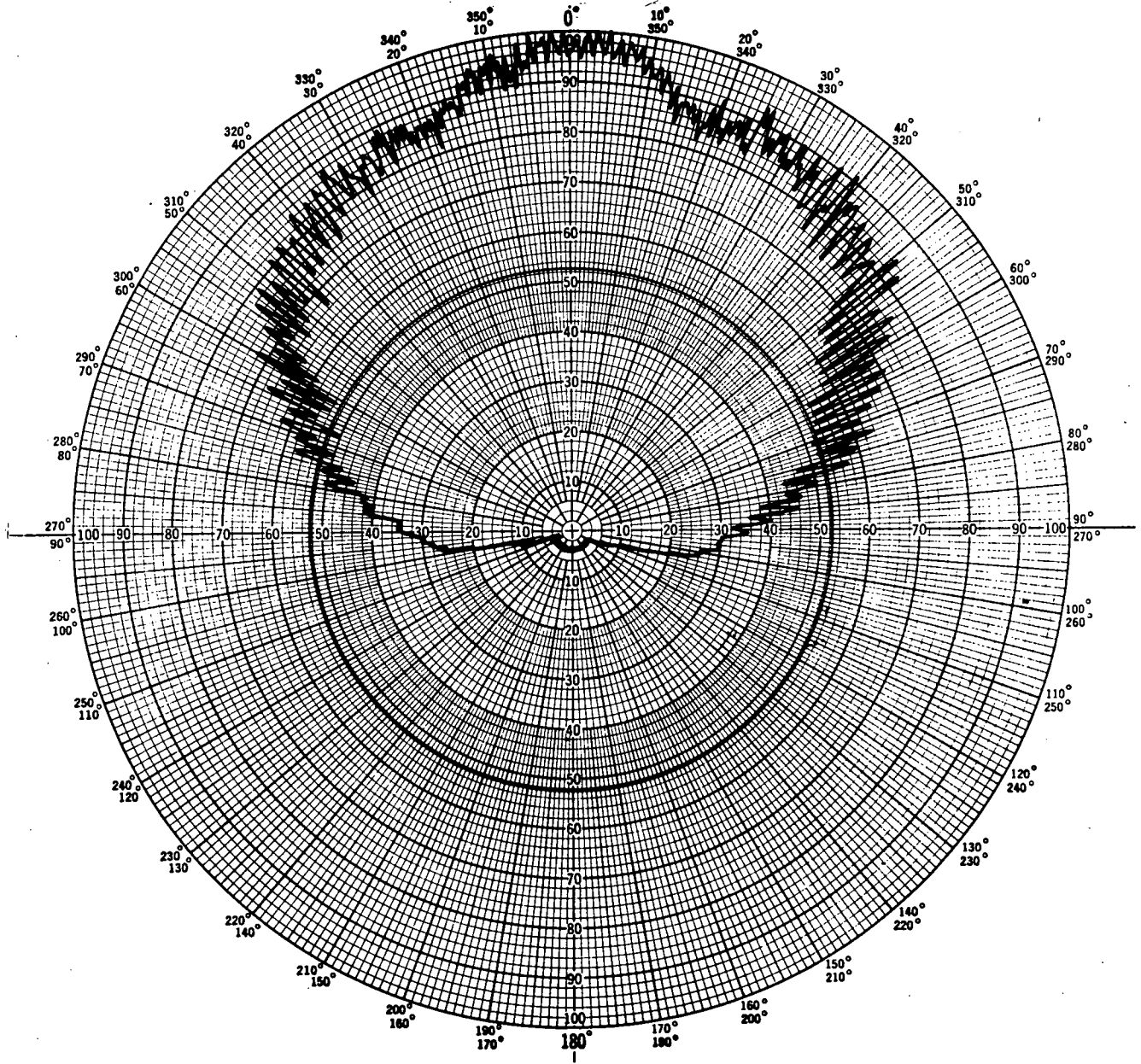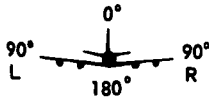
Maximum directivity: 5.6 dB
Curve plotted in voltage
Variable angle θ
Constant angle $\phi = 90°$

Model scale: 1/20
Full-scale frequency: 1600 MHz
Convair 880 airplane
Antenna location: top centerline at STA 820

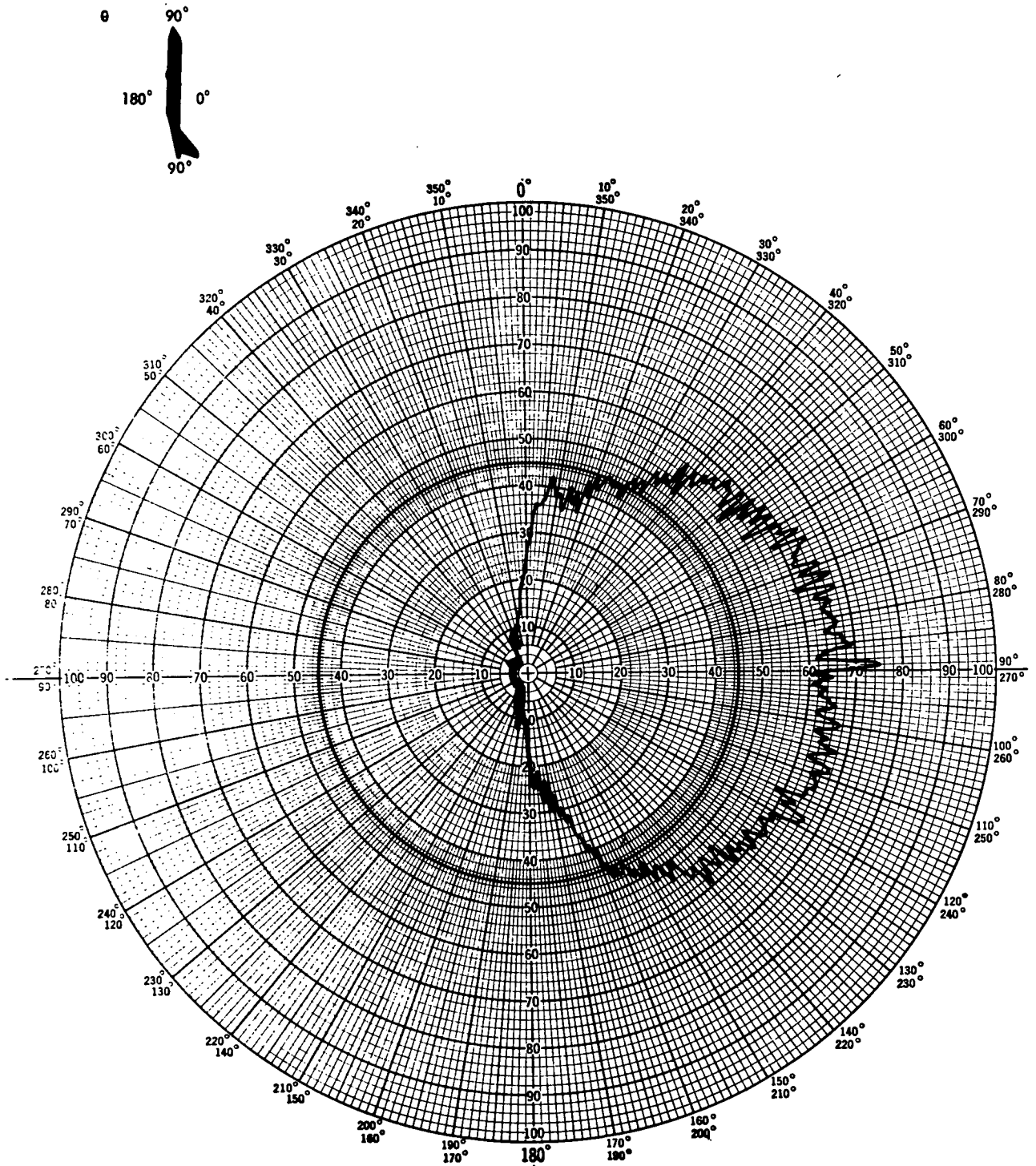*Figure 19.—Orthogonal-Mode Crossed-Slot Antenna Roll Plane Pattern,
Right Hand Circular (Principal) Polarization*
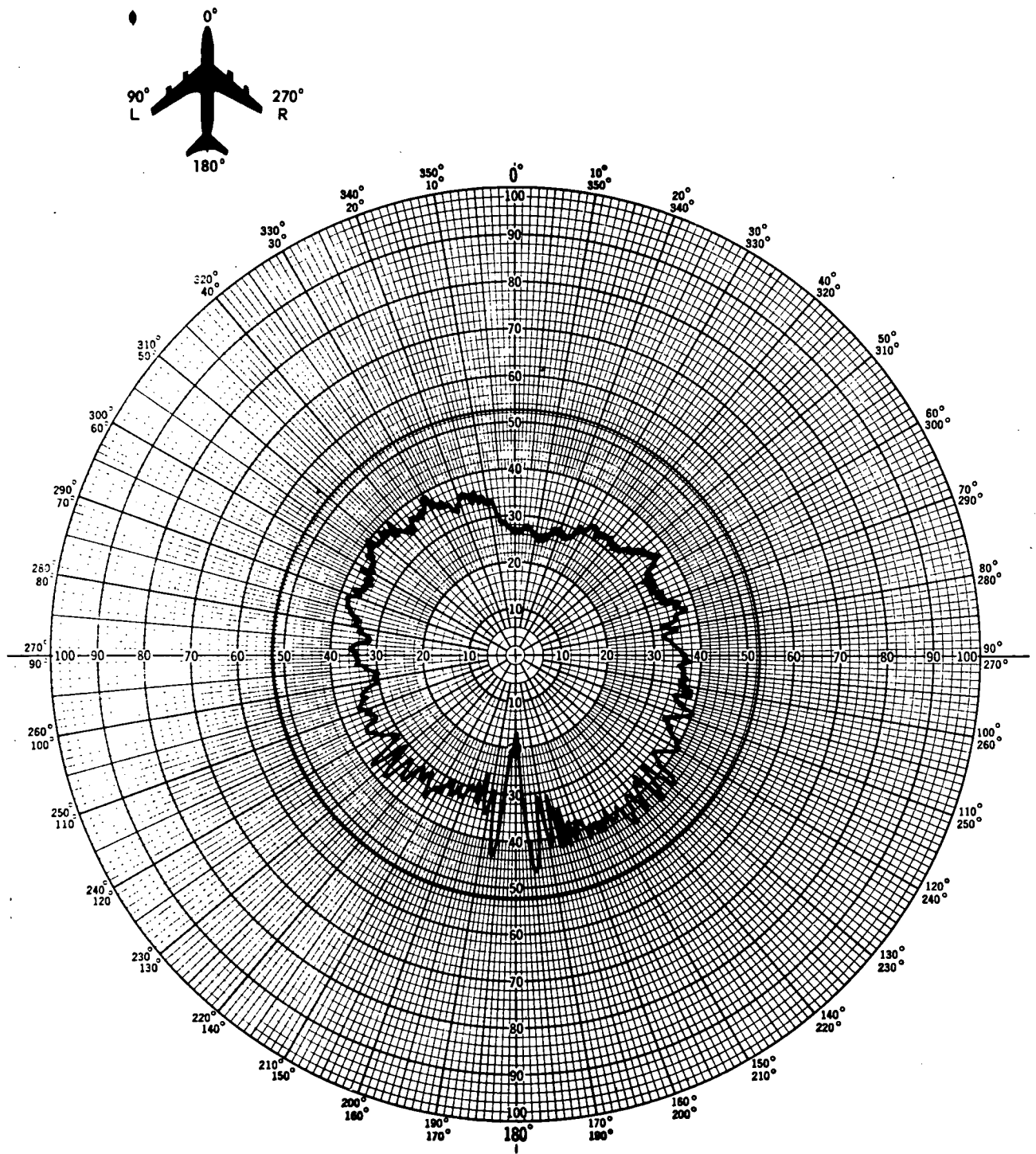
Maximum directivity: 5.6 dB

Curve plotted in voltage

Variable angle ϕ

Constant angle $\theta = 90°$

Model scale: 1/20

Full-scale frequency: 1600 MHz

Convair 880 airplane
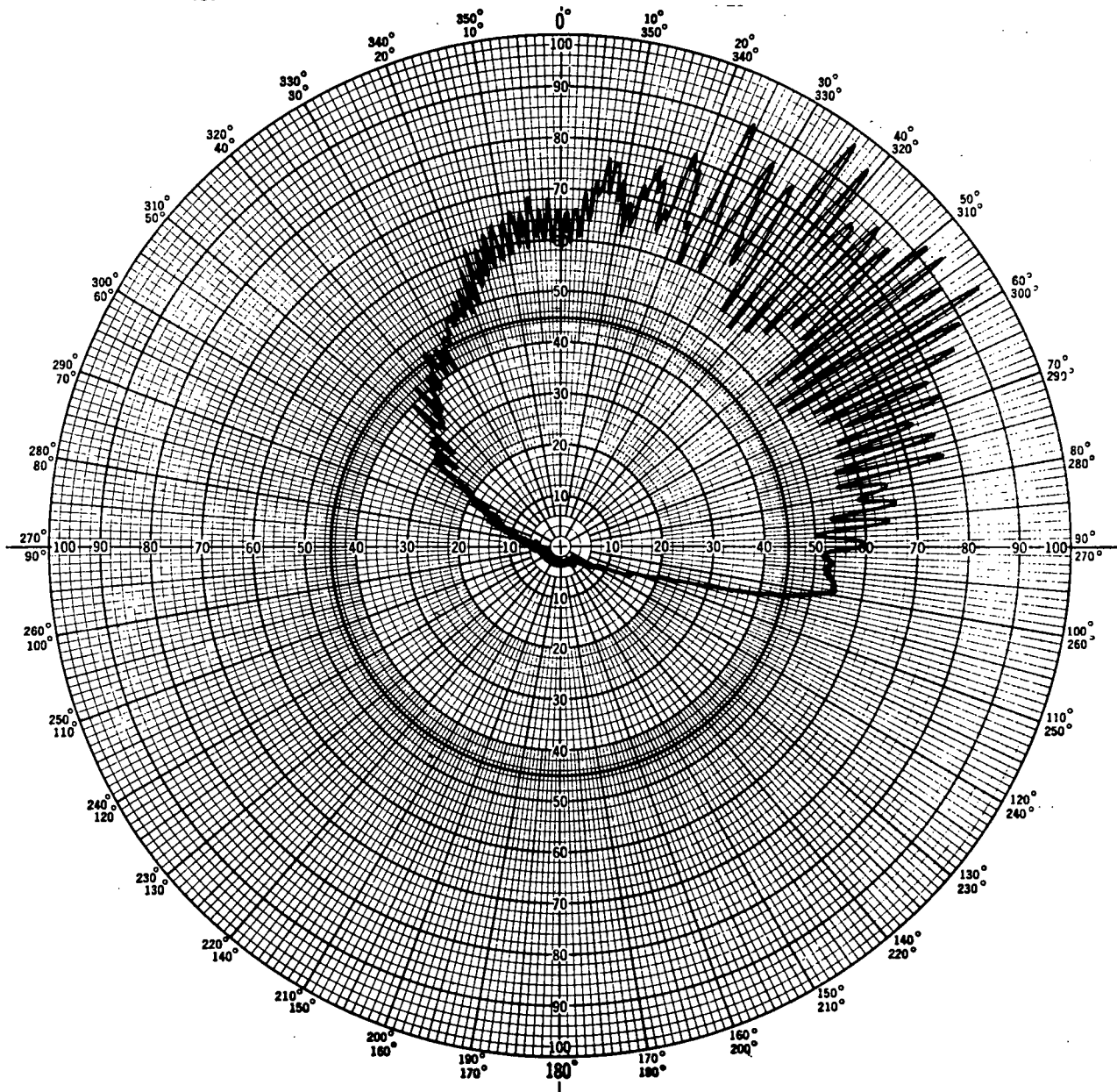
Antenna location: top centerline at STA 820

Figure 20.—Orthogonal-Mode Crossed-Slot Antenna Yaw Plane Pattern, Right Hand Circular (Principal) Polarization

Maximum directivity: 5.6 dB
Curve plotted in voltage
Variable angle θ
Constant angle $\phi = 0°$

Model scale: 1/20
Full-scale frequency: 1600 MHz
Convair 880 airplane
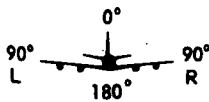Antenna location: top centerline at STA 820

Figure 21.—Orthogonal-Mode Crossed-Slot Antenna Pitch Plane Pattern,
Left Hand Circular (Cross) Polarization

Maximum directivity: 5.6 dB
Curve plotted in voltage
Variable angle θ
Constant angle $\phi = 90°$

Model scale: 1/20
Full-scale frequency: 1600 MHz
Convair 880 airplane
Antenna location: top centerline at STA 820

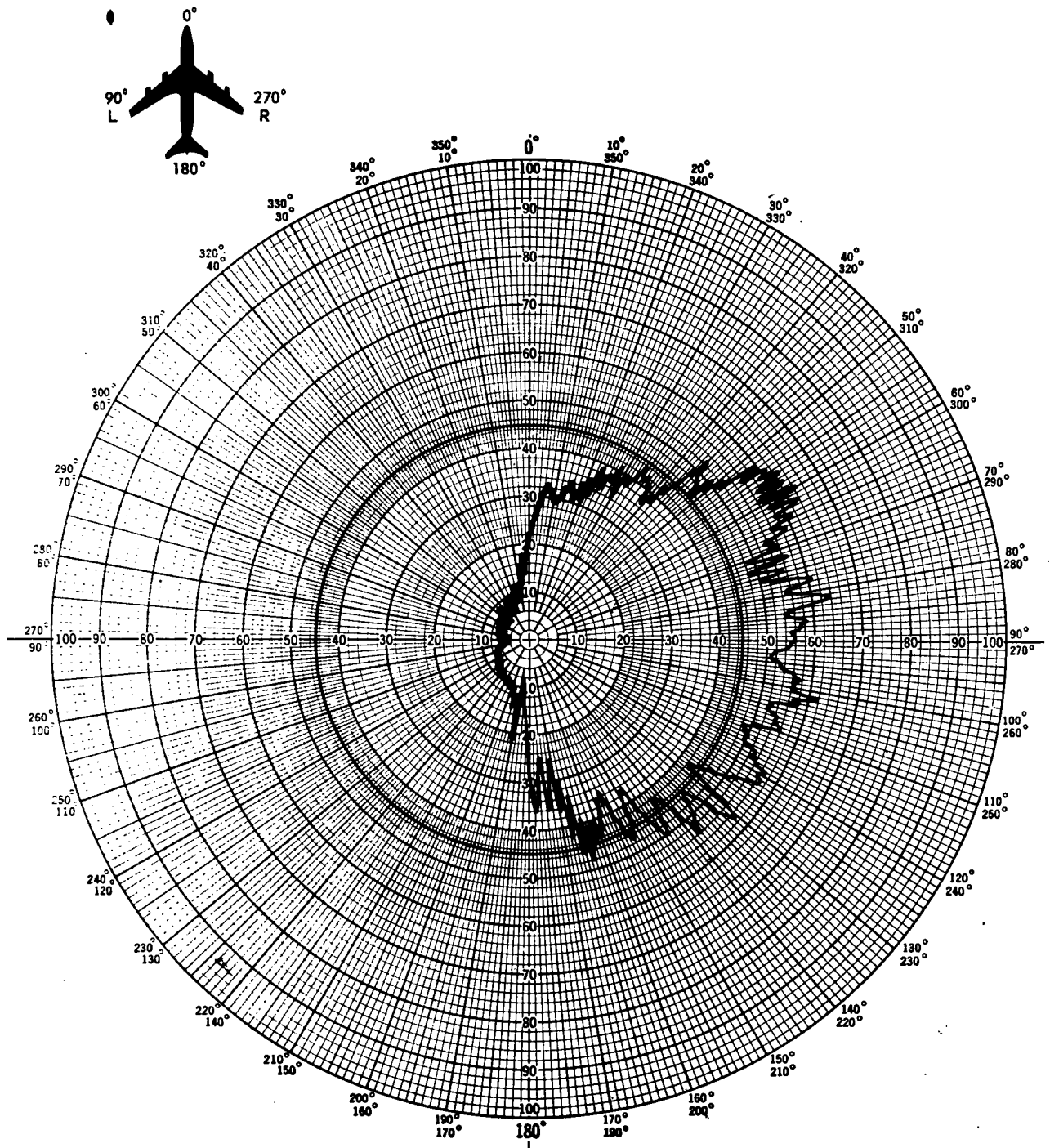*Figure 22.—Orthogonal-Mode Crossed-Slot Antenna Roll Plane Pattern,
Left Hand Circular (Cross) Polarization*

28

Maximum directivity: 5.6 dB
Curve plotted in voltage
Variable angle ϕ
Constant angle $\theta = 90°$

Model scale: 1/20
Full-scale frequency: 1600 MHz
Antenna location: top centerline at STA 820

Figure 23.—Orthogonal-Mode Crossed-Slot Antenna Yaw Plane Pattern,
Left Hand Circular (Cross) Polarization

Maximum directivity: 7.0 dB
Curve plotted in voltage
Variable angle θ
Constant angle $\phi = 0°$

Model scale: 1/20
Full-scale frequency: 1600 MHz
Convair 880 airplane
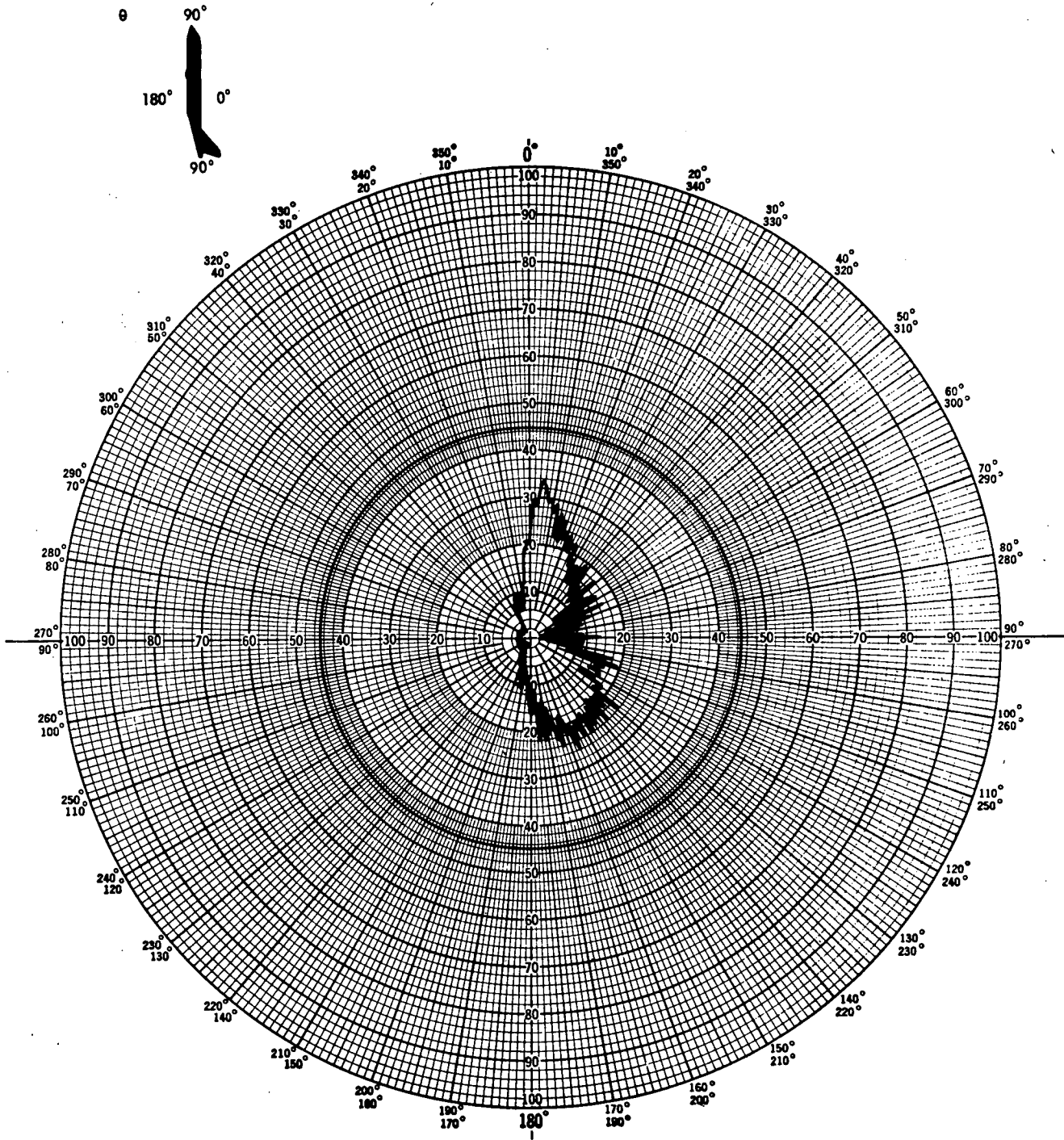Antenna location: 35° right of top centerline at STA 820

*Figure 24.—Orthogonal-Mode Crossed-Slot Antenna Pitch Plane Pattern,
Right Hand Circular (Principal) Polarization*

Maximum directivity: 7.0 dB
Curve plotted in voltage
Variable angle θ
Constant angle $\phi = 90°$

Model scale: 1/20
Full-scale frequency: 1600 MHz
Convair 880 airplane
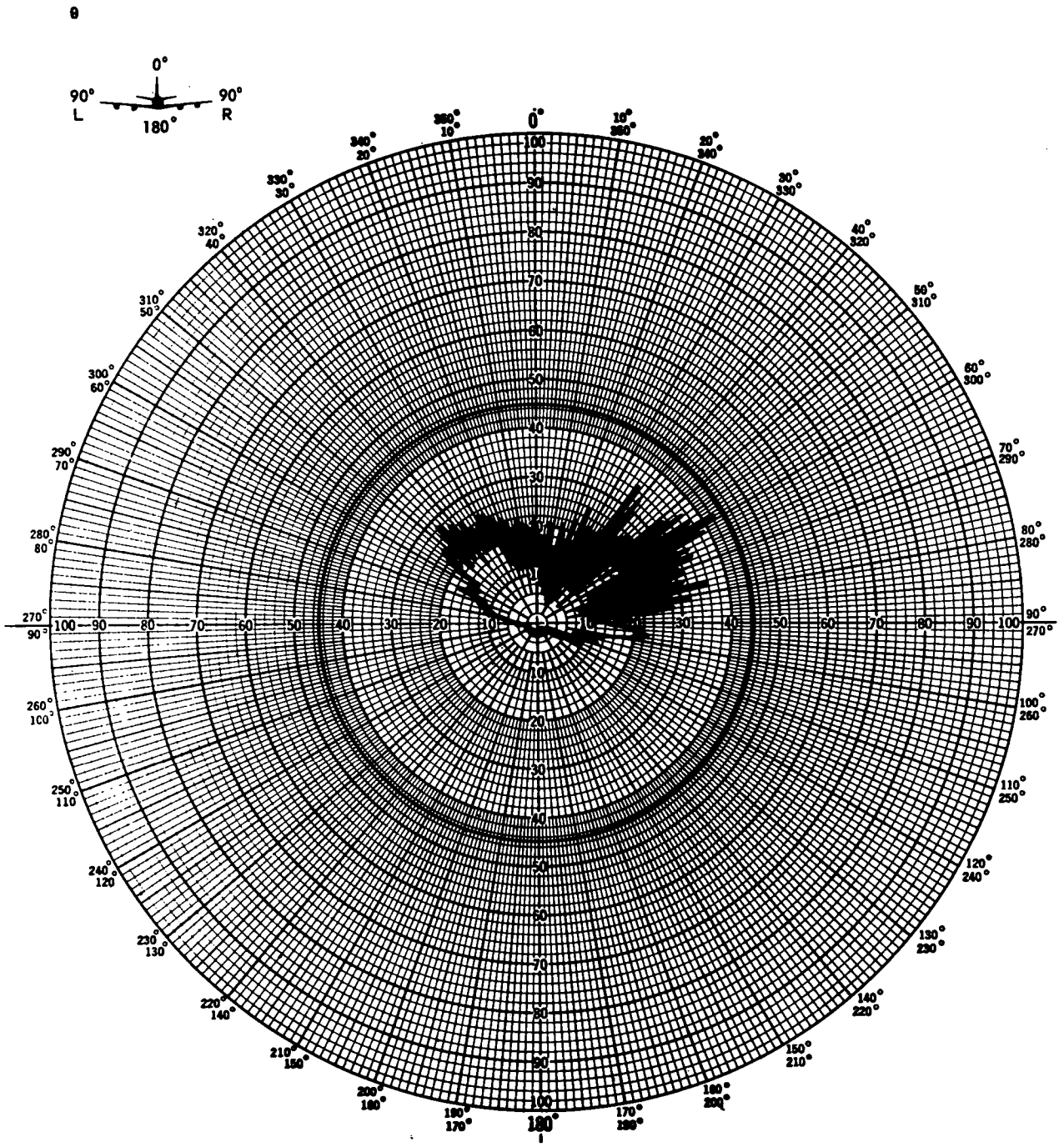Antenna location: 35° right of top centerline at STA 820

Figure 25.—Orthogonal-Mode Crossed-Slot Antenna Roll Pattern,
Right Hand Circular (Principal) Polarization

Maximum directivity: 7.0 dB
Curve plotted in voltage
Variable angle ϕ
Constant angle $\theta = 90°$

Model scale: 1/20
Full-scale frequency: 1600 MHz
Convair 880 airplane
Antenna location: 35° right of top centerline at STA 820

Figure 26.—Orthogonal-Mode Crossed-Slot Antenna Yaw Plane Pattern,
Right Hand Circular (Principal) Polarization

Maximum directivity: 7.0 dB
Curve plotted in voltage
Variable angle θ
Constant angle $\phi = 0°$

Model scale: 1/20
Full-scale frequency: 1600 MHz
Convair 880 airplane
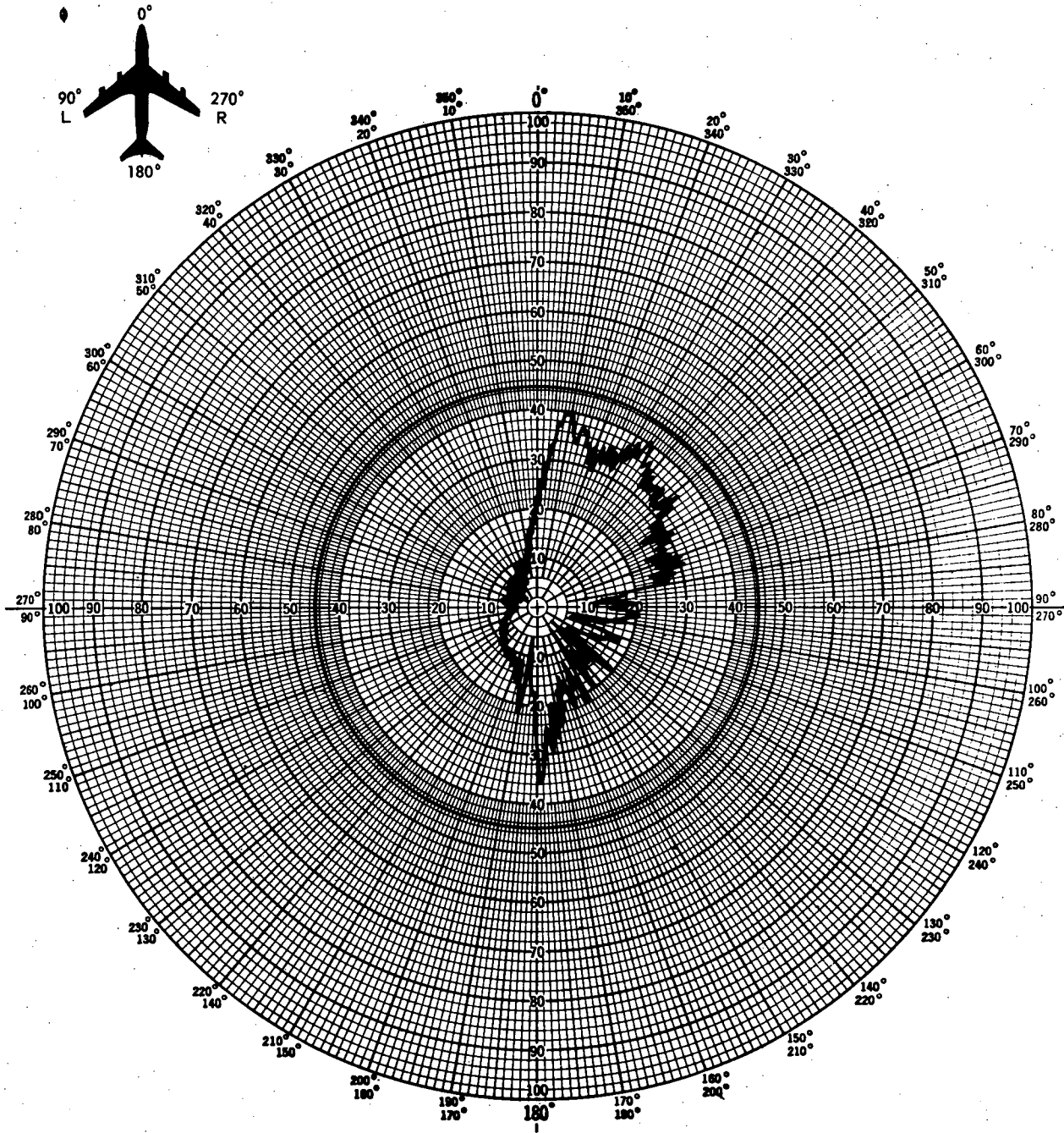Antenna location: 35° right of top centerline at STA 820

Figure 27.—Orthogonal-Mode Crossed-Slot Antenna Pitch Plane Pattern,
Left Hand Circular (Cross) Polarization

Maximum directivity: 7.0 dB
Curve plotted in voltage
Variable angle θ
Constant angle $\phi = 90°$

Model scale: 1/20
Full-scale frequency: 1600 MHz
Convair 880 airplane
Antenna location: 35° right of top centerline at STA 820

*Figure 28.—Orthogonal-Mode Crossed-Slot Antenna Roll Plane Pattern,
Left Hand Circular (Cross) Polarization*

Maximum directivity: 7.0 dB   Model scale: 1/20
Curve plotted in voltage   Full-scale frequency: 1600 MHz
Variable angle ϕ Convair 880 airplane
Constant angle $\theta = 90°$ Antenna location: 35° right of top centerline at STA 820

Figure 29.—Orthogonal-Mode Crossed-Slot Antenna Yaw Plane Pattern,
Left Hand Circular (Cross) Polarization

Figure 30.—Orthogonal-Mode Crossed-Slot Antenna Radiation Distribution Plot,
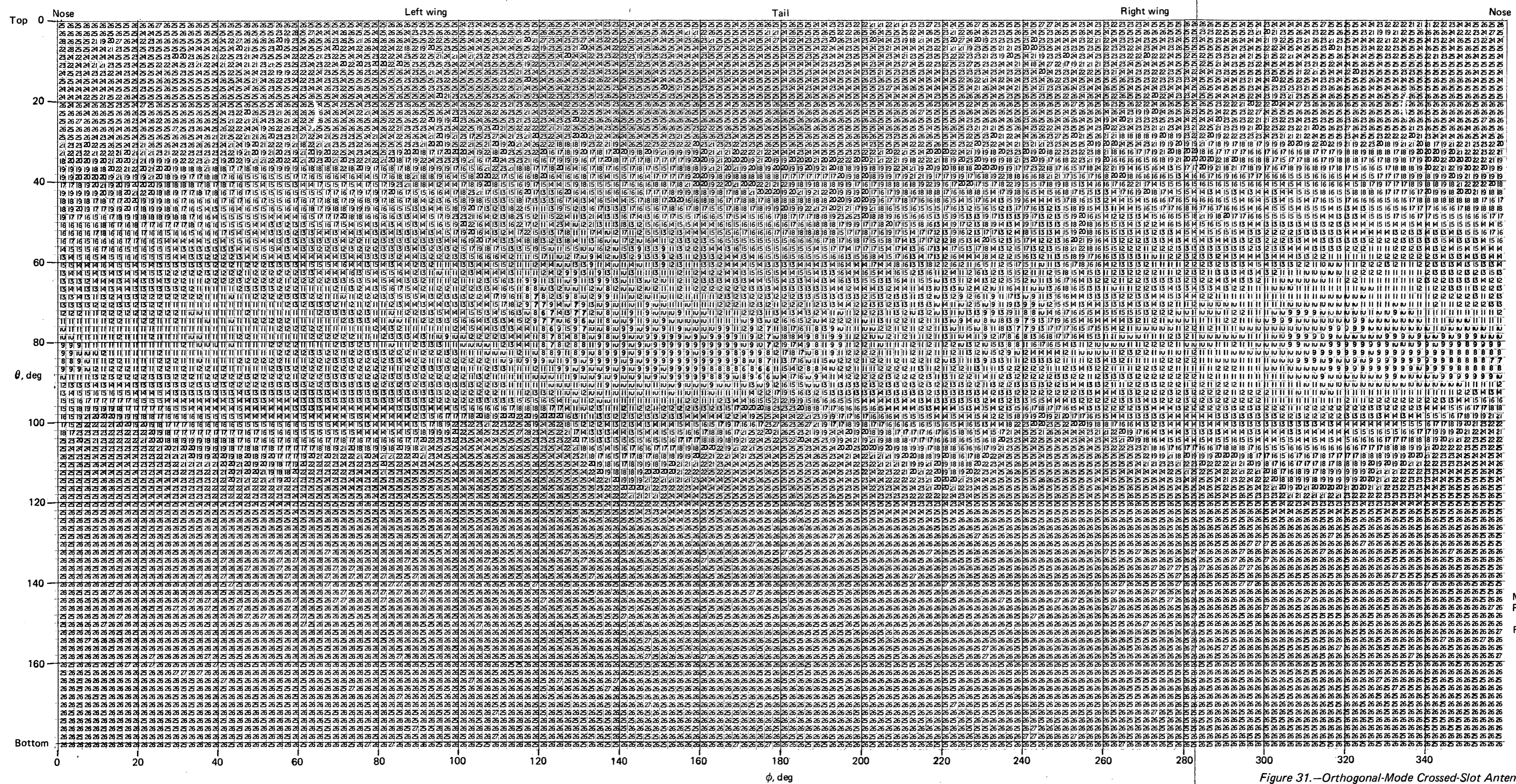Circular Principal Polarization
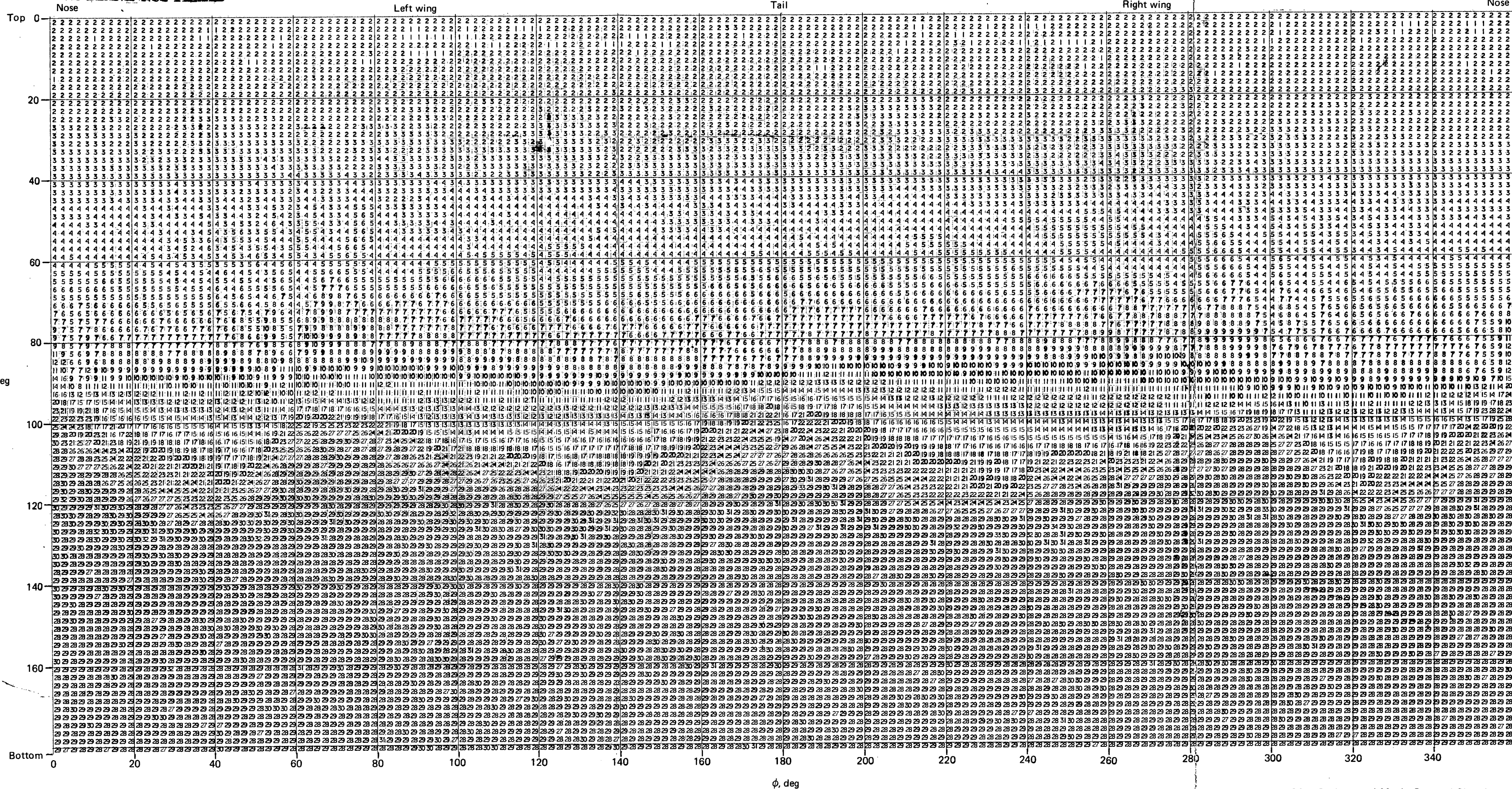
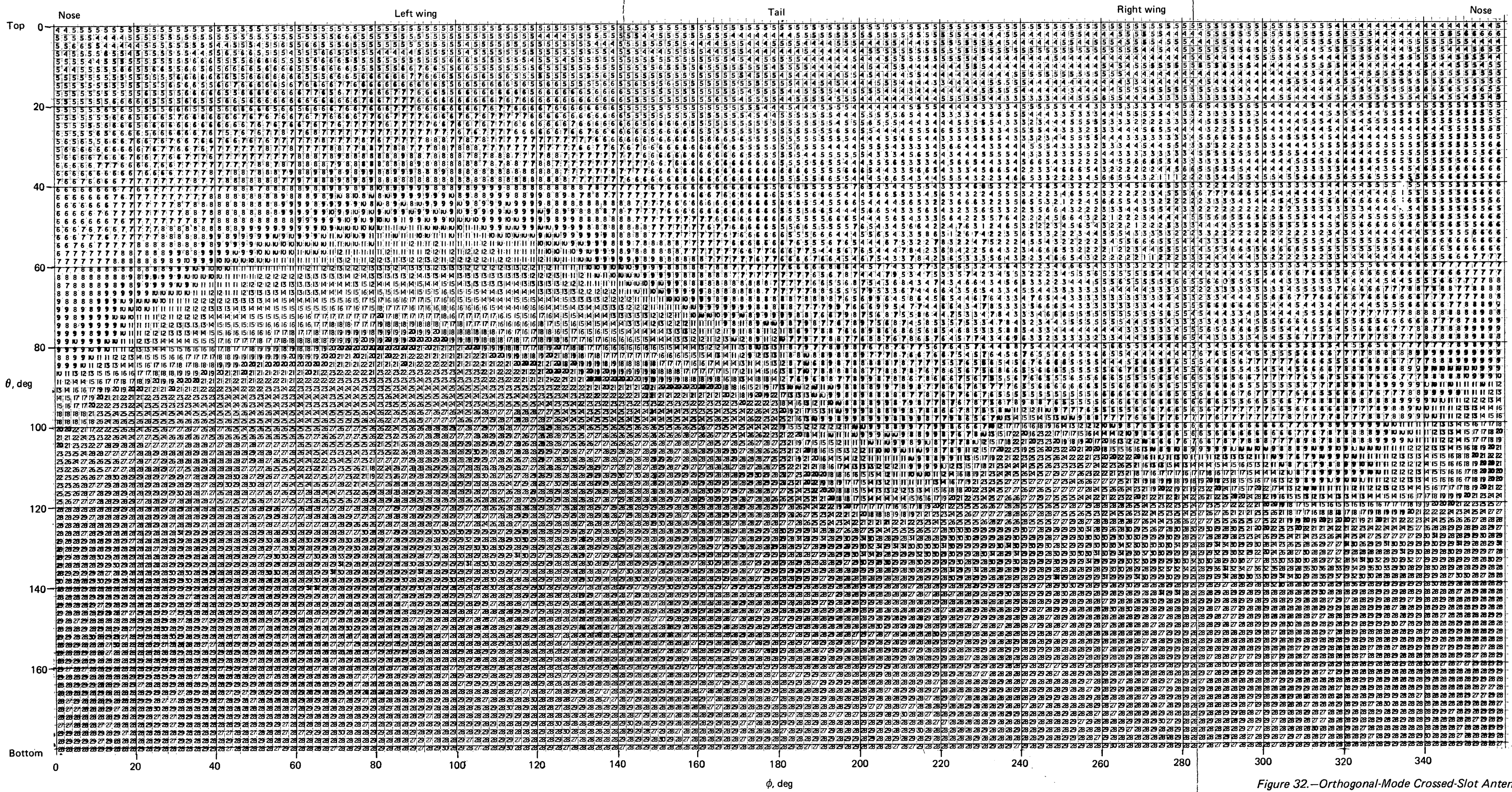Model scale: 1/20
Pattern measurement frequency: 32 GHz

Remarks:
The antenna is installed on the
top centerline on a Convair
880 at STA 820.
All figures in the plot are negative
and represent relative values
in dB.
The maximum level "1" is a peak
gain of 5.0 dB above isotropic
level.

37

Page intentionally left blank

Figure 31.—Orthogonal-Mode Crossed-Slot Antenna Radiation Distribution Plot, Circular Cross Polarization

Model scale: 1/20
Pattern measurement frequency: 32 GHz

Remarks:
The antenna is installed on the top centerline on a Conviar 880 airplane at STA 820.
All figures in the plot are negative and represent relative values in dB.
The maximum level "1" is a peak gain of 5.0 dB above isotropic level.

Page intentionally left blank

Top 0

θ, deg

20

40

60

80

100

120

140

160

Bottom

0 20 40 60 80 100 120 140 160 180 200 220 240 260 280 300 320 340

φ, deg

Model scale: 1/20
Pattern measurement frequency: 32 GHz

Remarks:
The antenna is installed 35° to the right of the top centerline on a Convair 880 airplane at STA 820. All figures in the plot are negative and represent relative values in dB. The maximum level "1" is a peak gain of 6.4 dB above isotropic level.
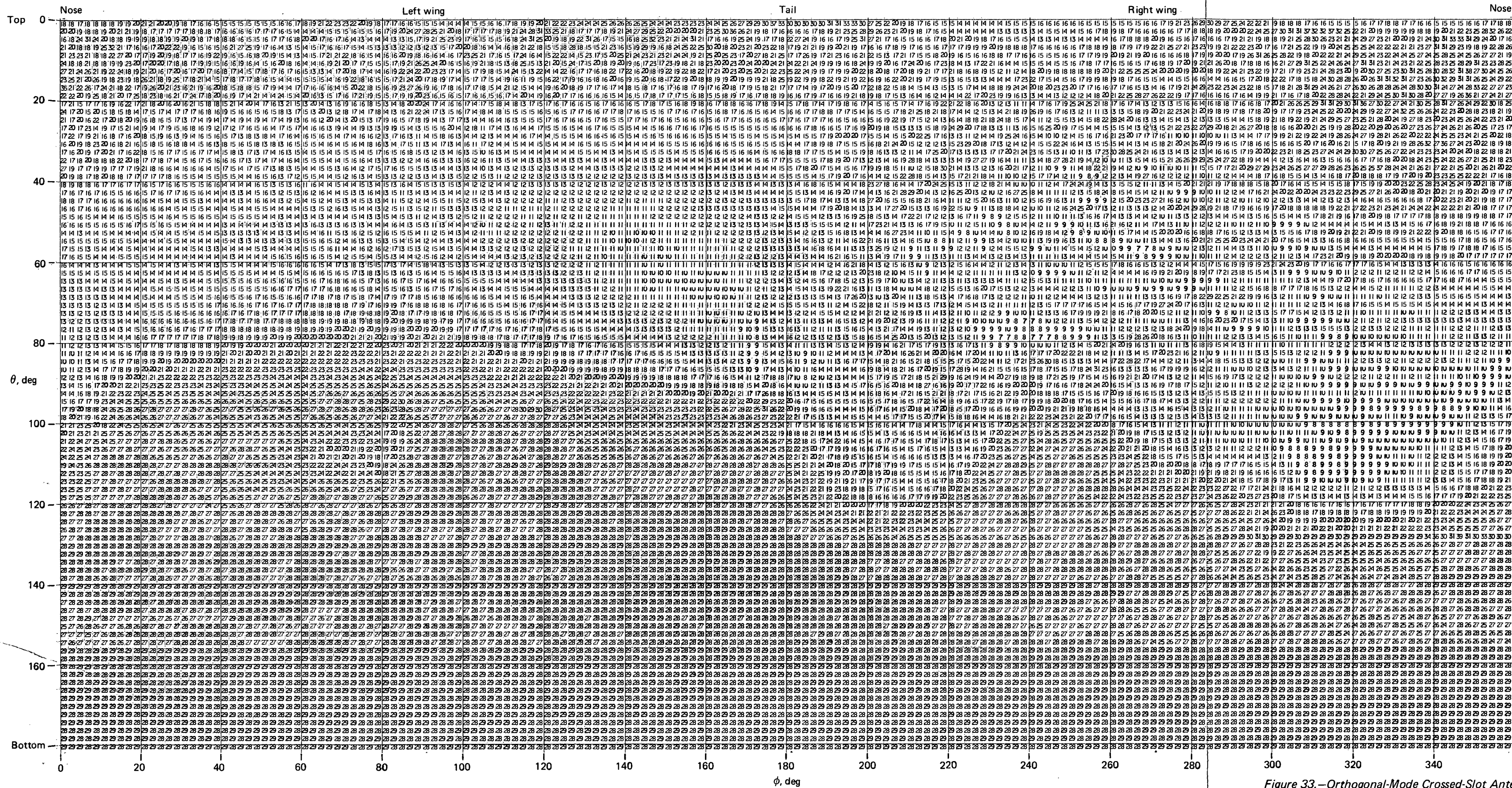
Figure 32.—Orthogonal-Mode Crossed-Slot Antenna Radiation Distribution Plot, Circular Principal Polarization

41

Page intentionally left blank

Figure 33.—Orthogonal-Mode Crossed-Slot Antenna Radiation Distribution Plot, Circular Cross Polarization

Model scale: 1/20
Pattern measurement frequency: 32 GHz

Remarks:
The antenna is installed 35° to the right of the top centerline on a Convair 880 airplane at STA 820. All figures in the plot are negative and represent relative values in dB. The maximum level "1" is a peak gain of 6.4 dB above isotropic level.

43

ORTHOGONAL-MODE CROSSED-SLOT ANTENNA–LINEARLY POLARIZED

Introduction

The linearly polarized orthogonal-mode crossed-slot antenna is intended as an experimental aid for airborne satellite communications studies in the 1540- to 1660-MHz frequency range. When mounted on the side of the forward fuselage, this antenna will provide nearly equal gain for vertical and horizontal polarization as well as equal gain for direct and sea-reflected satellite signals arriving from low elevations (near the horizon). The antenna is a cavity-backed, crossed-slot design where each half-wavelength slot is an independent, linearly polarized radiator.

The exterior of the antenna is identical to that of the circularly polarized antenna except for the connector mounting and marking shown in figures 1 and 2 in the previous section. The antenna has two output connectors marked "H" and "V" which will provide horizontal and vertical polarization, respectively, when the antenna is oriented properly on the side of the fuselage. Three production antennas were furnished under this contract. These units are intended to be operated as receiving antennas. However, tests on the feed network show that the antenna has a capability of handling 60 watts of CW power at 45,000-ft altitude and can also be used as a transmitting antenna.

Requirements

The basic requirements are that a single flush-mounted antenna installed on the side of the airplane fuselage shall provide essentially equal and constant gain for horizontal and vertical polarization in a sector 60° wide in azimuth and elevation. Furthermore, it is required that radiation pattern symmetry exist around the axis normal to the antenna aperture. To meet these requirements a cavity-backed iris consisting of two orthogonal half-wavelength slots is selected as the basic antenna configuration (see fig. 3).

Theory of the Antenna

In the following description the crossed-slot iris is assumed to be located in vertical ground plane and oriented so that one slot is horizontal and the other is vertical. The coordinate system for all pattern descriptions is shown in figure 4.

The principle of operation is illustrated in figure 34. Figures 34a and 34b show the idealized far field E-plane and H-plane patterns of the individual slots in the crossed-slot iris. The vertical slot pro-

vides E_ϕ polarization, which is horizontal, and the horizontal slot provides E_θ polarization, which is vertical (on the horizon). Figure 34c shows the pattern coverage of the crossed-slot iris, which is obtained by superposition of the individual slot patterns. The E_θ and E_ϕ components, which in any given direction are orthogonal, are equal in magnitude on the axis normal to aperture (0-dB axial ratio). For an antenna located on the left side of the fuselage this axis has the direction:

$(\theta, \phi) = (90°, 90°)$ (see fig. 4).

As one moves off axis, the axial ratio between the E_θ and the E_ϕ field components increases due to the asymmetry between E-plane and H-plane patterns of the individual slots. However, within a 90° cone around the above-mentioned axis, the axial ratio between $|\bar{E}_\theta|$ and $|\bar{E}_\phi|$ is less than 2 dB. Each slot has a separate output connector. Thus, it is possible to resolve an unknown signal into its E_θ and E_ϕ field components.

Mechanical Construction

The dual-mode linear version of the orthogonal-mode crossed-slot antenna is of the same basic construction as the circularly polarized antenna, i.e., the housing, dimensions, and materials are as outlined in figure 6.

In this antenna the hybrid is removed from the cavity and each slot is connected to a separate output connector by a short length of microstrip transmission line. Each slot is fed at one point rather than the balanced feed version shown in figure 7. The three production antennas furnished under this contract are identified by the serial numbers DOT-TSC-001 through -003.

Feed Network—Impedance Matching

Figure 35 shows schematically the antenna feed network and the external control circuit (coaxial transfer switch) which enables the remote selection of vertical or horizontal polarization.

Each slot is fed at one point, and the equivalent electrical network presented to each of the feed transmission lines is shown in figure 9. The technique for matching the antenna is outlined in the previous section on the circularly polarized antenna. The antenna output ports are marked "H" and "V." The H-port is connected to the vertical slot and provides horizontal (ϕ) polarization. The V-port is connected to the horizontal slot and provides vertical (θ) polarization. The impedance at each output port is matched to 50 ohms within a 2:1 VSWR limit. Impedance data measured at the H- and V-ports are given in the next section.

Electrical Data

The electrical performance data presented in this section are obtained from measurements on the production antenna, serial number DOT-TSC-003. These data are nearly identical to those measured on the other antennas, serial numbers DOT-TSC-001 and -002, and are therefore representative for all of the delivered "dual-mode linear" antennas.

All measurements were performed with the antenna installed in a 4- by 4-ft ground plane simulating a side fuselage section of the Convair 880 airplane as shown in figure 36.

Impedance—Figure 37 is a Smith chart plot of the individual slot impedances referred to the antenna output ports, H and V in figure 35.

The impedance was measured at each output port, with the other port terminated in 50 ohms. Table 6 shows the VSWR at H and V as a function of frequency. The data show that the antenna VSWR is within the specified 2:1 limit (50-ohm reference) over the 1540- to 1660-MHz frequency range.

TABLE 6.—ANTENNA INPUT VSWR

Frequency, MHz	Antenna VSWR	
	Port H	Port V
1540	1.45	1.46
1600	1.34	1.48
1660	1.75	1.68

Isolation—The isolation between the individual slots was measured at the output ports H and V, i.e., a reference power level was applied to one slot at H and the power coupled to the other slot was monitored at V. The values are given in table 7.

TABLE 7.—ISOLATION BETWEEN SLOTS

Frequency, MHz	Isolation between slots, dB
1540	15.2
1600	18.5
1660	14.5

Radiation Patterns

Radiation pattern measurements were performed on the production antenna to determine pattern characteristics, directivity, and gain. With the antenna installed in the ground plane as shown in figure 36, the radiation patterns for main polarization as well as cross polarization were measured in the following cuts of each slot:

● E-plane (plane normal to the ground plane and the slot axis)

● H-plane (plane through the slot axis and normal to the ground plane)

In addition to the pattern measurements, the maximum directivity of each slot of the antenna in the direction normal to the ground plane was measured to be 5.2 dB. By comparative measurements between the antenna and a reference standard gain horn antenna, the maximum antenna gain (in the same direction) was determined to be 4.6 dB. From the directivity and gain values the antenna efficiency is determined to be 87%.

Figures 38 through 45 show the polar diagram patterns measured on the H-port (vertical slot with horizontal main polarization) and the V-port (horizontal slot with vertical main polarization). As no significant pattern variations occur over the frequency band, only the patterns measured at 1600 MHz are submitted. The patterns are plotted in voltage with the maximum level referred to the edge of the polar diagram (the "100" level). To ease the pattern evaluation the isotropic radiation level is shown as a circle on the polar diagram.

These patterns do not show any influence of the airplane structure, since they are full-scale patterns of the antenna installed on a small ground plane. The scalloping in the E-plane cuts of figures 38 and 42 is caused by the finite size of the ground plane (edge effects).

Scale Model Pattern Study

Scale model pattern measurements were performed to obtain detailed pattern characteristics of the antenna installed on the airplane. Such patterns were measured for the following installation location on the Convair 880 airplane:

● STA 422, 78° to the left of the top centerline

Due to the similarity between the Convair 880 and the Boeing 707 airframes, a 1/20th-scale model 707 airplane was used for the measurements. A 1/20th-scale model antenna (half-wavelength slot) was fabricated and installed at the equivalent location (STA 390) on the 707 model airplane.

Thus, all patterns are marked Convair 880, although the measurements were performed on a 707 airplane. The frequency used for the scale-model pattern measurements was 32 GHz.

Before its installation in the model airplane, the model antenna was installed on a 2.4- by 2.4-in. ground plane (a 1/20th-scale version of the ground plane shown in fig. 36) and E-plane and H-plane patterns were measured on the half-wavelength slot antenna at the scale frequency (32 GHz). This was done to verify that the model antenna possesses the pattern characteristics of the production antenna. Figures 46 through 49 show these patterns, which compare favorably to the full-scale patterns shown in figures 38 through 41. The lack of "spillover" radiation behind the ground plane is caused by absorbent material behind and around the ground plane, which was applied to prevent reflections from the waveguide feed network. The results obtained with the antenna installed on the model aircraft are discussed in the following paragraphs.

Polar Diagram Patterns—The radiation distribution prints, which will be discussed later, include main-polarized as well as cross-polarized radiation levels over the full sphere with 2° increments. Therefore, the polar diagram patterns are only submitted for main polarization in the principal planes (pitch, roll, and yaw).

Figures 50 through 52 show the patterns of the vertical slot, which has horizontal main polarization. These patterns would be obtained at the H-port of the production antenna. Figures 53 through 55 show the patterns of the horizontal slot, which has vertical main polarization. These patterns would be obtained at the V-port of the production antenna.

The patterns are plotted in voltage, with the maximum radiation level referred to the edge of the polar diagram (the "100" level). The constant angle and the variable angle of the pattern cut as well as the polarization of the rf field are indicated on each polar diagram.

Integration—The total energy radiated over the sphere (main- and cross-polarized energy) was integrated to establish the directivity of the antenna as installed on the airplane. The maximum directivity of the antenna is:

● 8.50 dB for horizontal polarization (H-port)

● 5.68 dB for vertical polarization (V-port)

The higher directivity for horizontally polarized energy is due to the horizontal wing structure, which causes more pattern distortion (lobing) for this polarization. For vertical polarization the scattering effects of the wing structure are minimal, which is also indicated by the "smooth" patterns of figures 53 through 55.

Radiation Distribution Plot—Radiation distribution plots were obtained with the model antenna installed and operating as described in the previous paragraph. These data for horizontally and vertically polarized illumination (main and cross polarization) on each slot show the radiation levels over the full sphere in 2° increments, thus giving a detailed resolution of the radiation distribution. Figures 56 and 57 are the plots for the horizontal slot (V-port) and figures 58 and 59 are those for the vertical slot (H-port). The maximum directivity, which is represented by the lowest number in the radiation distribution plot, is indicated on each of the plots. The interpretation of the distribution plot is discussed in detail in the "VHF Crossed-Loop Antenna" section. Using the plot to determine the directivity in a given direction the gain at these coordinates can be determined by subtracting 0.6 dB from the directivity value found, since it was established that the production antenna has an efficiency of 86%.

Conclusions

The linearly polarized orthogonal-mode crossed-slot antenna is intended to provide essentially equal and constant gain for horizontal and vertical polarization in a sector 60° wide in azimuth and elevation with symmetry around the antenna axis. The radiation patterns and the distribution plots clearly show that the antenna meets these objectives satisfactorily. Although the vertical slot has more lobed patterns for horizontal polarization due to interference from the horizontal wing structure, the gain difference between the vertical and horizontal polarization is within 1 dB on the axis of the antenna and less than 2.5 dB in any direction within the 60° cone around the antenna axis. No pattern improvement is anticipated by moving the antenna either forward or aft on the fuselage. Moving the antenna aft will increase the wing structure interference, and moving the antenna further forward will distort the pattern symmetry.

50
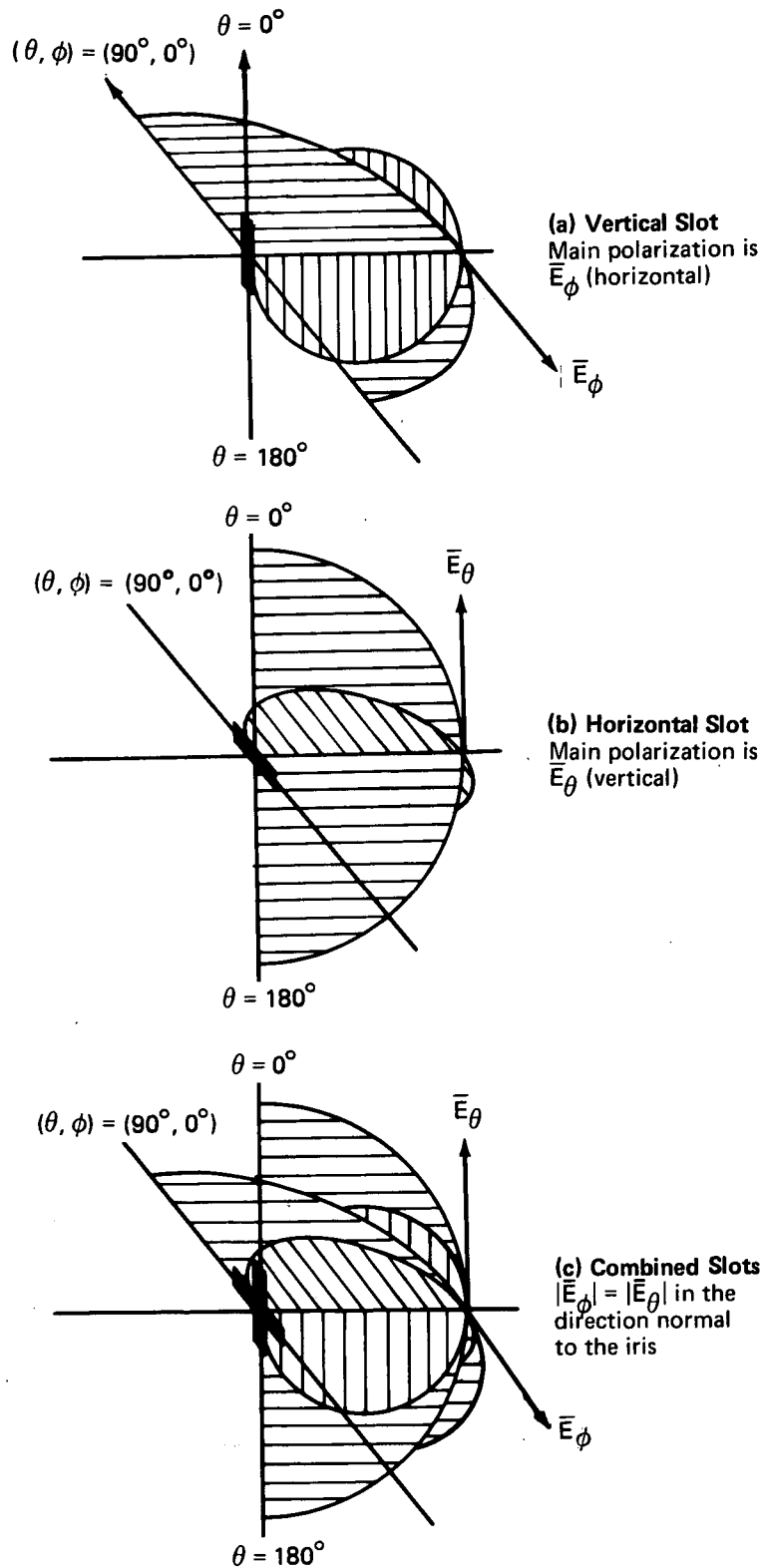
Figure 34.— Idealized Far-Field Patterns (E-Plane and H-Plane Cuts) From Individual Slots and Crossed-Slot Iris in a Vertical Ground Plane

51

Control
voltage
28Vdc

50-ohm
termination

Radiating aperture

V

H

To receiver

Coaxial transfer switch

Antenna unit
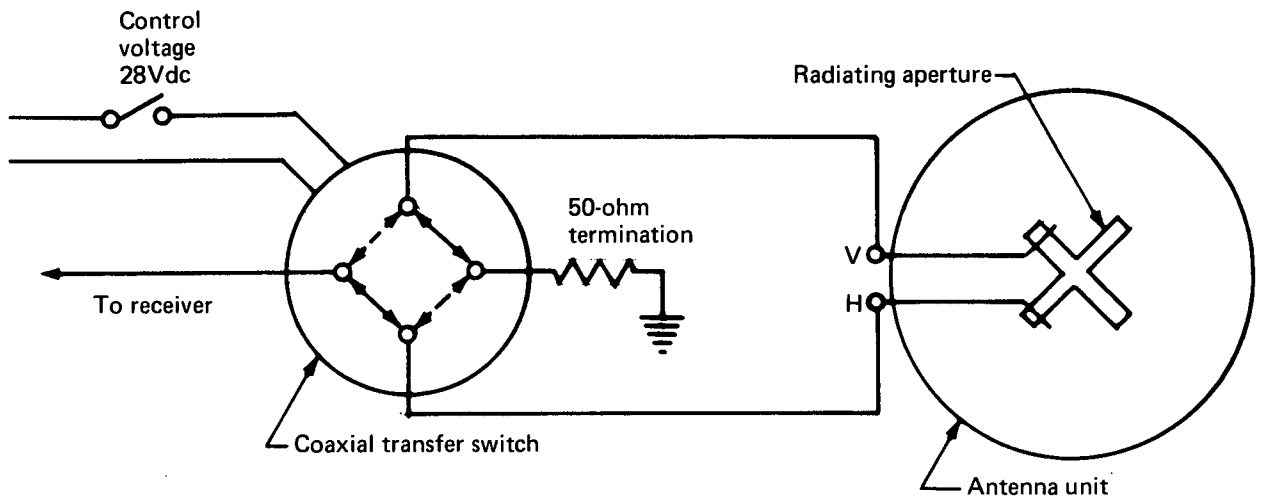
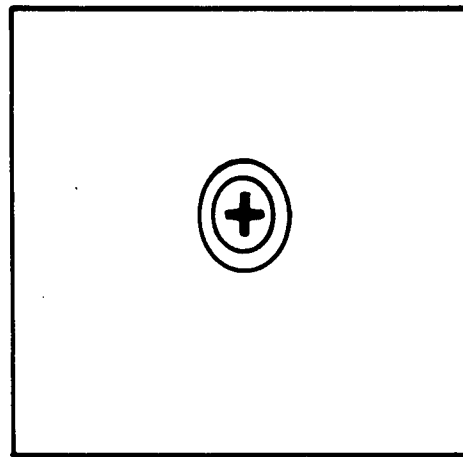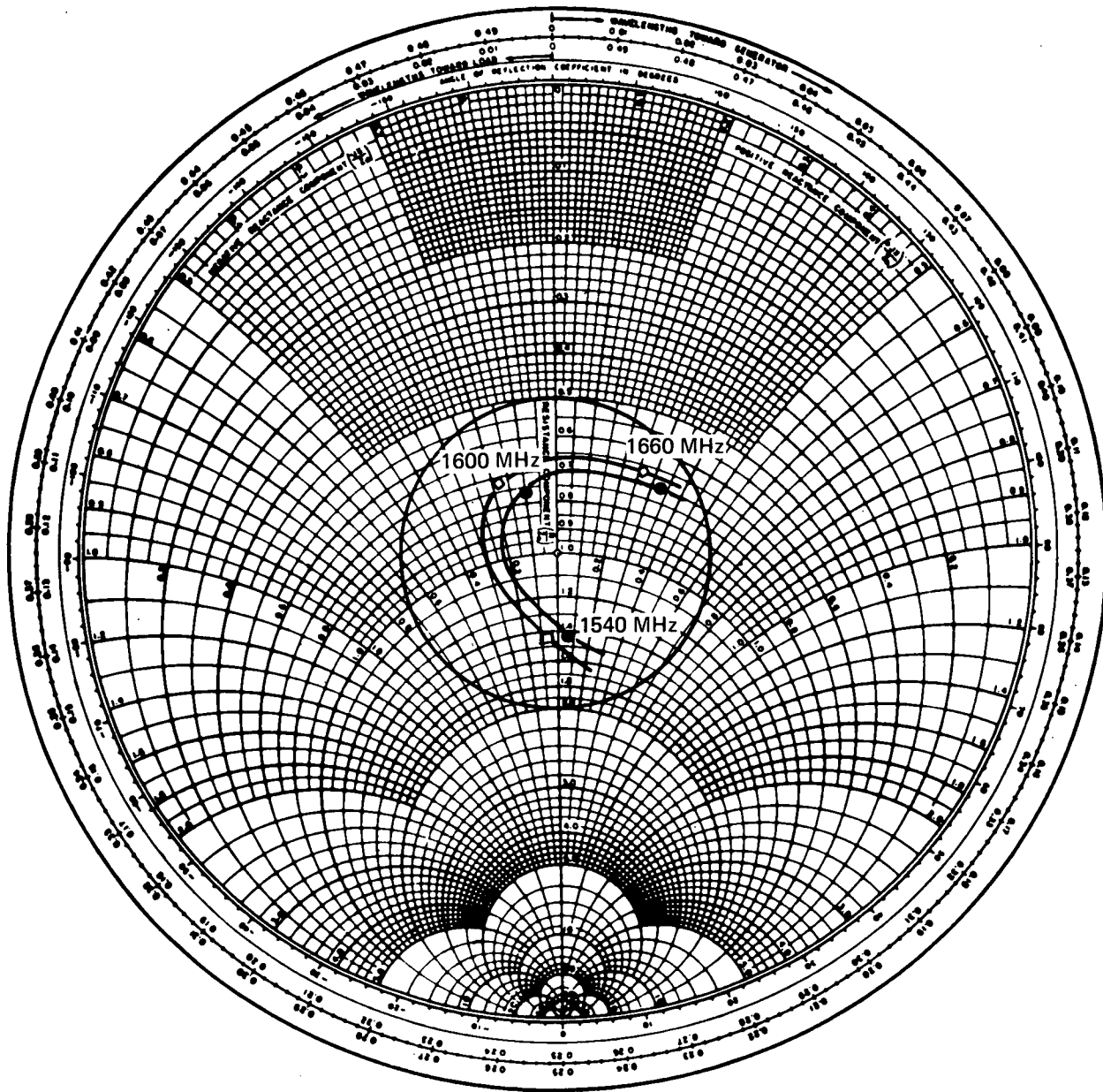Figure 35.—Antenna Feed Network and External Control Circuit

Figure 36.—Linearly Polarized Orthogonal-Mode Crossed-Slot Antenna Mounted on
Fuselage Section for Impedance and Pattern Measurements

◇ = impedance at horizontal port H   Specification-required frequency: 1540-1660 MHz
● = impedance at vertical port V   VSWR < 2:1
Z_0 = 50 ohms   Antenna S/N: DOT-TSC-003

Figure 37.— Impedance Plot of Orthogonal-Mode Crossed-Slot Antenna, Linear Polarization
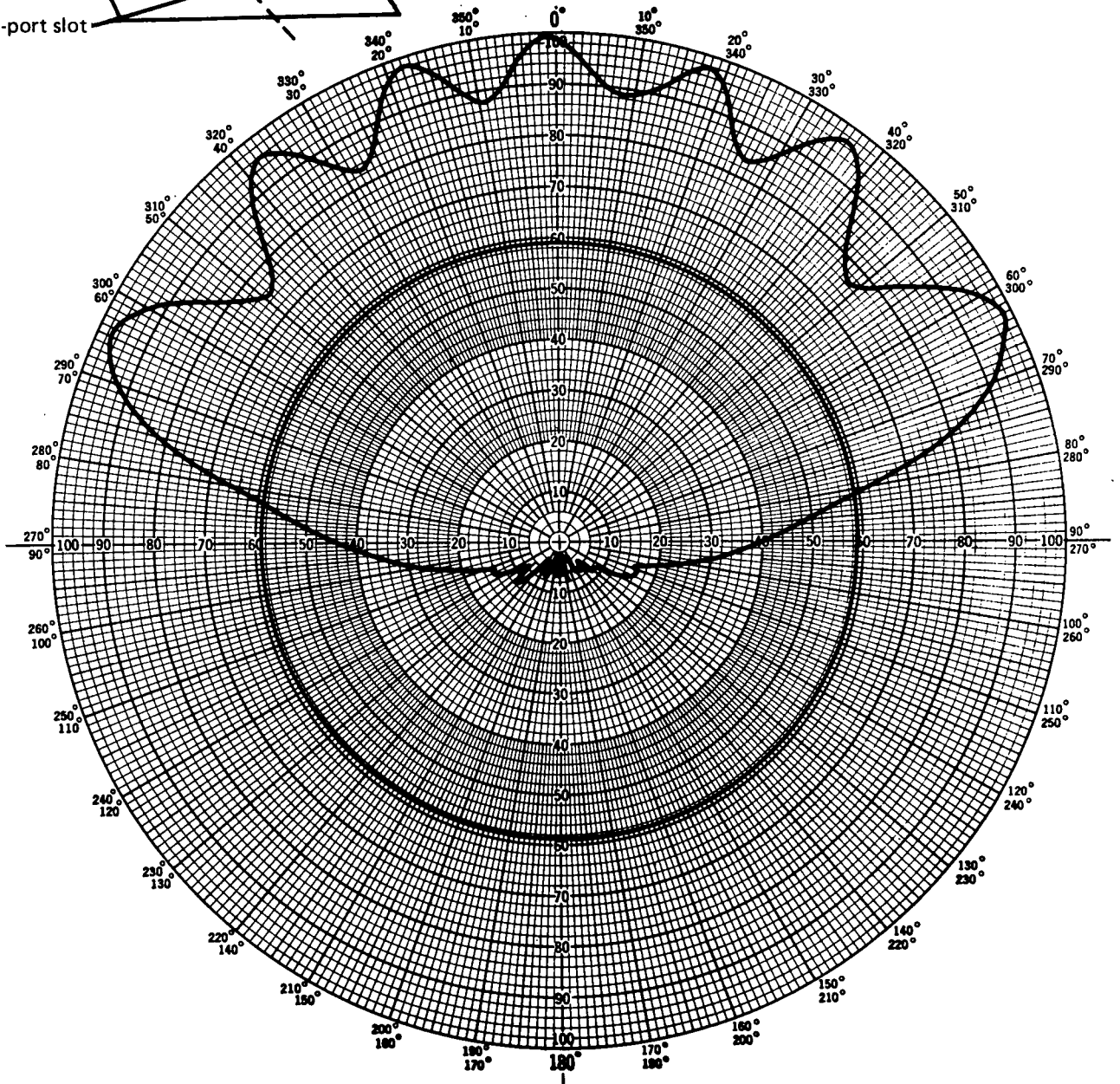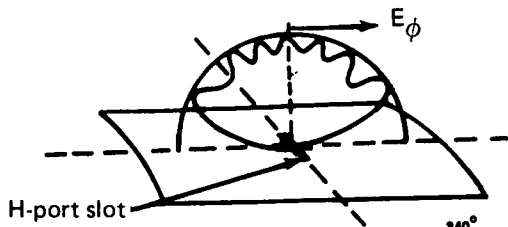
Maximum gain: 4.6 dB
Curve plotted in voltage
Variable angle ϕ
Constant angle $\theta = 90°$

Polarization: E_ϕ
Frequency: 1600 MHz
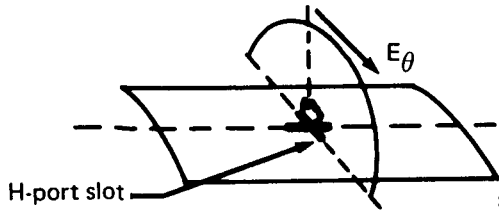Antenna location: 4-ft-square ground plane
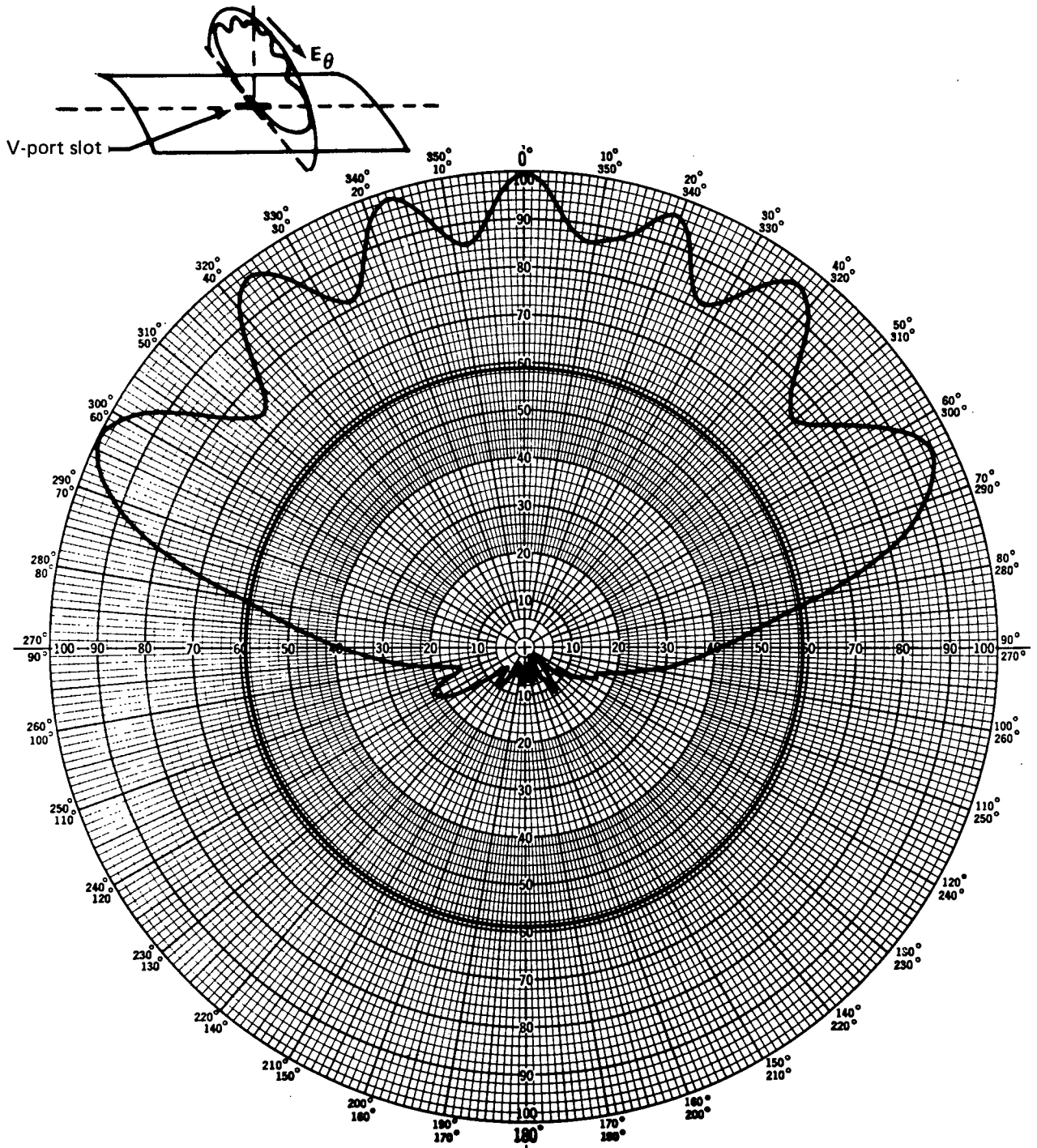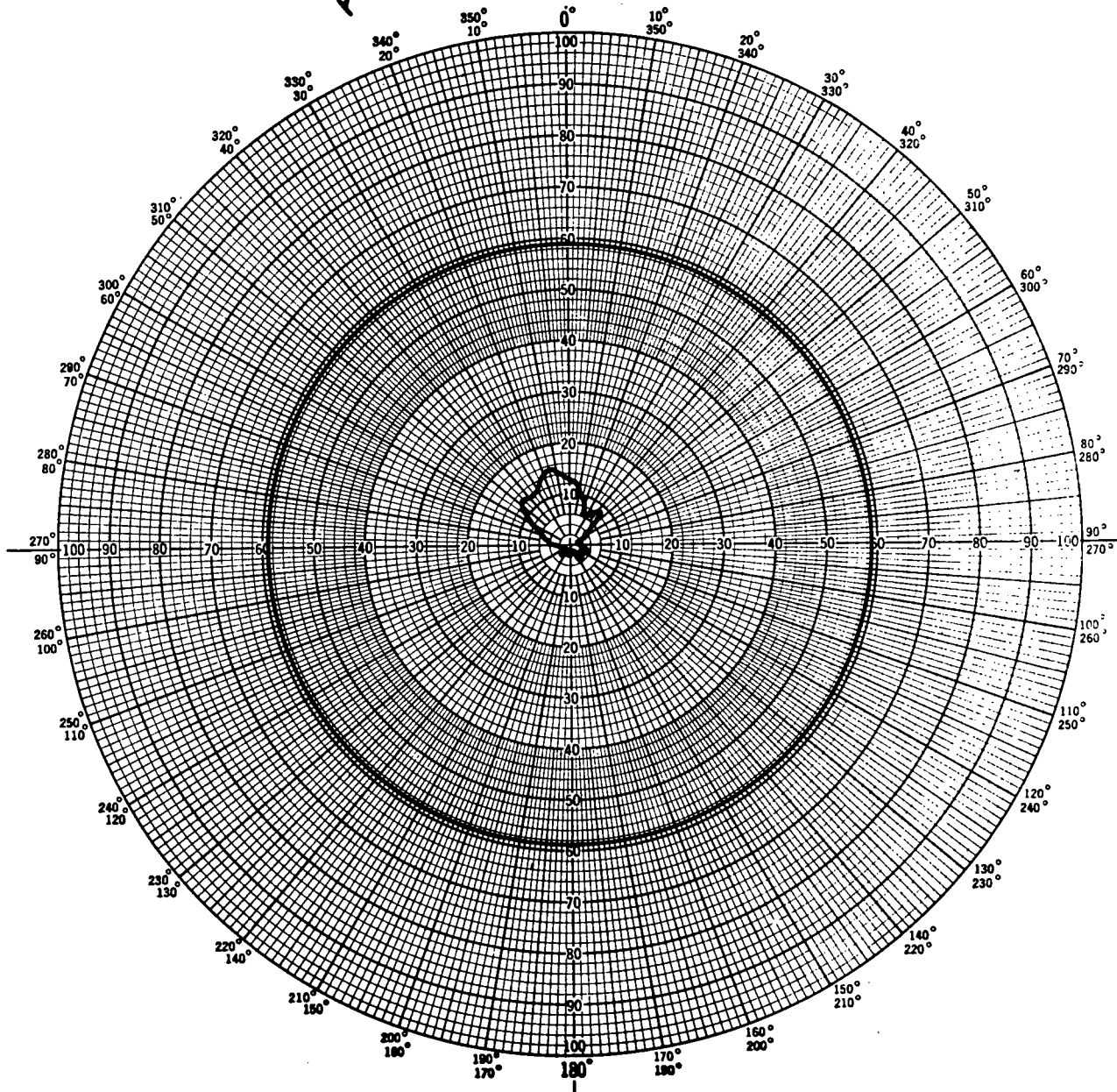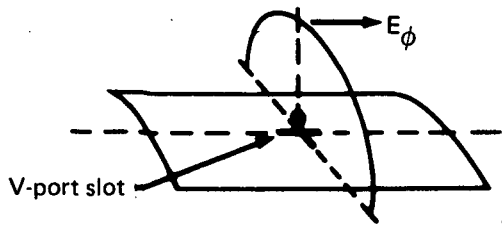Antenna S/N: DOT-TSC-003

*Figure 38.—Orthogonal-Mode Crossed-Slot Antenna E-Plane Pattern on H-Port Slot,
Principal Polarization*
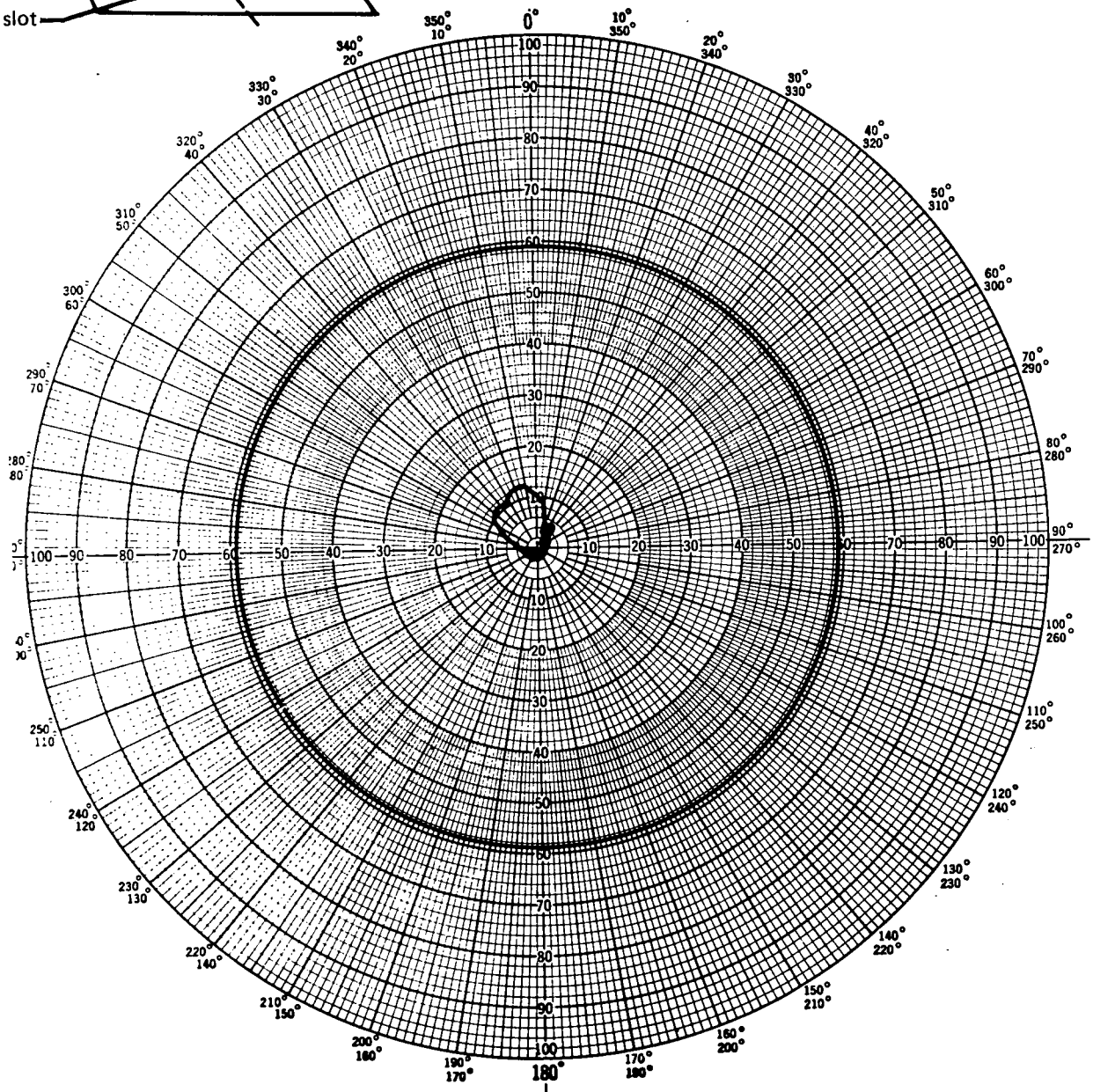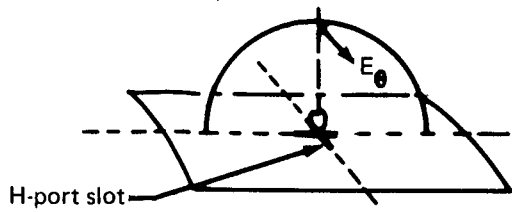
Maximum gain: 4.6 dB
Curve plotted in voltage
Variable angle ϕ
Constant angle $\theta = 90°$

Polarization: E_θ
Frequency: 1600 MHz
Antenna location: 4-ft-square ground plane
Antenna S/N: DOT-TSC-003

Figure 39.—Orthogonal-Mode Crossed-Slot Antenna E-Plane Pattern on
H-Port Slot, Cross Polarization
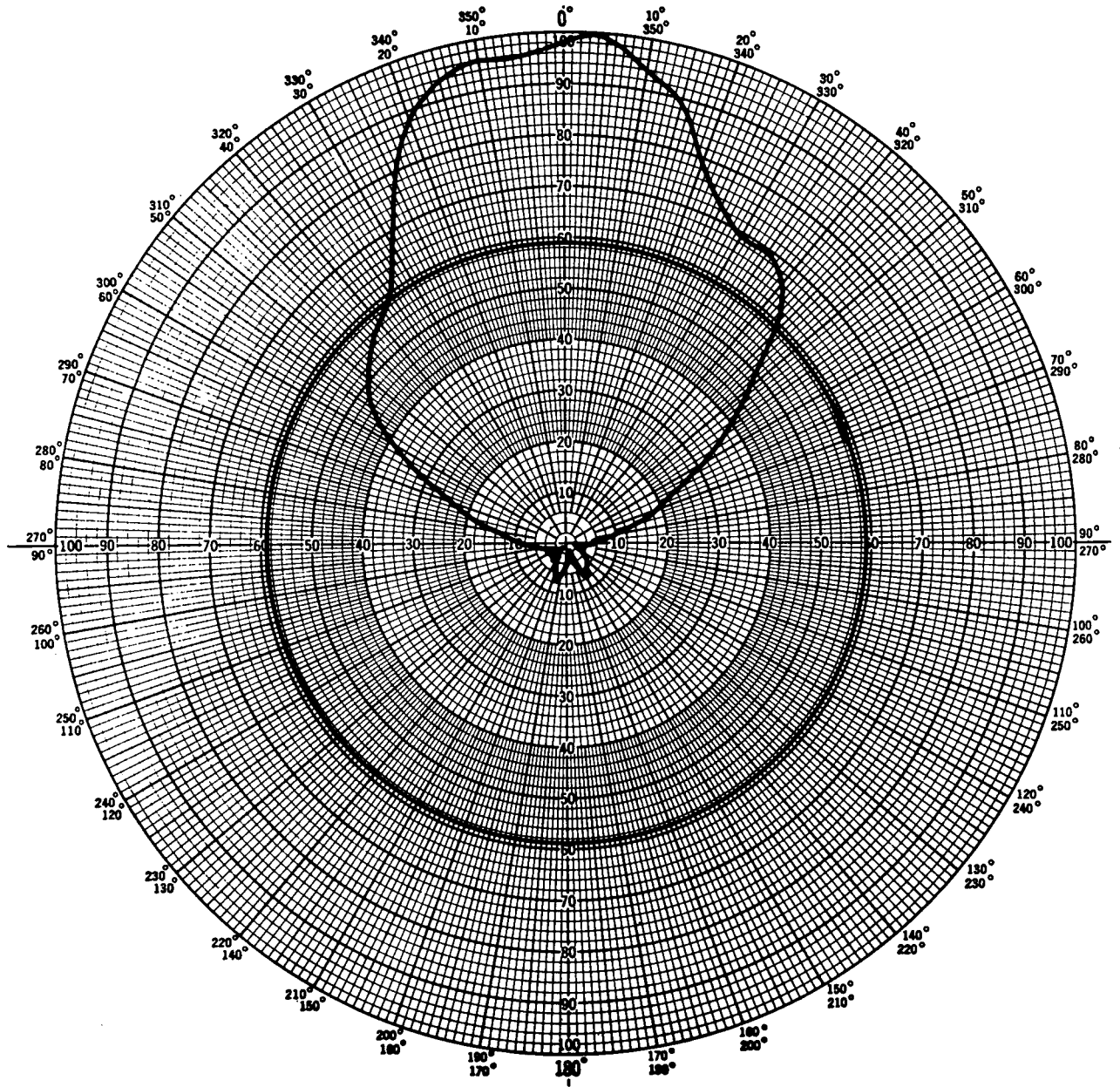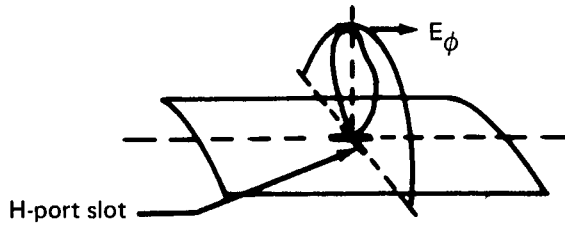
55

Maximum gain: 4.6 dB   Polarization: E
Curve plotted in voltage   Frequency: 1600 MHz
Variable angle θ Antenna location: 4-ft-square ground plane
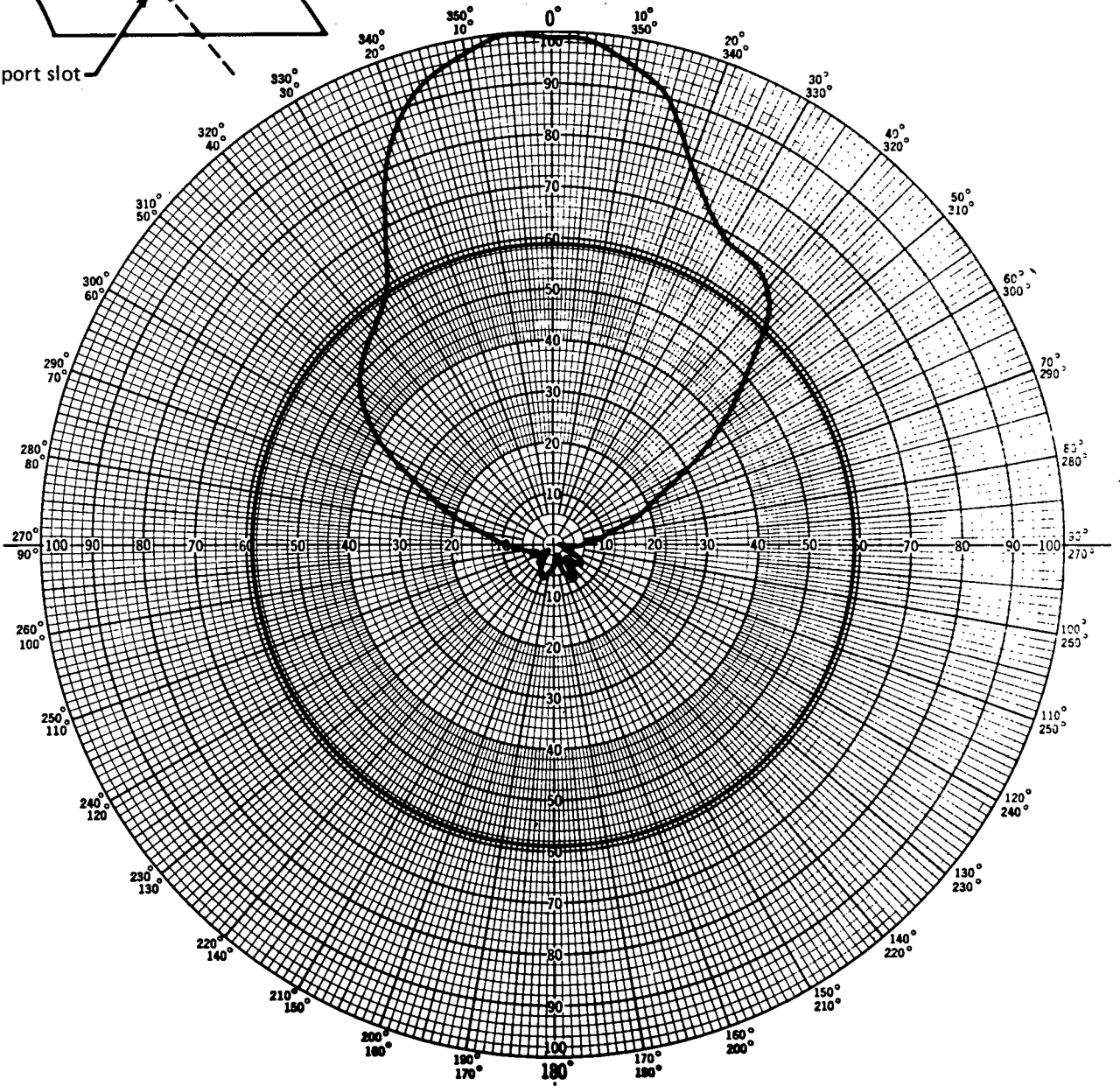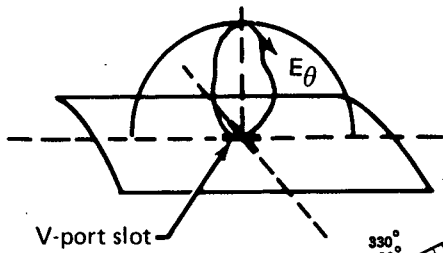Constant angle $\phi = 90°$ Antenna S/N: DOT-TSC-003

*Figure 40.—Orthogonal-Mode Crossed-Slot Antenna H-Plane Pattern
on H-Port Slot, Principal Polarization*
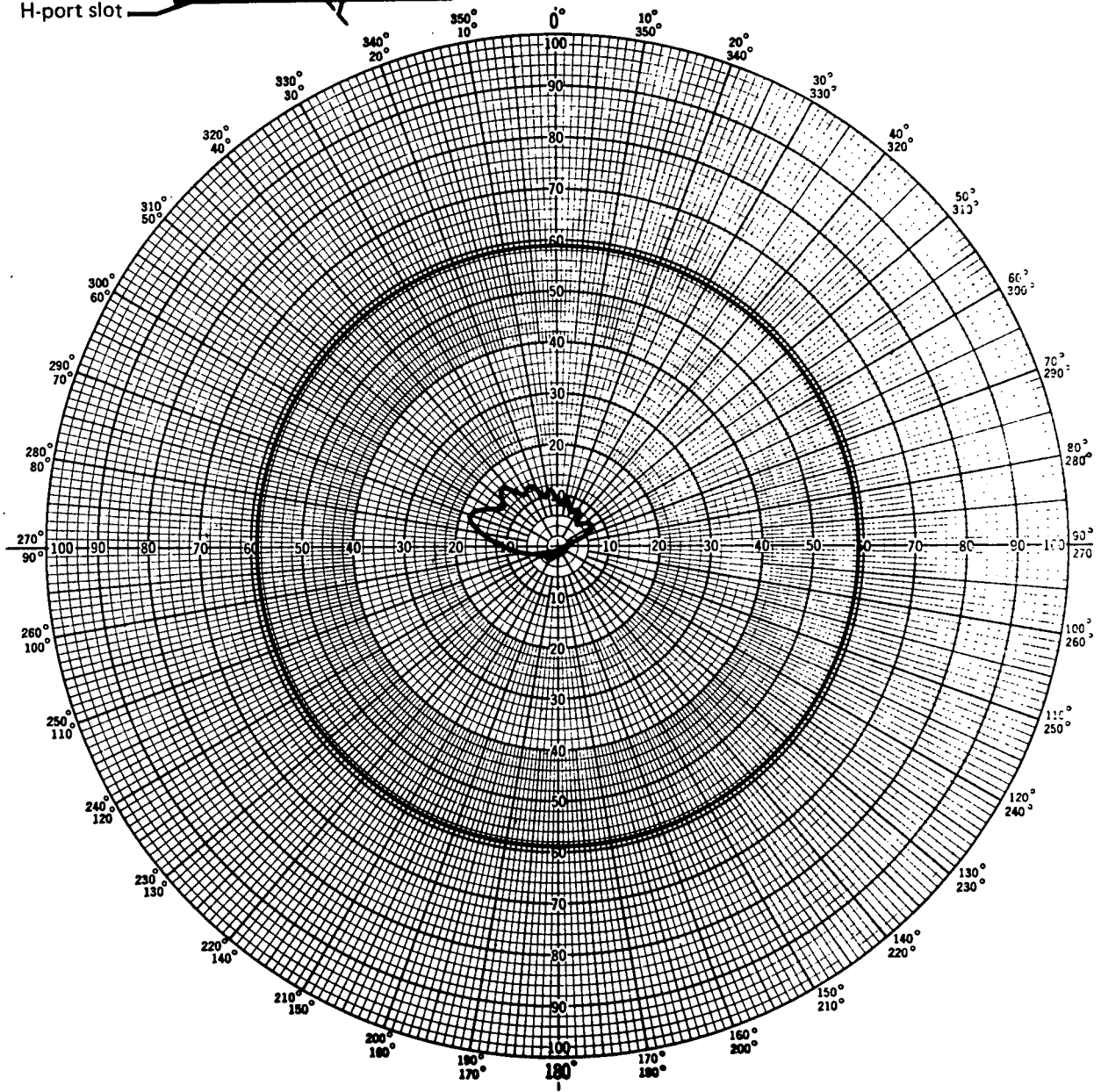
Maximum gain: 4.6 dB
Curve plotted in voltage
Variable angle θ
Constant angle $\phi = 90°$

Polarization: E_θ
Frequency: 1600 MHz
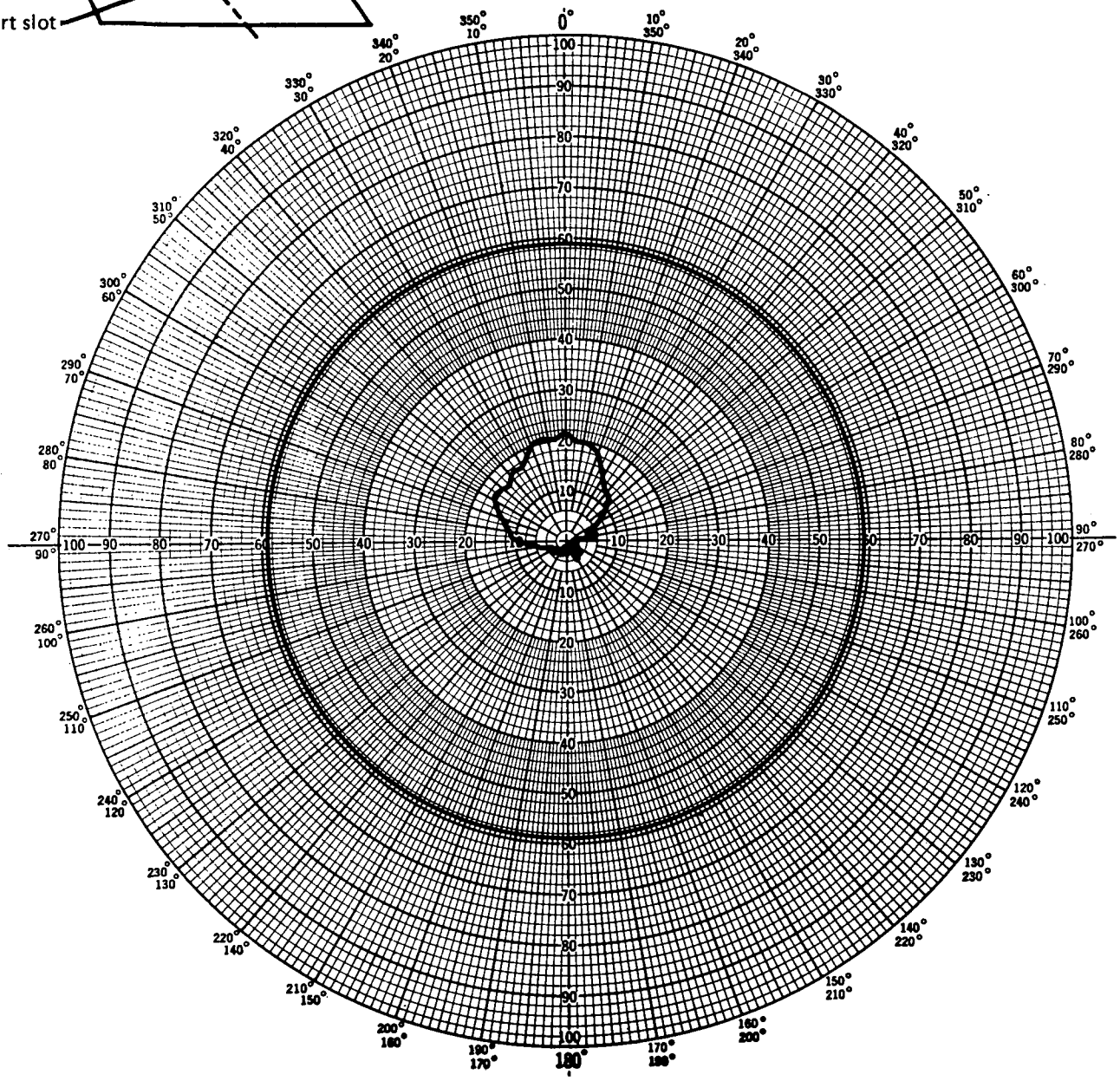Antenna location: 4-ft-square ground plane
Antenna S/N: DOT-TSC-003

Figure 41.—Orthogonal-Mode Crossed-Slot Antenna H-Plane Pattern on H-Port Slot,
Cross Polarization

Maximum gain: 4.6 dB
Curve plotted in voltage
Variable angle θ
Constant angle $\phi = 90°$

Polarization: E_θ
Frequency: 1600 MHz
Antenna location: 4-ft-square ground plane
Antenna S/N: DOT-TSC-003

*Figure 42.—Orthogonal-Mode Crossed-Slot Antenna E-Plane Pattern on V-Port Slot,
Principal Polarization*

Maximum gain: 4.6 dB
Curve plotted in voltage
Variable angle θ
Constant angle $\phi = 90°$

Polarization: E_ϕ
Frequency: 1600 MHz
Antenna location: 4-ft-square ground plane
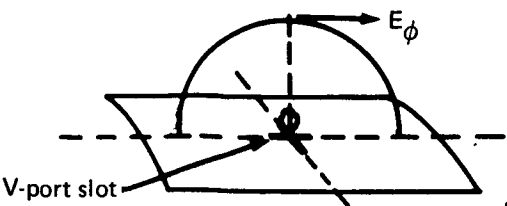Antenna S/N: DOT-TSC-003

Figure 43.—Orthogonal-Mode Crossed-Slot Antenna E-Plane Pattern on
V-Port Slot, Cross Polarization

Maximum gain: 4.6 dB
Curve plotted in voltage
Variable angle ϕ
Constant angle $\theta = 90°$

Polarization: E_θ
Frequency: 1600 MHz
Antenna location: 4-ft-square ground plane
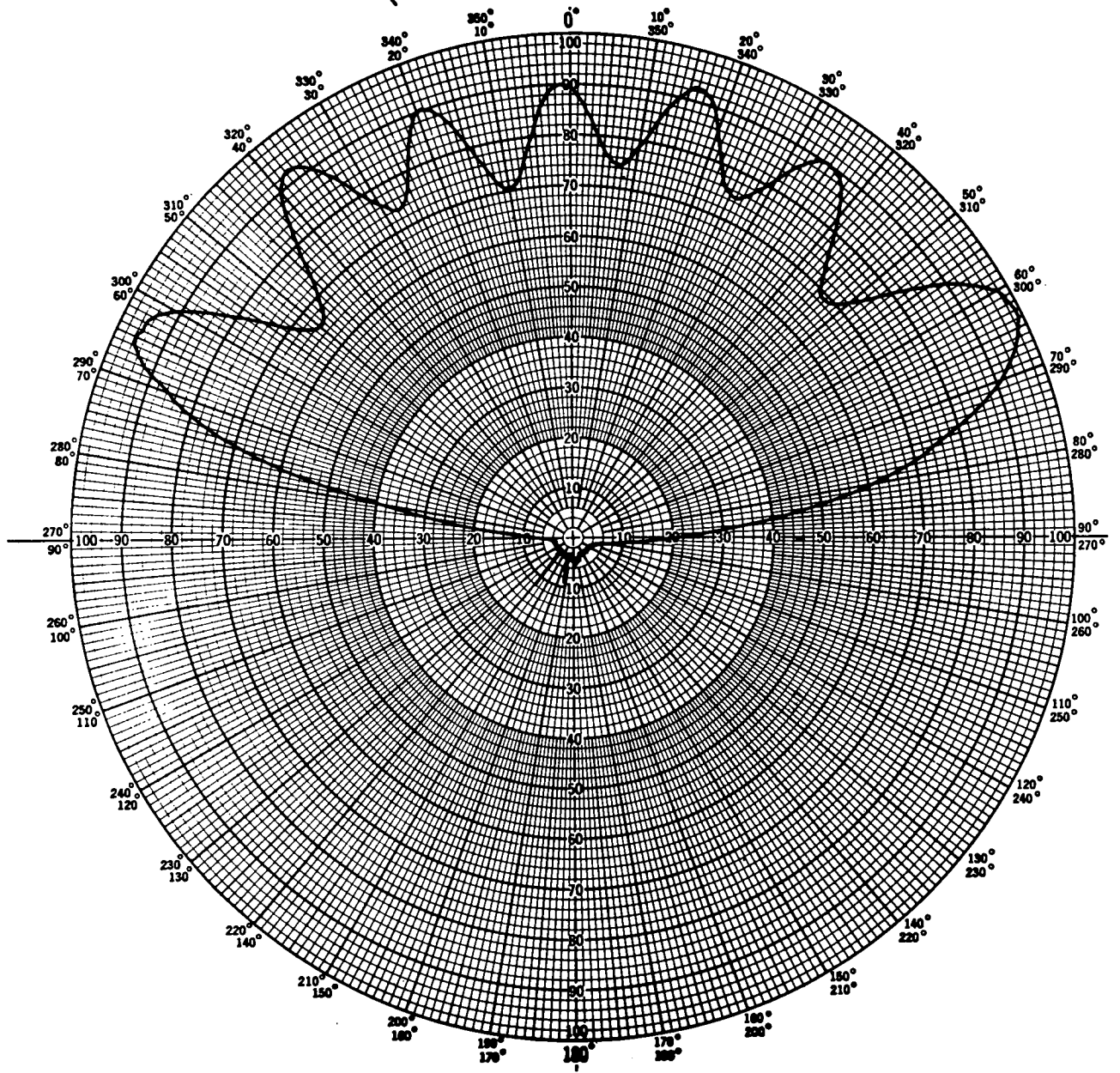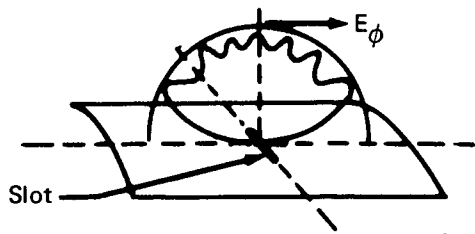Antenna S/N: DOT-TSC-003

Figure 44.— Orthogonal-Mode Crossed-Slot Antenna H-Plane Pattern on V-Port Slot, Principal Polarization

60

Maximum gain: 4.6 dB
Curve plotted in voltage
Variable angle ϕ
Constant angle $\theta = 90°$

Polarization: E_ϕ
Frequency: 1600 MHz
Antenna location: 4-ft-square ground panel
Antenna S/N: DOT-TSC-003

Figure 45.— Orthogonal-Mode Crossed-Slot Antenna H-Plane Pattern on V-Port Slot, Cross Polarization

61

Curve plotted in voltage   Polarization: E_ϕ
Variable angle ϕ Full-scale frequency: 1600 MHz
Constant angle $\theta = 90°$ Antenna location: 2.4-in.-square ground plane

Figure 46.— Orthogonal-Mode Crossed-Slot Antenna E-Plane Pattern on
1/20th-Scale Slot, Principal Polarization

Curve plotted in voltage
Variable angle ϕ
Constant angle $\theta = 90°$

Polarization: E_θ
Full-scale frequency: 1600 MHz
Antenna location: 2.4-in.-square ground plane

Figure 47.—Orthogonal-Mode Crossed-Slot Antenna E-Plane Pattern on
1/20-Scale Slot, Cross Polarization

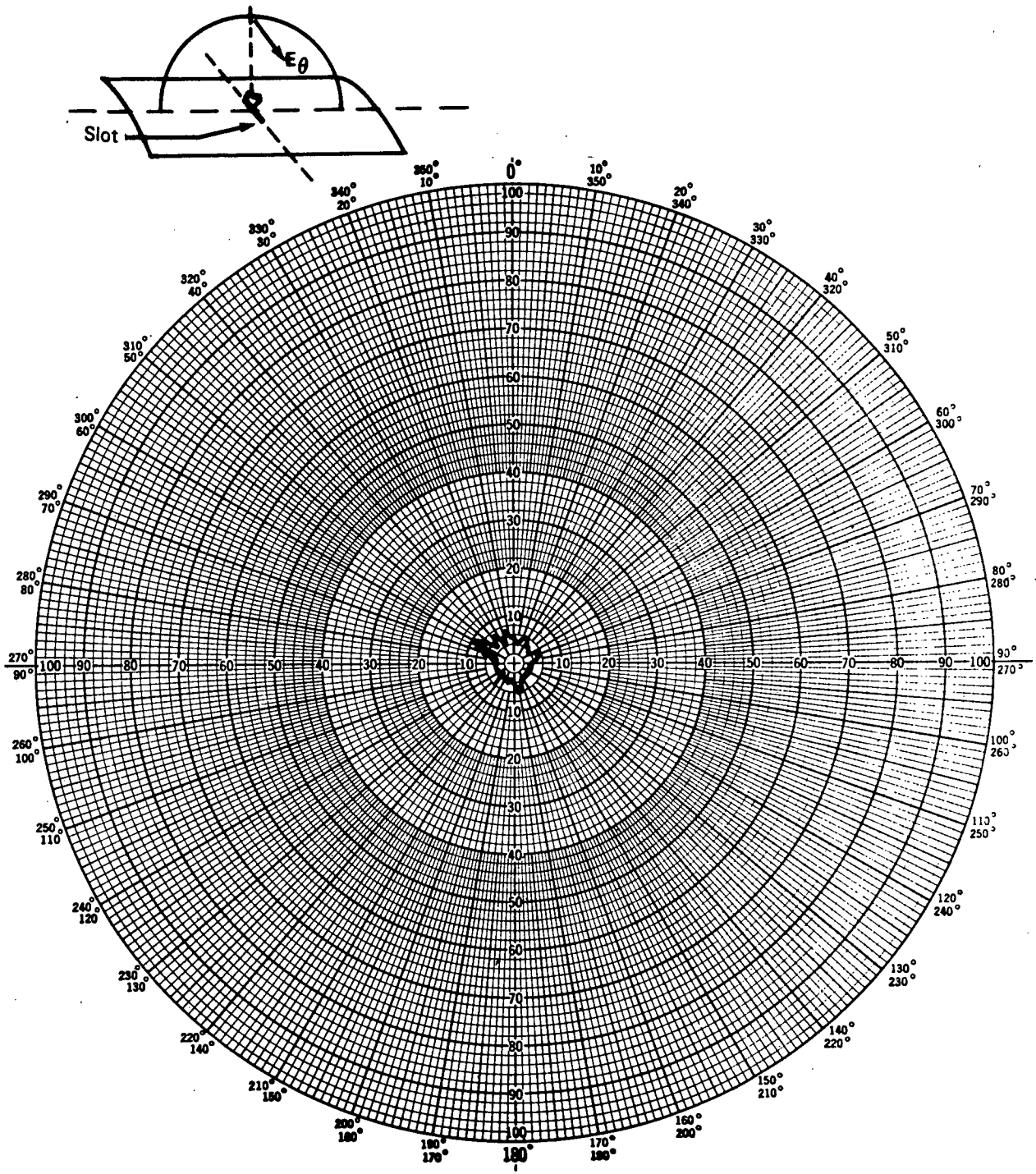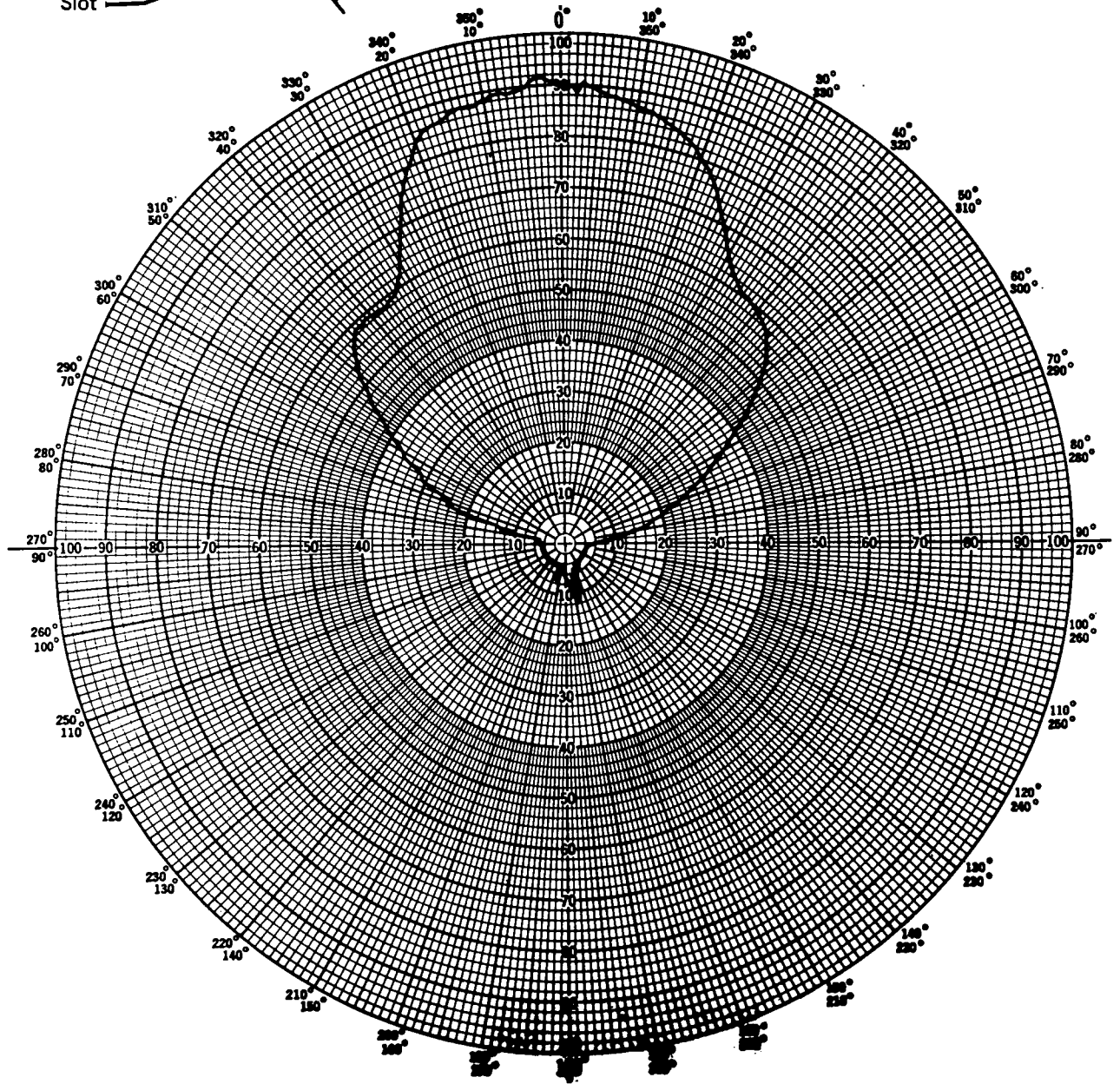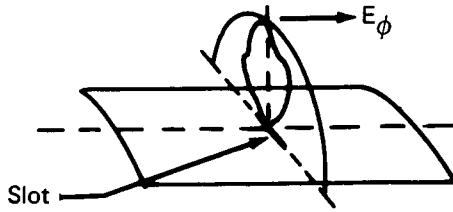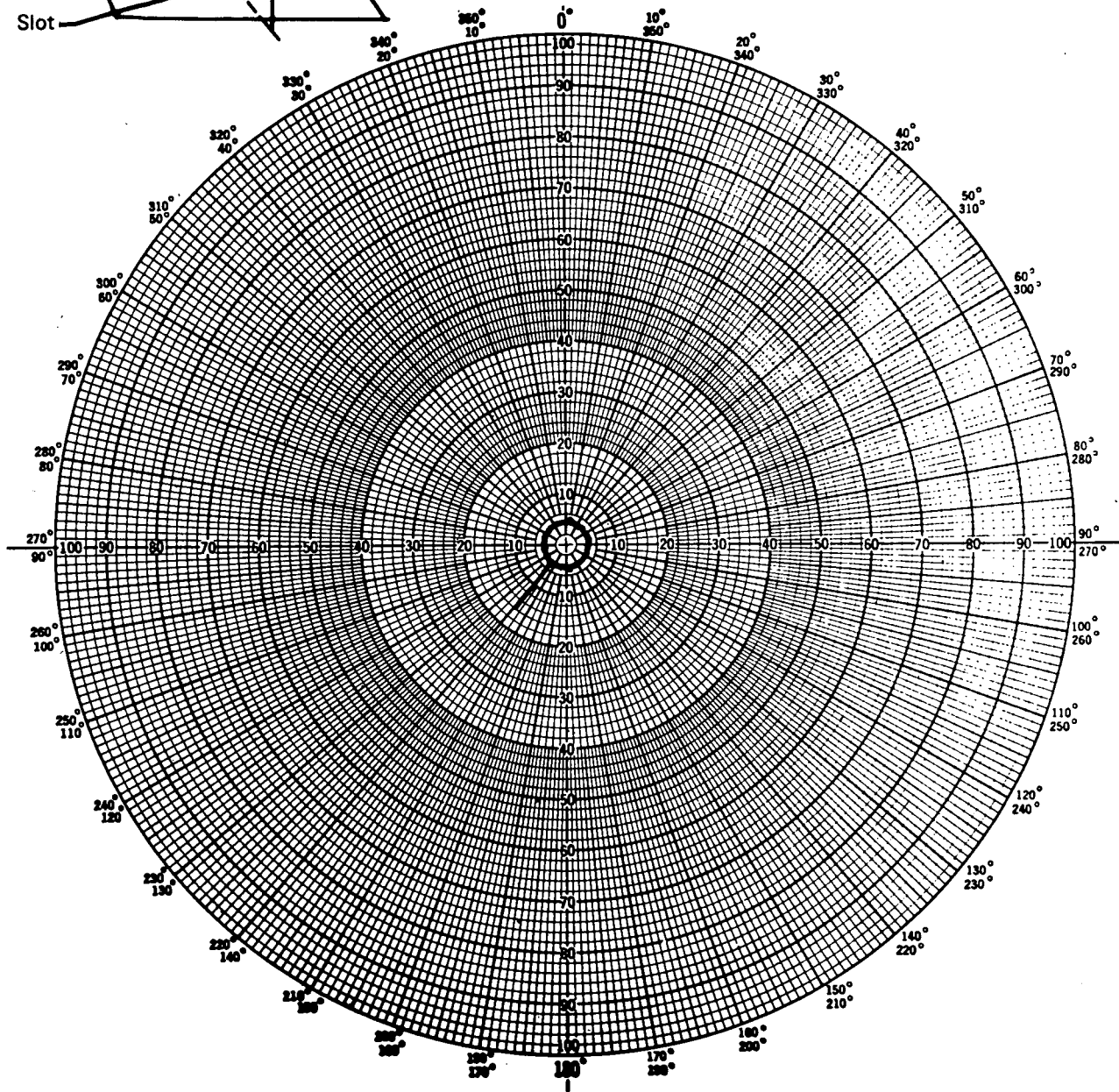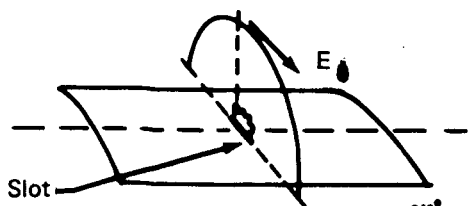Curve plotted in voltage
Variable angle θ
Constant angle $\phi = 90°$

Polarization: E_ϕ
Full-scale frequency: 1600 MHz
Antenna location: 2.4-in.-square ground plane

Figure 48.— Orthogonal-Mode Crossed-Slot Antenna H-Phane Pattern on 1/20th-Scale Slot, Principal Polarization

Curve plotted in voltage
Variable angle θ
Constant angle $\phi = 90°$

Polarization: Eθ
Full-scale frequency: 1600 MHz
Antenna location: 2.4-in.-square ground plane

*Figure 49.—Orthogonal-Mode Crossed-Slot Antenna H-Plane Pattern on
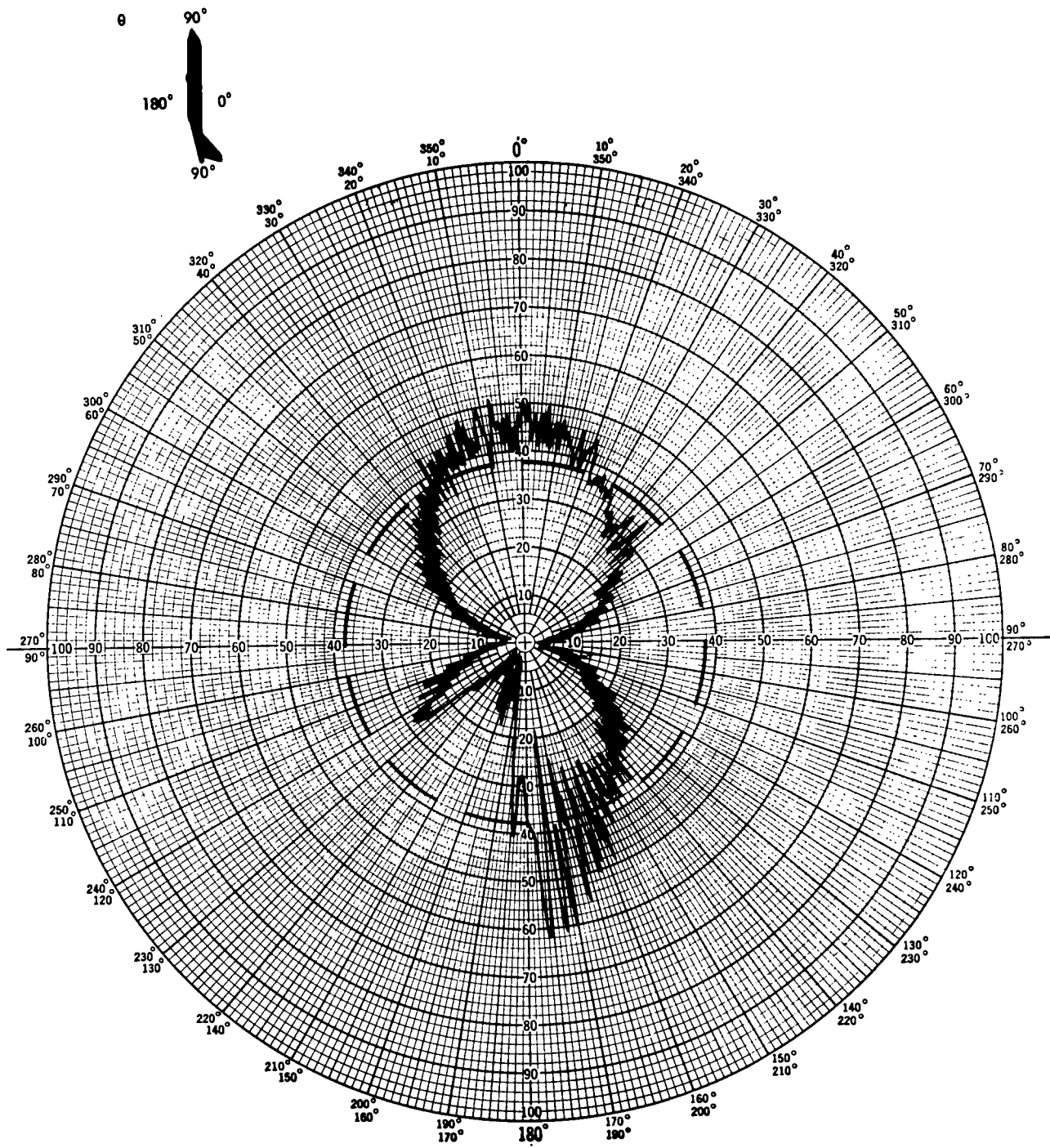1/20th-Scale Slot, Cross Polarization*

Maximum directivity: 8.5 dB
Curve plotted in voltage
Variable angle θ
Constant angle $\phi = 0°$

Polarization: Eϕ
Model scale: 1/20
Full-scale frequency: 1600 MHz
Convair 880 airplane
Antenna location: 78° left of top centerline at STA 422

Figure 50.—Orthogonal-Mode Crossed-Slot Antenna Pitch Plane Pattern on H-Port Slot, Principal Polarization

Maximum directivity: 8.5 dB
Curve plotted in voltage
Variable angle θ
Constant angle $\phi = 90°$
Polarization: E_ϕ

Model scale: 1/20
Full-scale frequency: 1600 MHz
Convair 880 airplane
Antenna location: 78° left of top centerline at STA 422

Figure 51.—Orthogonal-Mode Crossed-Slot Antenna Roll Plane Pattern on H-Port Slot, Principal Polarization
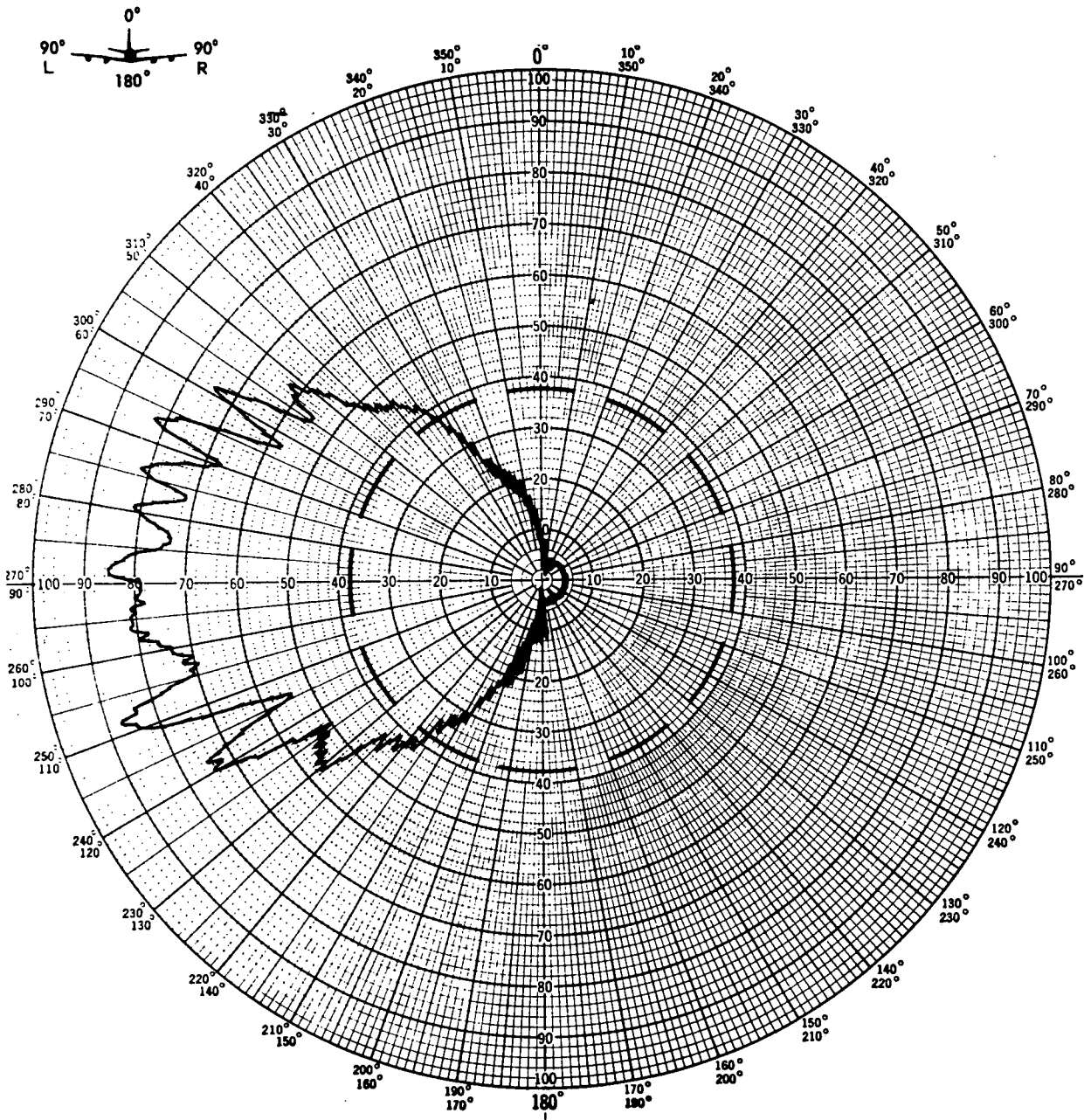
Maximum directivity: 8.5 dB
Curve plotted in voltage
Variable angle ϕ
Constant angle $\theta = 90°$
Polarization: E_ϕ

Model scale: 1/20
Full-scale frequency: 1600 MHz
Convair 880 airplane
Antenna location: 78° left of top centerline at STA 422

*Figure 52.— Orthogonal-Mode Crossed-Slot Antenna Yaw Plane Pattern on H-Port Slot,
Principal Polarization*

Maximum directivity: 5.68 dB
Curve plotted in voltage
Variable angle θ
Constant angle $\phi = 0°$
Polarization: E_θ

Model scale: 1/20
Full-scale frequency: 1600 MHz
Convair 880 airplane
Antenna location: 78° left of top centerline at STA 422

*Figure 53.—Orthogonal-Mode Crossed-Slot Antenna Pitch Plane Pattern on V-Port Slot,
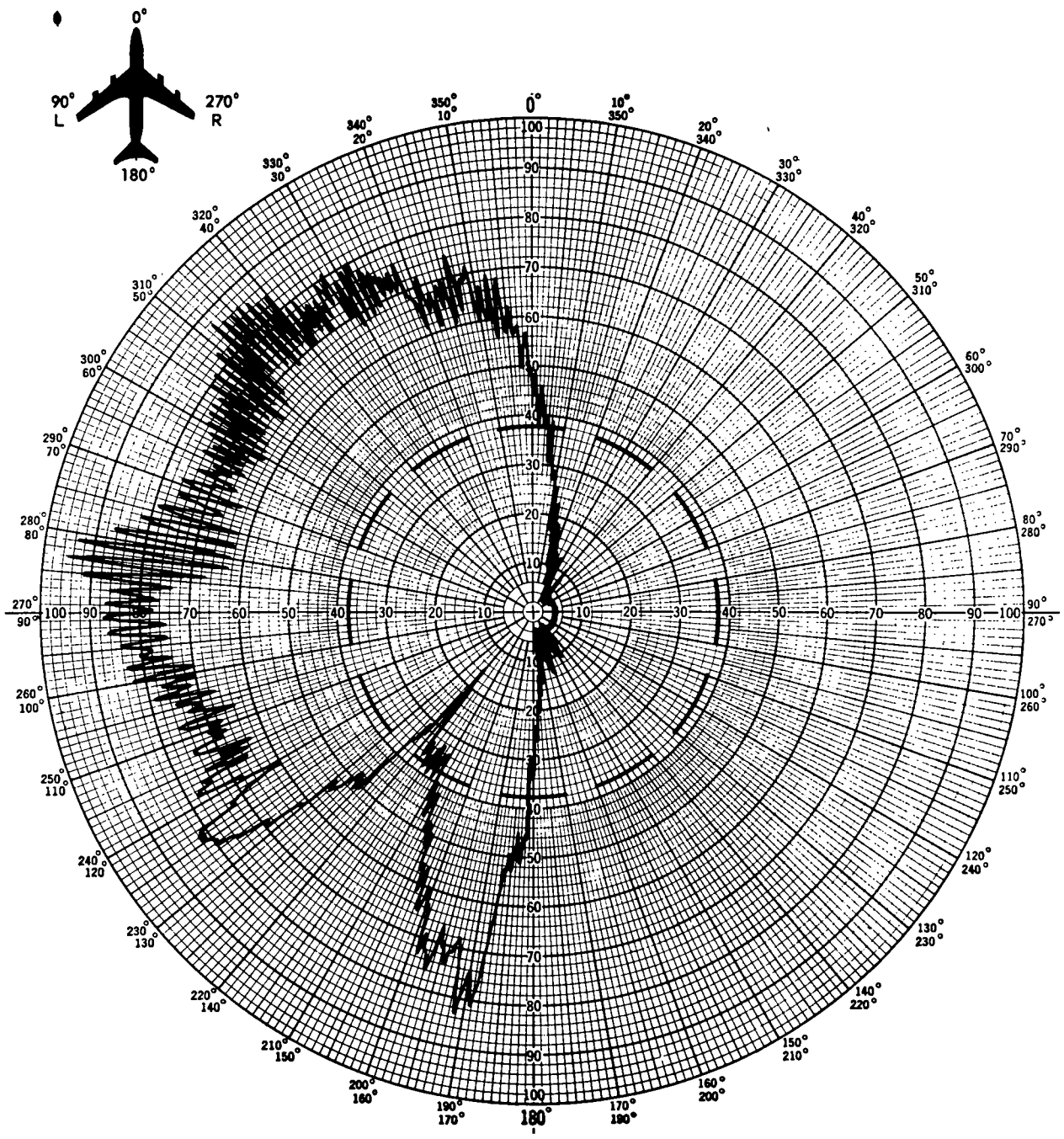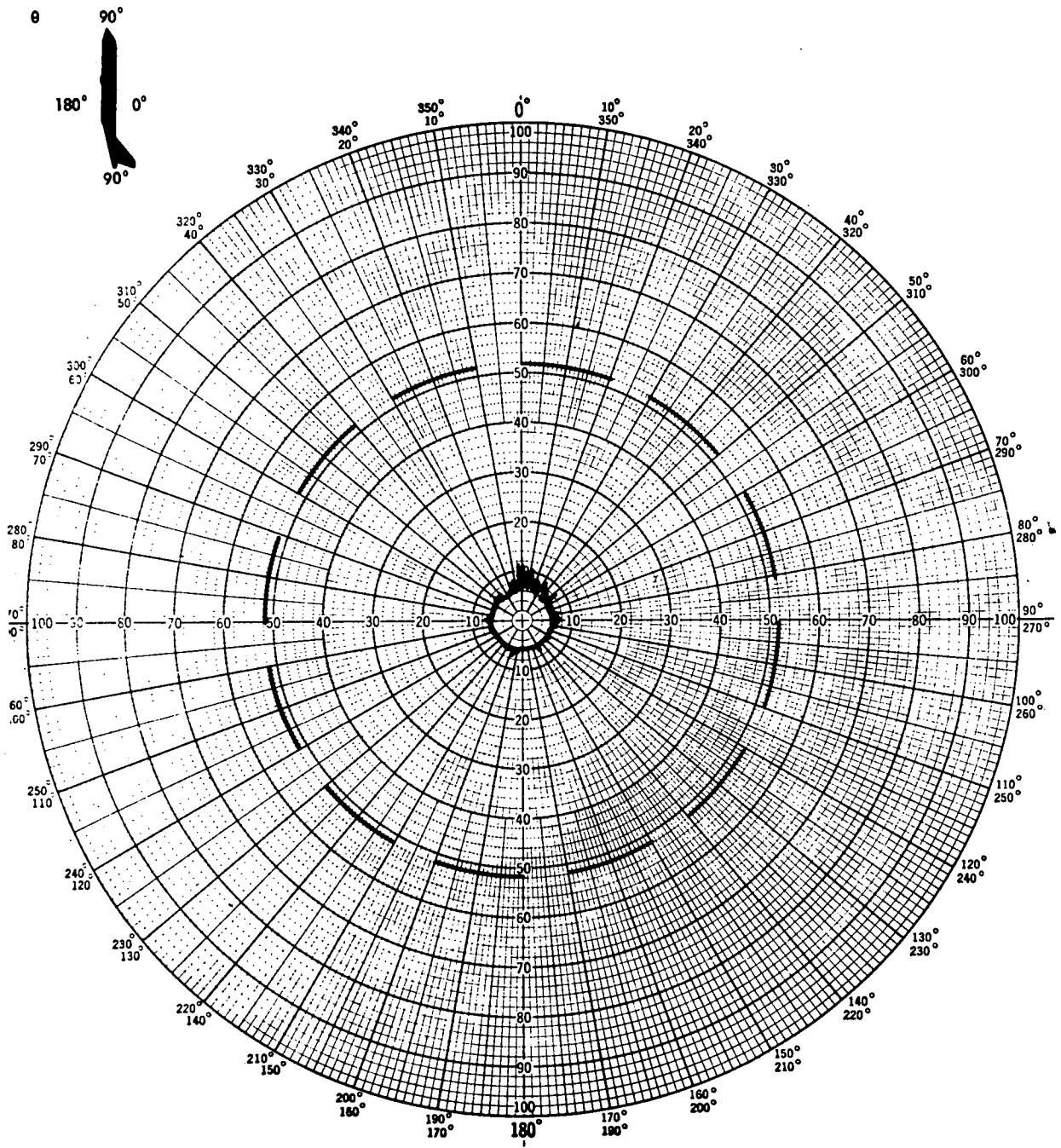Principal Polarization*

Maximum directivity: 5.68 dB   Model scale: 1/20
Curve plotted in voltage   Full-scale frequency: 1600 MHz
Variable angle θ Convair 880 airplane
Constant angle $\phi = 90°$ Antenna location: 78° left of top centerline at STA 422
Polarization: Eθ

Figure 54.—Orthogonal-Mode Crossed-Slot Antenna Roll Plane Pattern on V-Port Slot,
Principal Polarization

70

Maximum directivity: 5.68 dB
Curve plotted in voltage
Variable angle ϕ
Constant angle $\theta = 90°$
Polarization: E_θ

Model scale: 1/20
Full-scale frequency: 1600 MHz
Convair 880 airplane
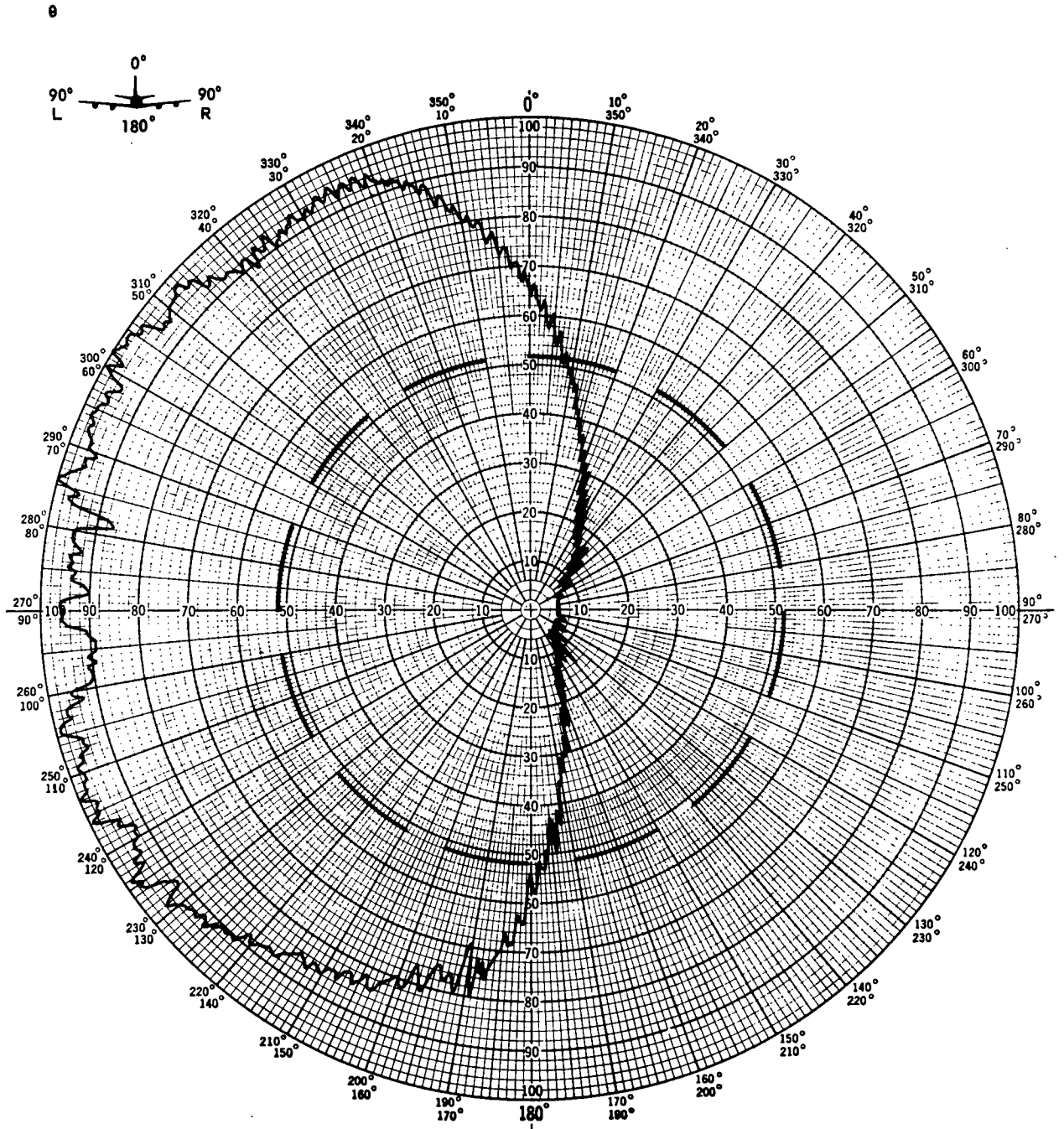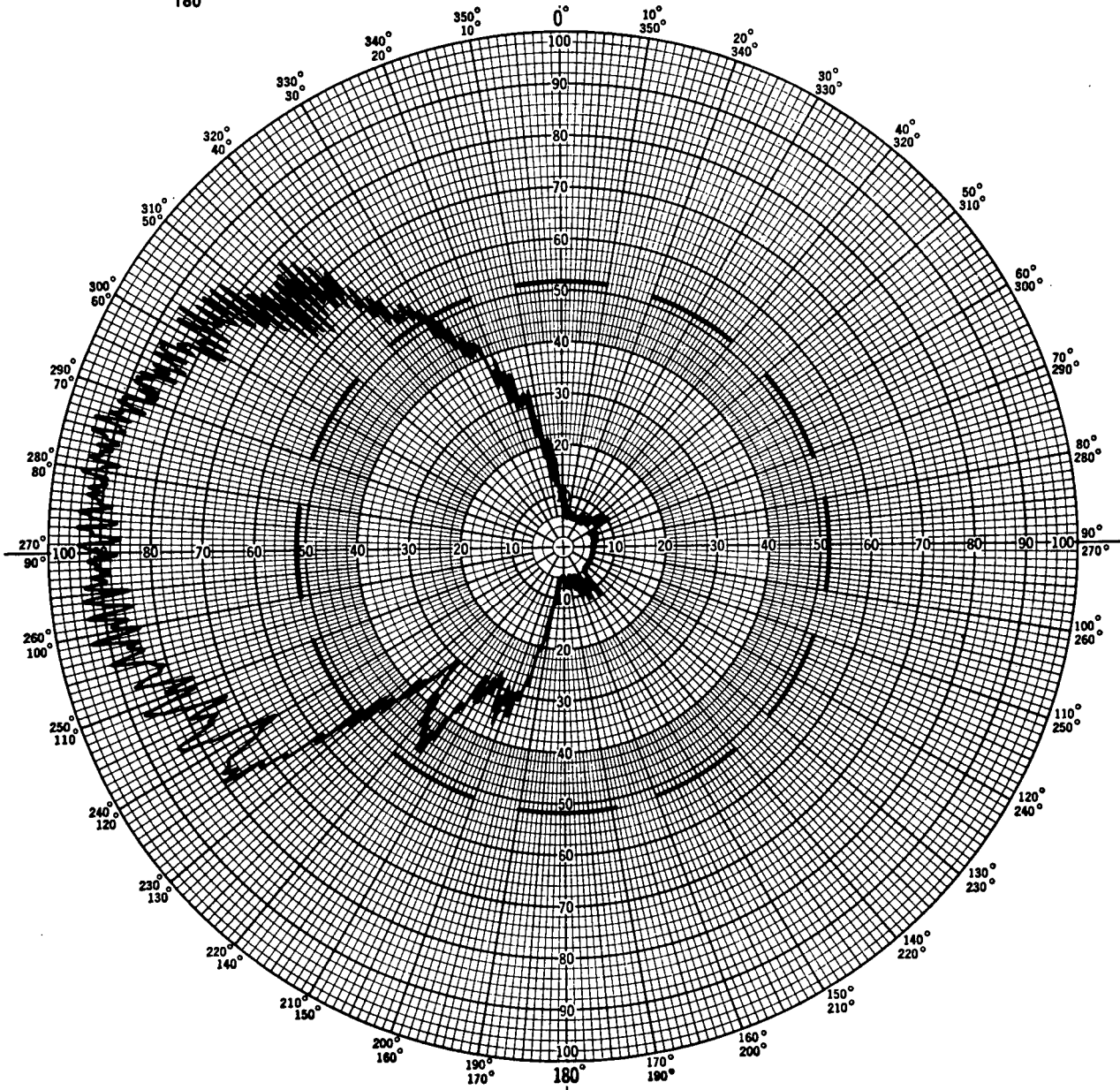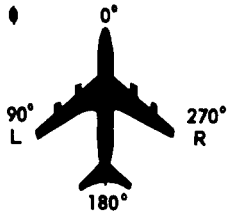Antenna location: 78° left of top centerline at STA 422

*Figure 55.—Orthogonal-Mode Crossed-Slot Antenna Yaw Plane Pattern
on V-Port Slot, Principal Polarization*
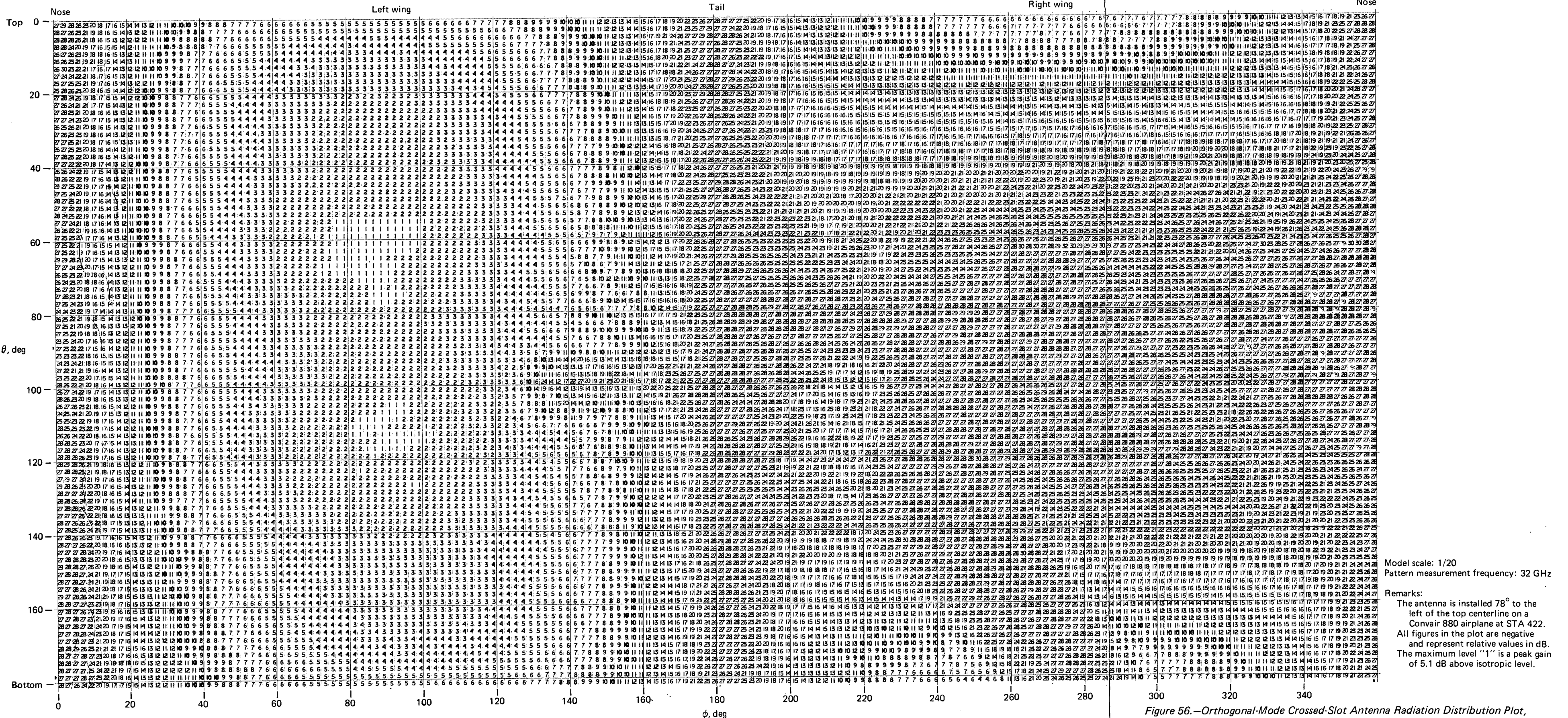
Figure 56.—Orthogonal-Mode Crossed-Slot Antenna Radiation Distribution Plot, Vertical Principal Polarization Measured at V-Port
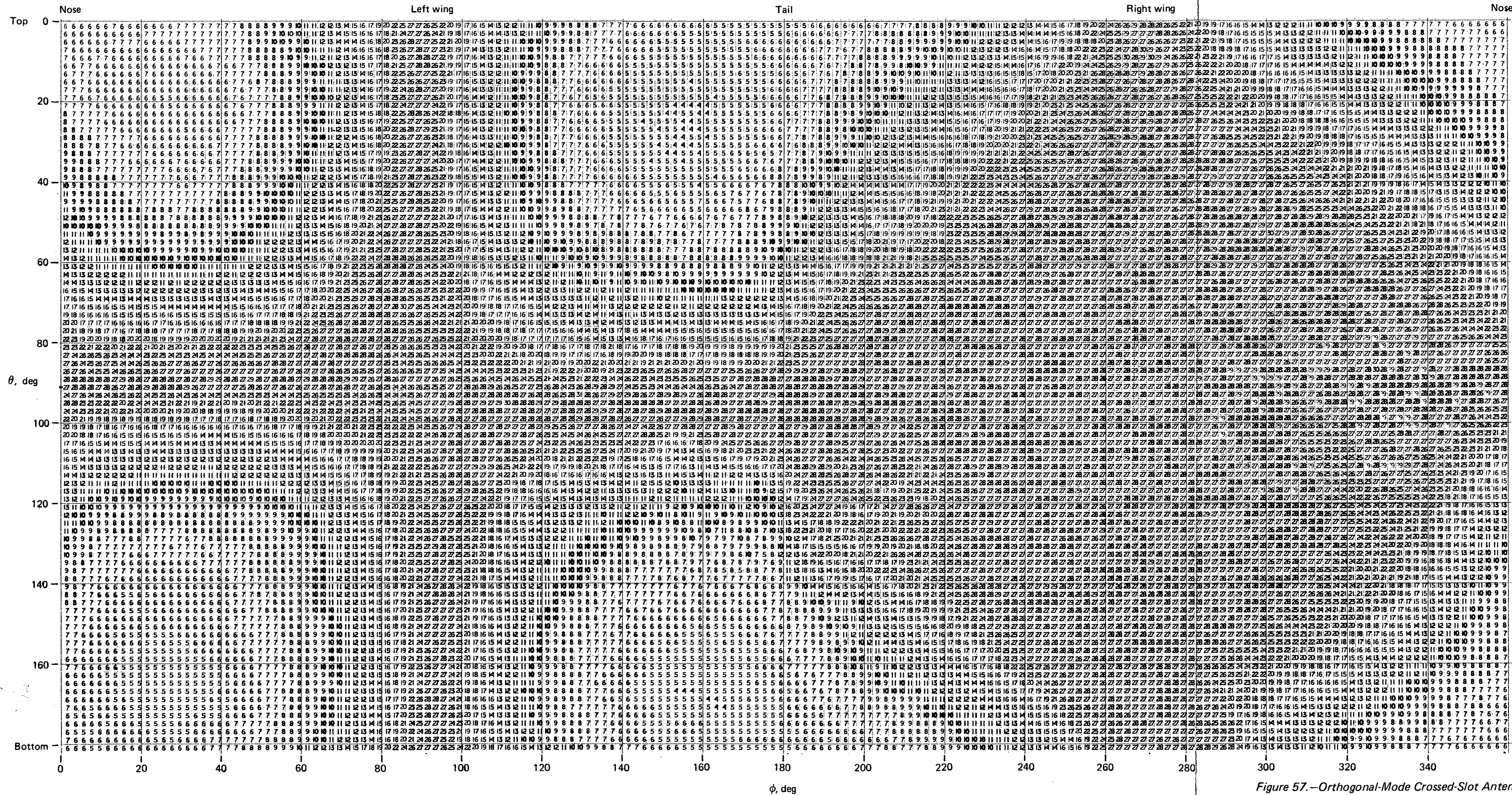
Model scale: 1/20
Pattern measurement frequency: 32 GHz

Remarks:
The antenna is installed 78° to the left of the top centerline on a Convair 880 airplane at STA 422. All figures in the plot are negative and represent relative values in dB. The maximum level "1" is a peak gain of 5.1 dB above isotropic level.

73

Top 0

Nose   Left wing   Tail   Right wing   Nose

θ, deg

20

40

60

80

100

120

140

160

Bottom

0   20   40   60   80   100   120   140   160   180   200   220   240   260   280   300   320   340

φ, deg

Model scale: 1/20
Pattern measurement frequency: 32 GHz

Remarks:
The antenna is installed 78° to the
left of the top centerline on a
Convair 880 airplane at STA 422.
All figures in the plot are negative
and represent relative values in dB.
The maximum level "1" is a peak gain
of 5.1 dB above isotropic level.

*Figure 57.—Orthogonal-Mode Crossed-Slot Antenna Radiation Distribution Plot,
Horizontal Cross Polarization Measured at V-Port*

75

Nose Left wing Tail Right wing Nose

Top 0

θ, deg

20

40

60

80

100

120

140

160

Bottom

0 20 40 60 80 100 120 140 160 180 200 220 240 260 280 300 320 340

φ, deg

Model scale: 1/20
Pattern measurement frequency: 32 GHz

Remarks:
The antenna is installed 78° to the left of the top centerline on a Convair 880 airplane at STA 422. All figures in the plot are negative and represent relative values in dB. The maximum level "0" is a peak gain of 7.9 dB above isotropic level.

Figure 58.—Orthogonal-Mode Crossed-Slot Antenna Radiation Distribution Plot, Horizontal Principal Polarization Measured at H-Port
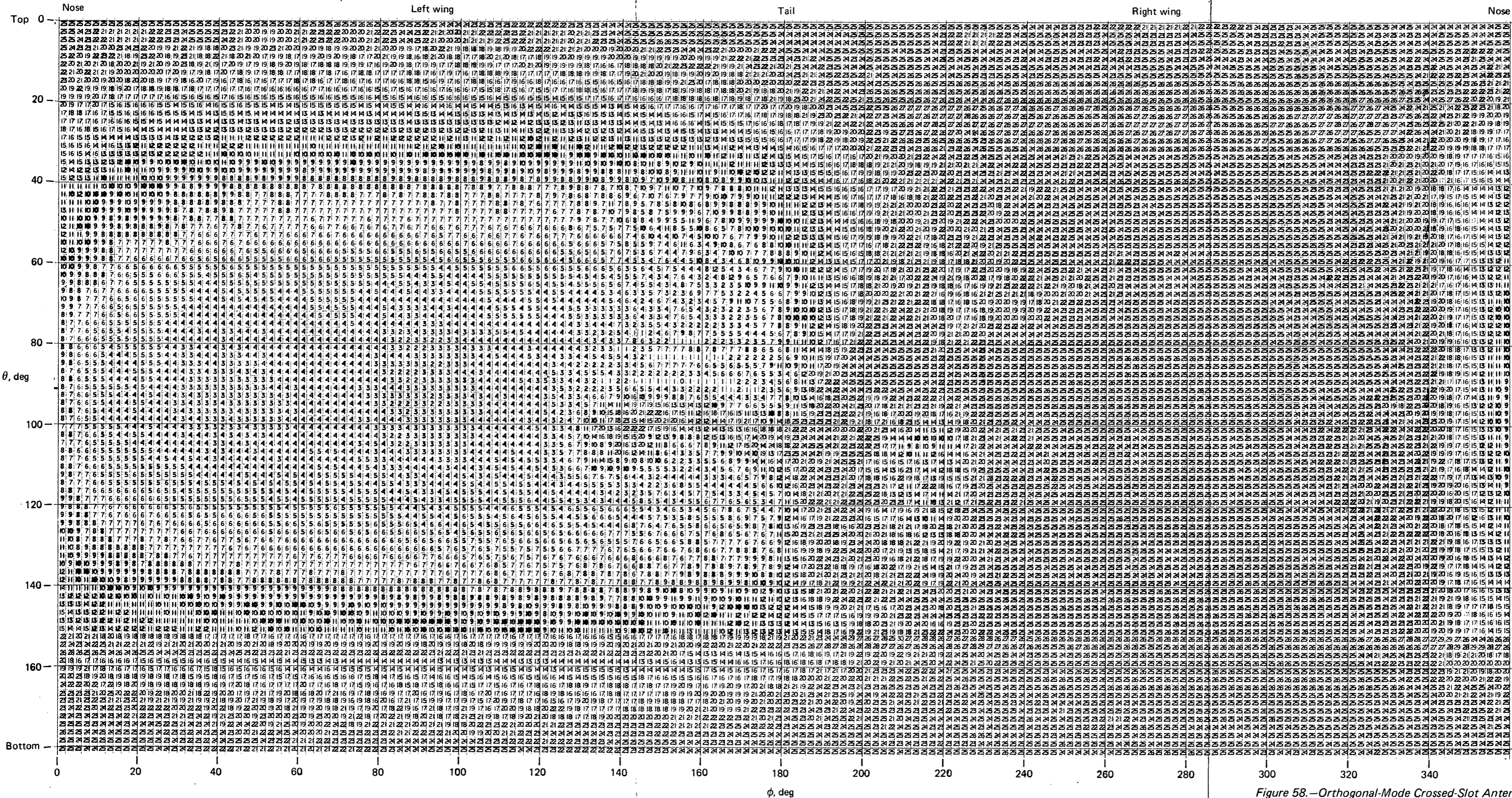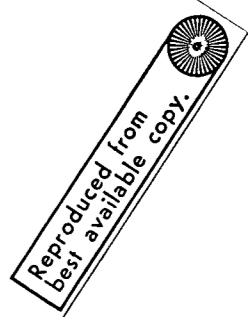
77

Model scale: 1/20
Pattern measurement frequency: 32 GHz

Remarks:
The slot antenna is installed 78° to the
left of the top centerline on a
Convair 880 airplane at STA 422.
All figures in the plot are negative and
represent relative values in dB.
The maximum level "0" is a peak gain
of 7.9 dB above isotropic level.

Figure 59.—Orthogonal-Mode Crossed-Slot Antenna Radiation Distribution Plot,
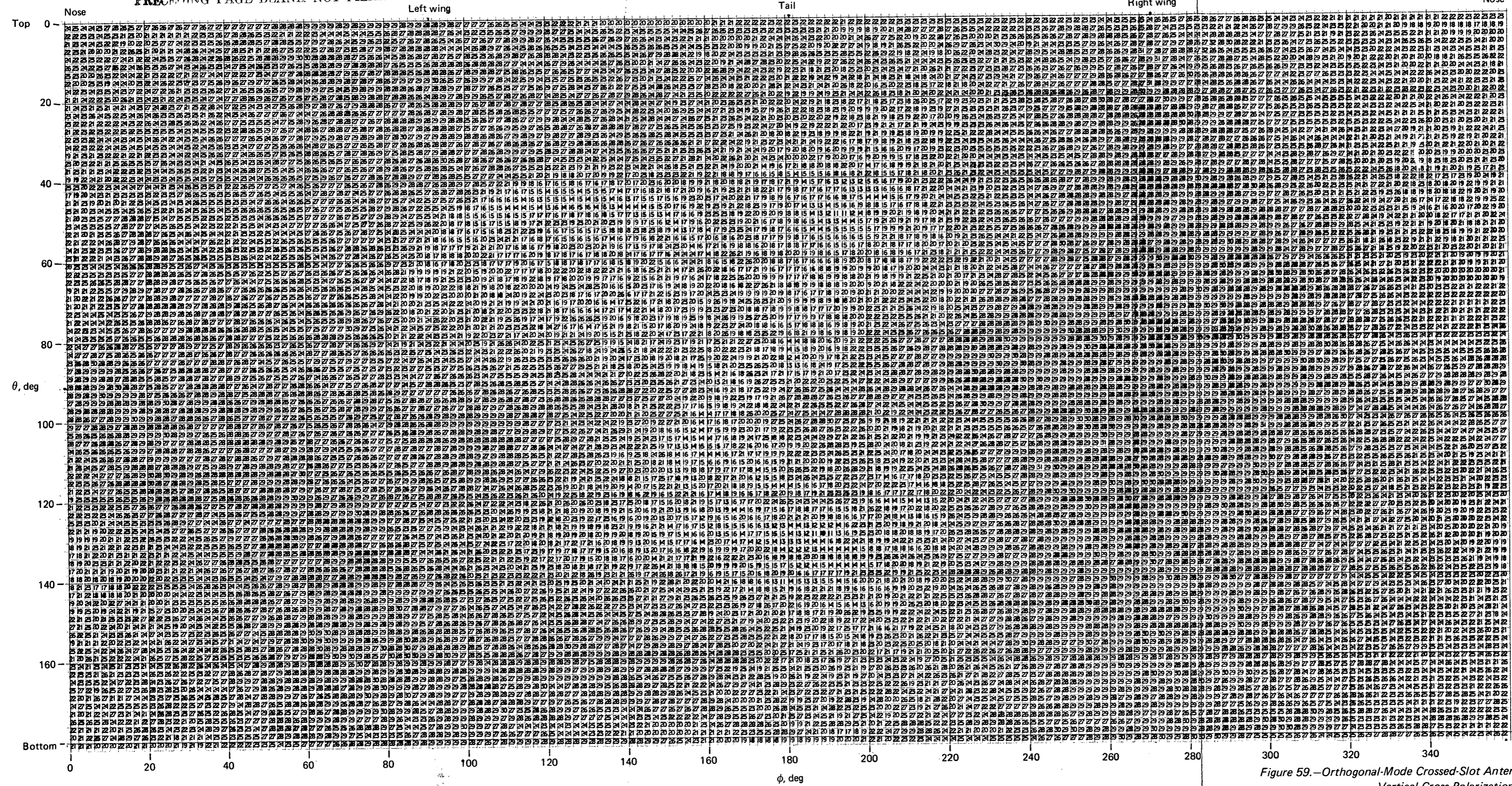Vertical Cross Polarization Measured at H-Port

79

VHF CROSSED-LOOP ANTENNA

Introduction

The VHF crossed-loop antenna is intended to provide upper hemisphere VHF satellite coverage when installed on the top centerline of the fuselage of a Convair 880 airplane. The basic antenna consists of two half loops housed under an aerodynamically shaped fiberglass radome. A switching scheme using a quadrature hybrid is included with the antenna design to select either right- or left-hand circular polarization. The antenna is designed for a maximum power input of 500 watts of VHF CW power at 45,000-ft altitude. Figure 60 shows the antenna furnished by this contract installed on a mocked-up section of fuselage.

The weight of the antenna is 11.5 lb. Aerodynamic drag calculations on the radome indicate a drag weight penalty of 5 lb at 35,000-ft altitude at Mach 0.85 when installed at station (STA) 1130 on a 707-type airplane. The production antenna furnished under this contract is intended to work at the center frequencies of 134.05 MHz (receive) and 135.7 MHz (transmit). Boeing drawings that cover the installation of the antenna at STA 590 on a Convair 880 airplane are:

65-82127, "Fairing Instl—VHF Crossed-Loop Antenna"

65-63483, "Pan—Components VHF Crossed-Loop Antenna"

65-63487, "Zee Assy—VHF Crossed-Loop Antenna"

Theory of Crossed-Loop Antenna

To provide upper hemisphere coverage, a low-gain basic radiating element is chosen. A small half loop with a constant current distribution will be omnidirectional in its E-plane, i.e., the plane of the electric field E. Arraying two half loops perpendicular to each other and feeding them in phase quadrature will yield a perfectly circularly polarized radiation pattern directly overhead which becomes linear at the horizon, since only the vertical electric field can exist at the surface of a conductor, i.e., the skin of the airplane. Figure 61 is a pitch plane pattern of a 1/20th-scale crossed loop installed on the top centerline of a 707-type airplane. The pattern was taken using a rotating linear polarization which shows the axial ratio at all points of the pattern.

The axial ratio is defined as the ratio of the maximum electric field to the minimum electric field, as measured by a linear antenna that can be rotated in time. In general, as the linear antenna is rotated, the response will be a varying voltage at the output of the antenna. This is because the most general type of radiation is elliptical and can be thought of as being generated by both right- and left-hand circular polarization. The maximum electric field E_{max} will be at the angle where the right- and left-hand circular fields add in phase producing $E_{max} = E_{right} + E_{left}$. The minimum electric field E_{min} is measured at the angle where the right- and left-hand circular fields subtract; $E_{min} = E_{right} - E_{left}$. E_{max} corresponds to the semimajor axis of the polarization ellipse, and E_{min} corresponds to the semiminor axis of the polarization ellipse. The axial ratio in dB is defined by

$$\text{Axial ratio} = 20 \log_{10} \frac{E_{max}}{E_{min}} = 20 \log_{10} \frac{E_{right} + E_{left}}{E_{right} - E_{left}}$$

Figure 61 was obtained by rotating a linearly polarized illuminating antenna at a rate such that the maximum and minimum electric fields were recorded at all points of the pitch-plane pattern. The low-axial-ratio (nearly perfect circular radiation) areas are directly above the aircraft. Here E_{max} and E_{min} are nearly the same. As one moves toward the nose or the tail, the axial ratio becomes larger, as indicated by the large excursions of the recording pen.

Early in the development of this antenna a 1/10th-scale half loop was built and tested to check the basic radiating element's current distribution. Figure 62 is an E-plane cut of the 1/10th-scale half loop installed on a 4-ft-square ground plane. The finite size of the ground plane causes the pattern to be lifted somewhat from the horizon, but the pattern does show a nearly constant radiation pattern (within 2 dB) over approximately 150° of beamwidth.

Impedance Matching and Physical Construction

Figure 63 is an equivalent circuit of a half-loop element together with its matching elements.

The inherent impedance of a half-loop element consists of a radiation resistance (R) and a loop inductance (L). To match the loop, capacitance (C) is added in series with the loop to cancel its inductive reactance. Four series capacitors are used in each half loop to improve the antenna's high-altitude power-handling capability. The balun accomplishes two functions in one element. First, it serves as an inductive stub to match the loop element to 50 ohms at the center frequency (135 MHz). It is built as a short section of open wire line with an air dielectric. A short is installed approximately 2 in. from the loop feed point. Such an element will have an inductive reactance equal to $+ jZ_0 \tan \beta\ell$ where Z_0 is the characteristic impedance of the line determined by the diameter of the conductors and the spacing between them, β is the phase constant of the transmission line equal to $2\pi/\lambda$ where λ is the wavelength, and ℓ is the physical length of the stub. If ℓ equals $\lambda/4$

the impedance becomes infinite. This is the familiar quarter-wave balun. Using a shorter stub length than ℓ/4 presents an inductive reactance at the input of the stub, which serves to match the loop and still accomplishes the transition from the balanced loop element to the unbalanced (coaxial) feedline.

Figure 64 is an underside view of the antenna. The radiating elements are made from 0.032-in.-thick, 2-in.-wide copper strips. The four radiators are bolted to the dielectric radome. Two fiberglass brackets hold the two aft radiating elements in a radius of curvature similar to that of the two forward radiators. These brackets are required to make the antenna elements completely symmetrical. Symmetrical construction is required to provide a high degree of isolation between the orthogonal half-loop elements so there will be a minimum of mutual coupling effects.

The series capacitors are made from Teflon-loaded fiberglass with 2-oz copper clad on one side. The copper has been partially removed to form the correct value of parallel plate capacitance for impedance matching at the center frequency. One piece of Teflon-loaded fiberglass actually forms two series capacitors, as shown in the cross section of figure 65. The dielectric properties of the Teflon-loaded fiberglass are a dielectric constant of 2.5 and a loss tangent of 0.002. The Teflon-loaded fiberglass has operational capabilities up to 500° F. The radome material is a polyimide-resin-preimpregnated fiberglass fabric per BMS 8-144, type 7581, class I, grade 1, with a dielectric constant of 4.4 and a maximum loss tangent of 0.01. It is capable of operation at temperatures in excess of 500° F.

Qualification Testing

Two series capacitors are in each radiator; a total of four series capacitors are used in each half loop. Originally one series capacitor was used to match the half-loop element. Severe corona problems were encountered at 45,000-ft pressure altitude with less than full power on a single half loop. By installing four series capacitors the voltage across any one capacitor is one-fourth of its original value. Such a design has passed qualification testing in a pressure altitude of 45,000 ft at room temperature. For the altitude test, 250 watts was applied to one half-loop element in a vacuum chamber at 45,000-ft pressure altitude. The test frequency was 135.585 MHz and the full 250 watts was applied for 45 minutes. Forward and reflected power were measured during the test. Upon completion of the test the prototype antenna was removed from the chamber and visually inspected for corona and dielectric heating. No corona damage was visible and the dielectric capacitors were only slightly warm.

The prototype antenna was also installed on the fuselage mockup shown in figure 66. The antenna was wired for right-hand circular polarization and a full 500 watts applied for 45 minutes. Again, the capacitors showed only a slight amount of heating after 45 minutes of full-power application; there was no sign of heating in the quadrature hybrid.

Figure 67 is a wiring diagram for the installed antenna. Figure 68 shows the hybrid, transfer switch, and dummy load installed on a mounting plate intended for installation inside the aircraft beneath the antenna.

Quadrature Hybrid

The hybrid furnished is constructed in stripline form with 2-oz copper clad on Teflon-loaded fiberglass. The electrical parameters of the hybrid are given in tables 8, 9, and 10.

TABLE 8.—POWER DIVISION CHARACTERISTICS

Frequency, MHz	Insertion loss between ports, dB			
	A–C	A–D	B–C	B–D
134	3.20	3.05	3.13	3.25
135	3.11	2.97	3.02	3.13
136	3.07	3.01	3.05	3.08

TABLE 9.—PHASE CHARACTERISTICS

Frequency, MHz	Phase shift between ports, deg	
	A–B	C–D
134	90.5	89.8
135	90.5	89.9
136	90.5	89.9

TABLE 10.—ISOLATION CHARACTERISTICS

Frequency, MHz	Isolation between adjacent ports, dB	
	A–B	C–D
134	17.5	17.5
135	18.5	18.5
136	19.5	19.5

The hybrid's function in the antenna design is to provide equal power division so that each half-loop element receives equal power and simultaneously to maintain a relative phase shift of 90° between output ports. The data in table 8 show a maximum amplitude unbalance of 0.15 dB over the frequency range of the antenna. This amplitude unbalance will yield an axial ratio of 0.15 dB if driven into identical antenna impedances and is definitely below the specification limit. Table 9 showing relative phase shift, indicates a maximum phase deviation of 0.5° from the ideal 90°. This

phase error in itself will yield an axial ratio of 0.3 dB if the hybrid's output ports are connected to half loops with identical driving point impedances.

The isolation data in table 10 were obtained with flat loads on the two opposite output ports and are intended to represent the highest isolation obtainable with the two antenna ports fully matched. With the actual antenna connected, the isolation is less since there is more reflected power from a VSWR of 2:1 than from a flat load. These data are given in table 11.

TABLE 11.—SYSTEM ISOLATION

Frequency, MHz	Isolation from ports C–D, dB
134	6.0
135	15.5
136	13.8

Impedance Data

To enable the crossed-loop antenna to work correctly in both the right- and left-hand circular mode the impedance plot of a half-loop element must track the other half-loop element. Also, there should be a sufficiently high isolation value between the half loops to prevent cross-coupling energy from one half loop to the other introducing mutual impedances. The measured isolation between the two antenna ports of the production antenna is in excess of 20 dB over the frequency band from 134 to 136 MHz. Figure 69 is an impedance plot of each half-loop element for the production antenna driving one half-loop element at a time. The impedance is referred to the actual antenna feed point. With the individual loop's impedances tracking one another, the antenna was then wired for right-hand circular polarization. Figure 70 is an impedance plot of each antenna element when driven in the right-hand circular mode. The impedances are referred to the male TNC connectors which connect to ports A and B of the hybrid. Figure 71 is an impedance plot in the left-hand circular mode.

The impedances presented to the transmitter-receiver or actual load impedances of the antenna system are given in figures 72 and 73 for right- and left-hand circular polarization, respectively. These data are measured at the input ports (ports C and D) of the hybrid. The measured isolation values between ports C and D of the hybrid with the antenna feedlines connected to ports A and B were given in table 11. The higher isolation values correspond to the lower antenna VSWR values.

Note that the lowest isolation value occurs at 134 MHz, the frequency which has the highest antenna VSWR values, as shown in figures 70 and 71.

Antenna Patterns

Both polar plots and radiation distribution plots were obtained for the 1/20th-scale crossed loop. Figure 74 shows the scaled antenna installed on the 1/20th-scale 707 model airplane. The location was chosen to position the antenna relative to the same position in which it will be installed on a Convair 880 airplane. Integration of the antenna yields a maximum directivity of 4.5 dB when installed on the airplane. The coordinate system used is shown in figure 4.

On both the polar plots and the radiation distribution plots, the polarization is referred to as circular principal polarization and circular cross polarization. Since the antenna can be polarized for either right- or left-hand circular polarization, the principal polarization is the right-hand circular response to right-hand circular illumination when the antenna is polarized to receive right-hand circular polarization. In this case, the circular cross polarization patterns are the response of the antenna to left-hand circular illumination. Placing the antenna in the left-hand circular mode will make the principal circular polarization patterns representative of the antenna's response to left-hand circular illumination, and the cross polarization circular patterns will refer to the antenna's response to right-hand circular illumination.

The patterns shown in figures 75 through 78 indicate nearly perfectly circular radiation directly above the airplane, with the cross polarization down in excess of 20 dB at this point. The cross polarization increases with the increase in θ conic angles due to two factors. First, the axial ratio of the ideal antenna increases as one moves off the point $\theta = 0°$ due to the decrease of the horizontal polarization in the conic angles closer to the horizon. Second, reflections from the wings and other airplane surfaces will cause reversal of the sense of the circular polarization, causing the principal polarization to become cross polarized after reflection from the aircraft surfaces. These two conditions can contribute to a loss in overall antenna directivity since so much radiation is present in the cross-polarized conics near the horizon. Note that maximum cross polarization appears in the conics between 60° and 90° in the aft directions with combinations of sense-reversed radiation due to reflections from the horizontal stabilizer and direct path cross polarization due to the basic crossed-loop antenna configuration becoming more linearly polarized near the horizon. Also, the size of the fuselage in terms of wavelengths at VHF is not sufficiently large to confine the radiation to the upper hemisphere. The principally polarized roll pattern (fig. 76) shows this clearly. This condition also serves to decrease the overall antenna directivity since the ground plane, i.e., the fuselage, is incapable of adequately confining the energy to the upper hemisphere.

Multipath rejection is also poor due to the small size of the fuselage when compared to the wavelength at VHF frequencies. Typically, at the 80° conic, the directivity of the crossed loop off the left wing (ϕ = 90°) to principal circular polarization is -0.78 dB. The multipath signal at this point will be arriving from θ = 100° and ϕ = 90°. The directivity of the antenna to the opposite sense polarization (assuming sense reversal) is -7.4 dB below isotrope. Thus, the multipath rejection is (7.40 - 0.78 = 6.62 dB).

Figure 79 shows the percent coverage of the antenna inside the cone defined by θ = 80°. The horizontal axis gives the antenna directivity in decibels, and the vertical axis gives the percent coverage for any antenna directivity value. The cone θ = 80° was chosen to limit the sector coverage to only the intended coverage cone, i.e., from directly overhead to 10° above the horizon.

The use of the radiation distribution plots is best explained by the following example (the same airplane coordinate system is used throughout the report):

- Find the directivity of the crossed-loop antenna in both principal polarization and crossed polarization with respect to the circular isotrope for the point θ = 80° and ϕ = 50° using the radiation distribution plots (figs. 80 and 81). First, the peak reading on the radiation distribution plots must be known. Inspection of the plots yields a pattern maximum of 2 dB. This represents the peak directivity of the antenna, which is known by integration to be 4.5 dB with respect to a circular isotrope. Thus, all data points will be referred to decibels below the maximum of 2 dB, which corresponds to a maximum pattern directivity of 4.5 dB. The radiation distribution plots are recorded in 2° increments in both ϕ and θ.

- Knowing the peak directivity and pattern maximum, go to the point θ = 80° and ϕ = 50° on the principally polarized radiation plot. The figure obtained at this point is 7 dB or 2 - 7 = 5 dB below the maximum directivity of 4.5 dB. Thus, the actual directivity of the antenna at this point is 4.5 - 5.0 = -0.5 dB below a circular isotrope.

- Similarly, the directivity of this antenna to cross-polarized radiation can be found from the cross-polarized radiation plot. At θ = 80° and ϕ = 50°, the number 14 dB is obtained. This is 2 - 14 = -12 dB below the pattern maximum or 4.5 - 12 = -7.5 dB below a circular isotrope.

Conclusions

A VHF crossed-loop antenna has been developed and qualification tested to an aircraft environment. The impedance plot of the individual loop antenna (fig. 69) indicates a high Q antenna. No absolute gain measurement has been made on the actual antenna since the ground plane required to sufficiently confine the antenna's radiation to one side cannot be supported on the Boeing antenna

ranges. Figure 62 shows a representative radiation pattern for a half-loop element mounted on a scaled 40-ft-square ground plane. Impedance measurements conducted early in the development program yielded a basic loop radiation resistance of 16 ohms at 135 MHz, with the loop tuned to resonance by a high Q variable air dielectric capacitor having a Q exceeding 2,000 at the measurement frequency. No dielectric radome was present for this measurement, merely the 2-in.-wide copper radiators mounted on a 12-ft-square ground plane. The measured value of radiation resistance, i.e., 16 ohms, indicates that an efficient radiator is possible if low-loss materials are used in the antenna construction. These facts, as well as the electrical properties of the materials used on the production antenna which were discussed under "Impedance Matching and Physical Construction," indicate that the production antenna meets and probably exceeds the minimum efficiency requirement of the specification.

The antenna coverage performance can best be summarized by referring to figure 79. For 80% of the coverage area, the antenna directivity meets or exceeds a directivity of -1 dB (the specification limit) in the cone defined by $\theta = 80°$.

As discussed earlier, the multipath rejection of the antenna is poor for certain azimuth angles near the horizon due to the relative size of the fuselage at VHF. The radiation is shielded from below in the azimuth direction of the wings. The result is that the poorest multipath rejection occurs in the two forward quadrants ($\phi = 0°$ to 90° and $\phi = 270°$ to 360°).
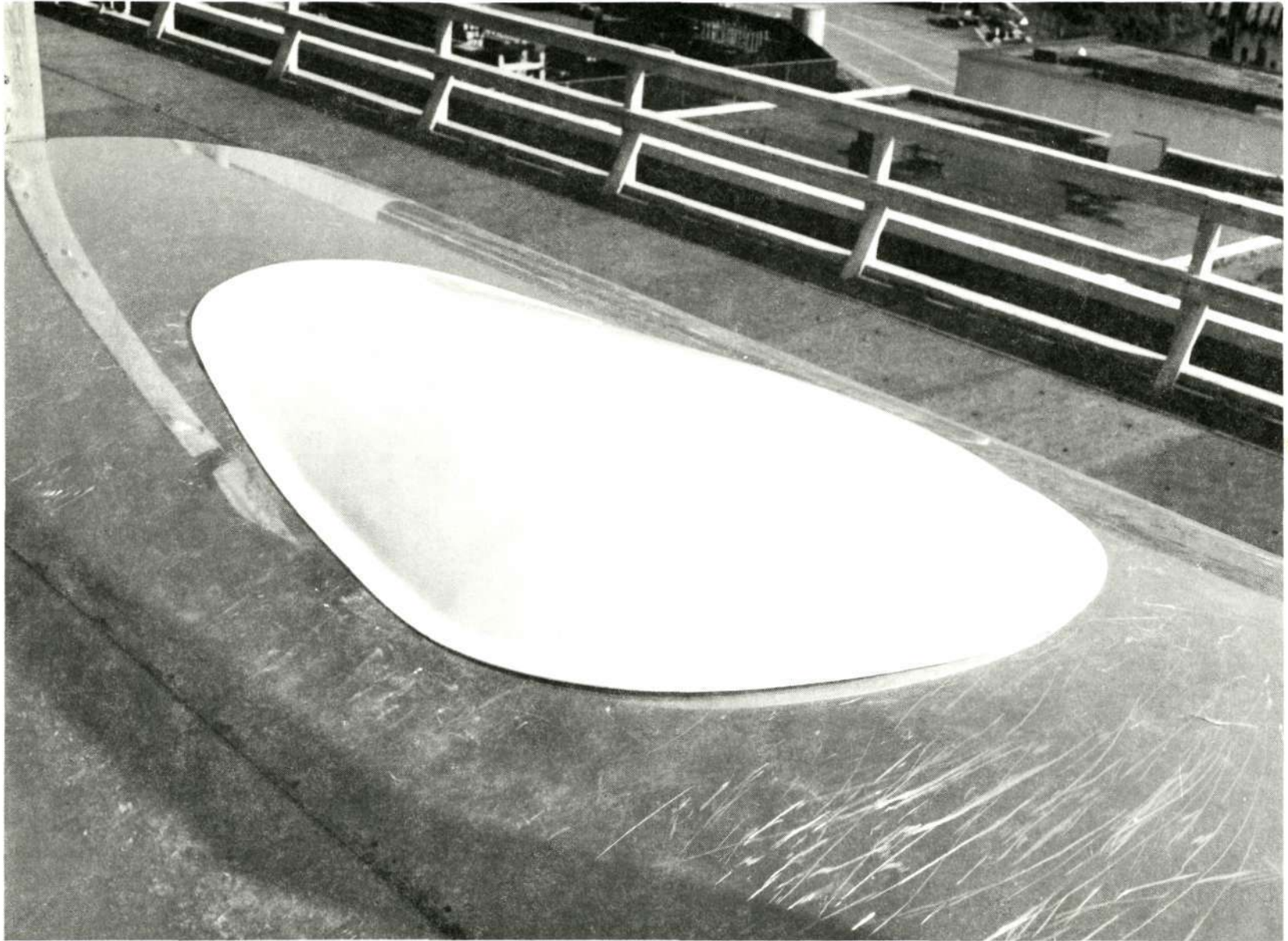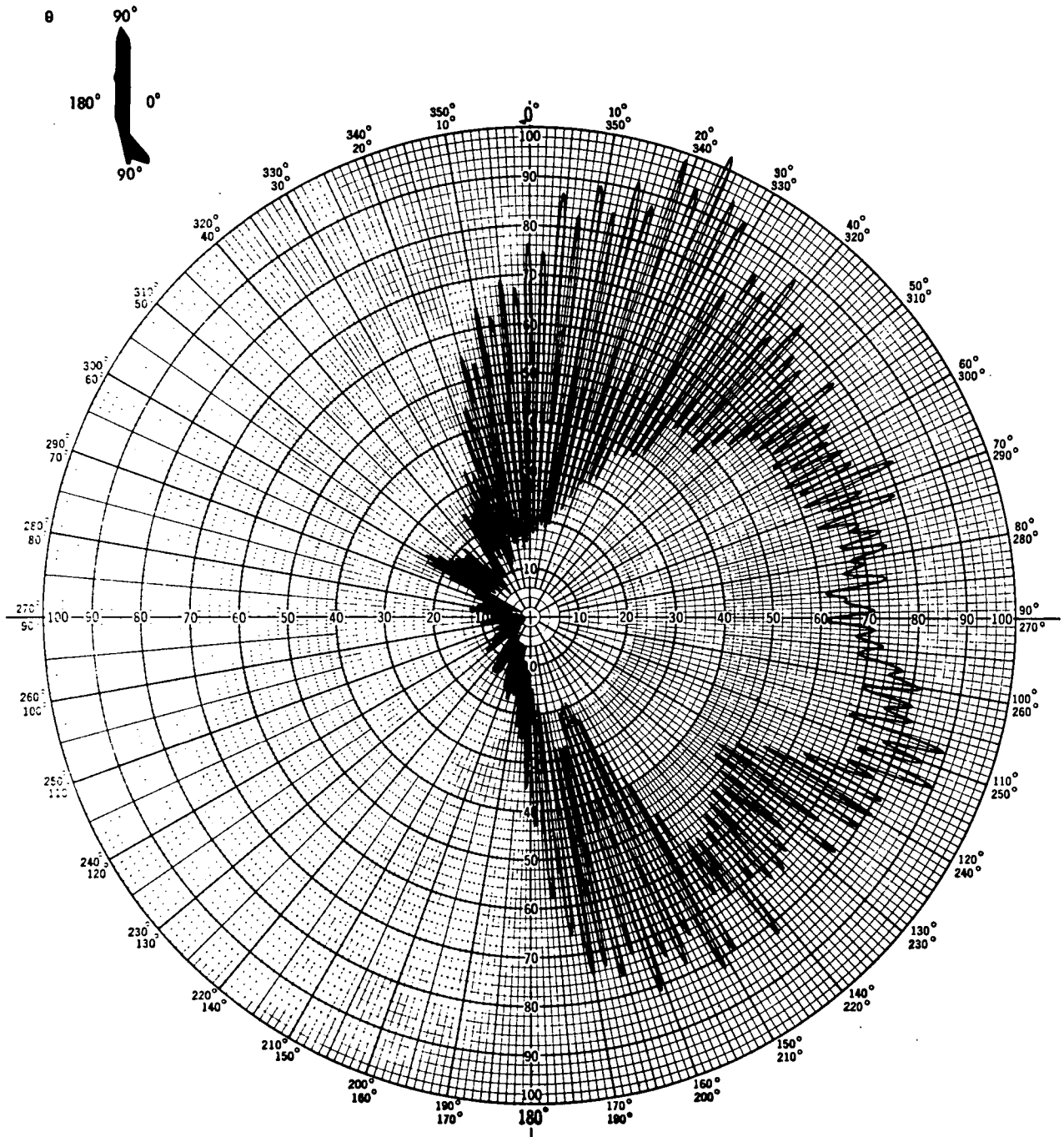
Figure 60.—VHF Crossed-Loop Antenna
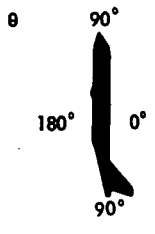
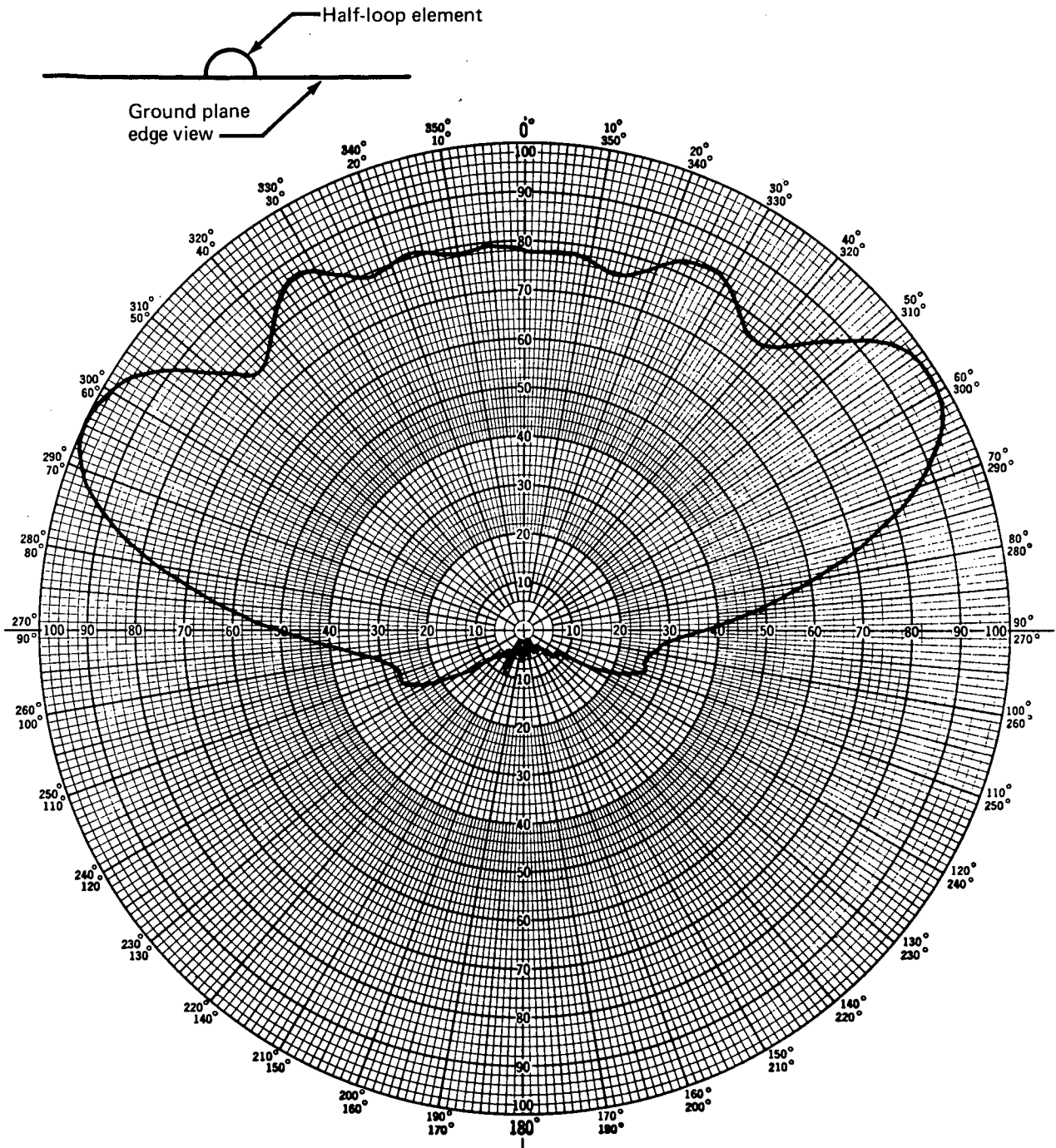Curve plotted in voltage   Full-scale frequency: 135 MHz
Variable angle θ 707 airplane
Constant angle $\phi = 0°$ Antenna location: top centerline at STA 600
Model scale: 1/20

Figure 61.—VHF Crossed-Loop Antenna Pitch Plane Pattern, Rotating Linear Polarization

Half-loop element

Ground plane
edge view

Curve plotted in voltage
Variable angle θ
Constant angle $\phi = 90°$

Model scale: 1/10
Full-scale frequency: 135 MHz
Antenna location: 4-ft-square ground plane

Figure 62.—Half-Loop Element Antenna E-Plane Cut

91
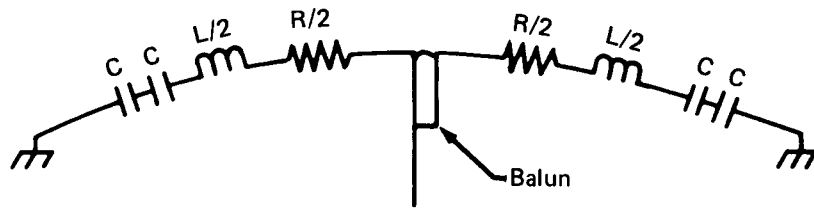
Figure 63.—Equivalent Circuit Half-Loop Element
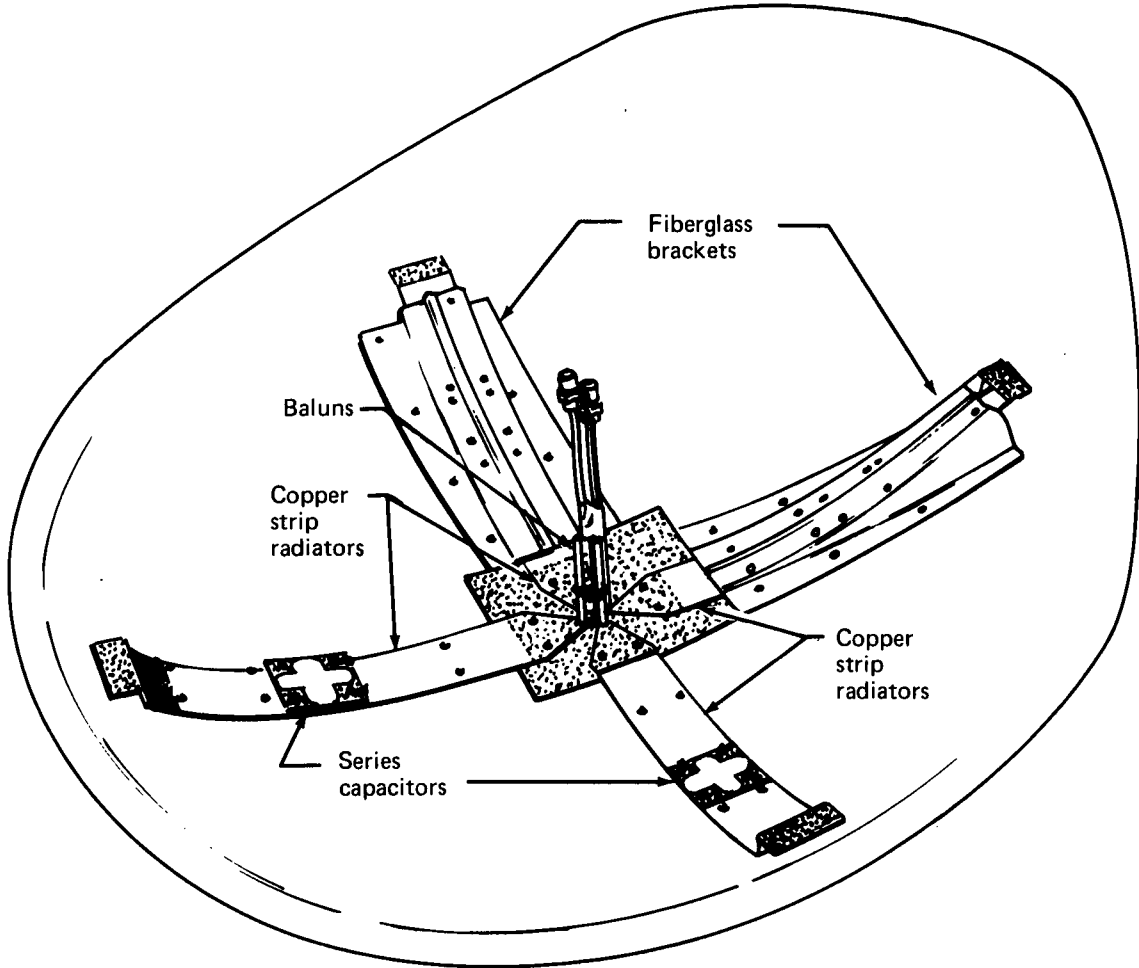
Figure 64.—Underside View—VHF Crossed-Loop Antenna
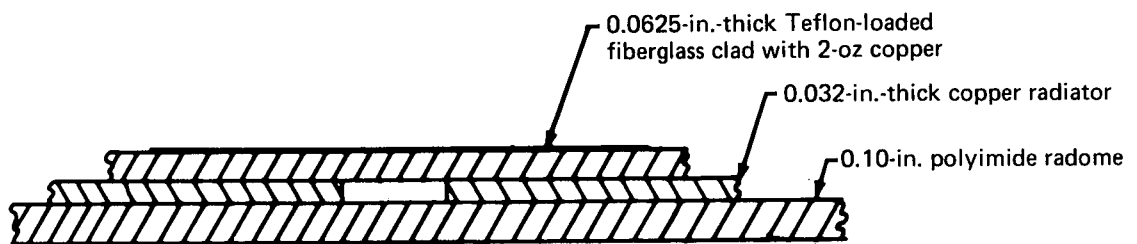
Figure 65.—Series Capacitor Detail

Figure 66.—Fuselage Mockup

Series capacitors

VHF crossed-loop antenna
(viewed from bottom)

Series
capacitors

These two lines
identical length

A   B

Quadrature hybrid

C   D

Note: With transfer switch
de-energized, the antenna is
polarized left hand circular.
Energizing the switch gives
right hand circular polarization.
The transceiver is connected to J_1.

50-W load
Bendix 633.7

Polarization selector switch

J_4
J_2 J_3
J_1

28 Vdc
at
150 mA

Transfer switch
Electronic Resources, Inc.
part 09-56-12111

Figure 67.—Wiring Diagram of VHF Crossed-Loop Antenna
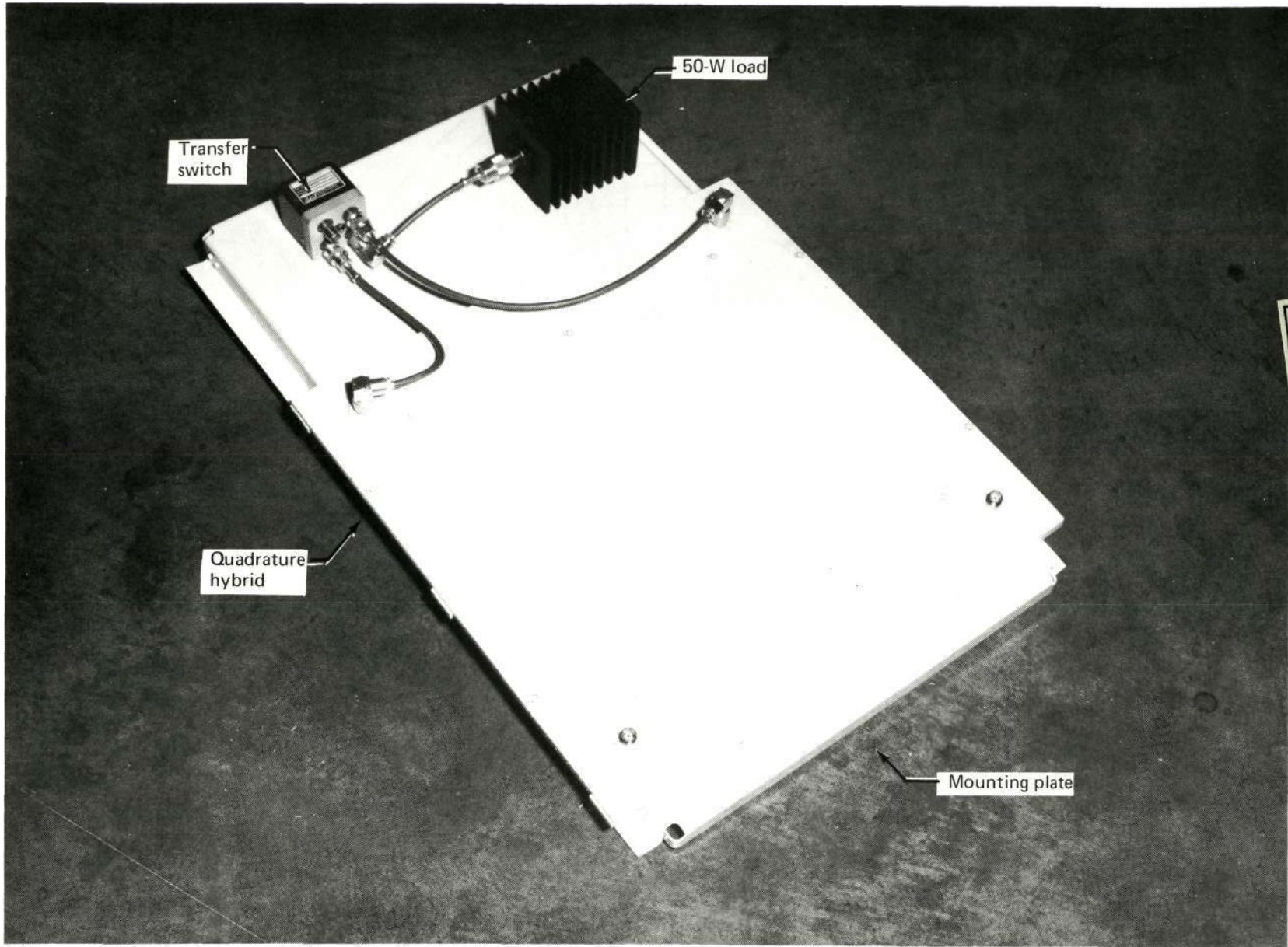
Figure 68.—VHF Antenna Components

Labels in figure:
- 50-W load
- Transfer switch
- Quadrature hybrid
- Mounting plate
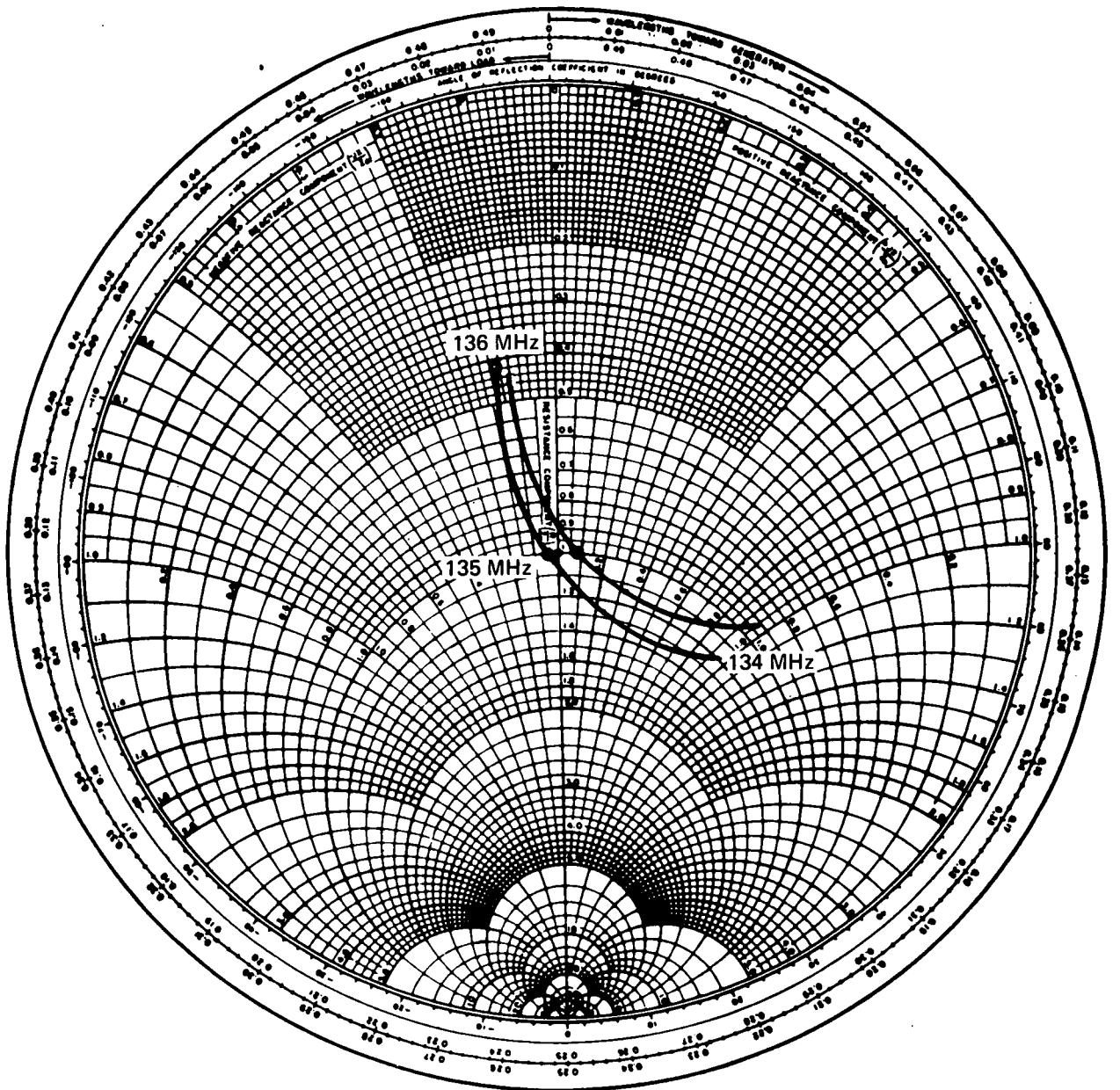
$Z_0 = 50$ ohms

Remarks: Impedance measured at feed point of each loop.
Each loop driven alone.

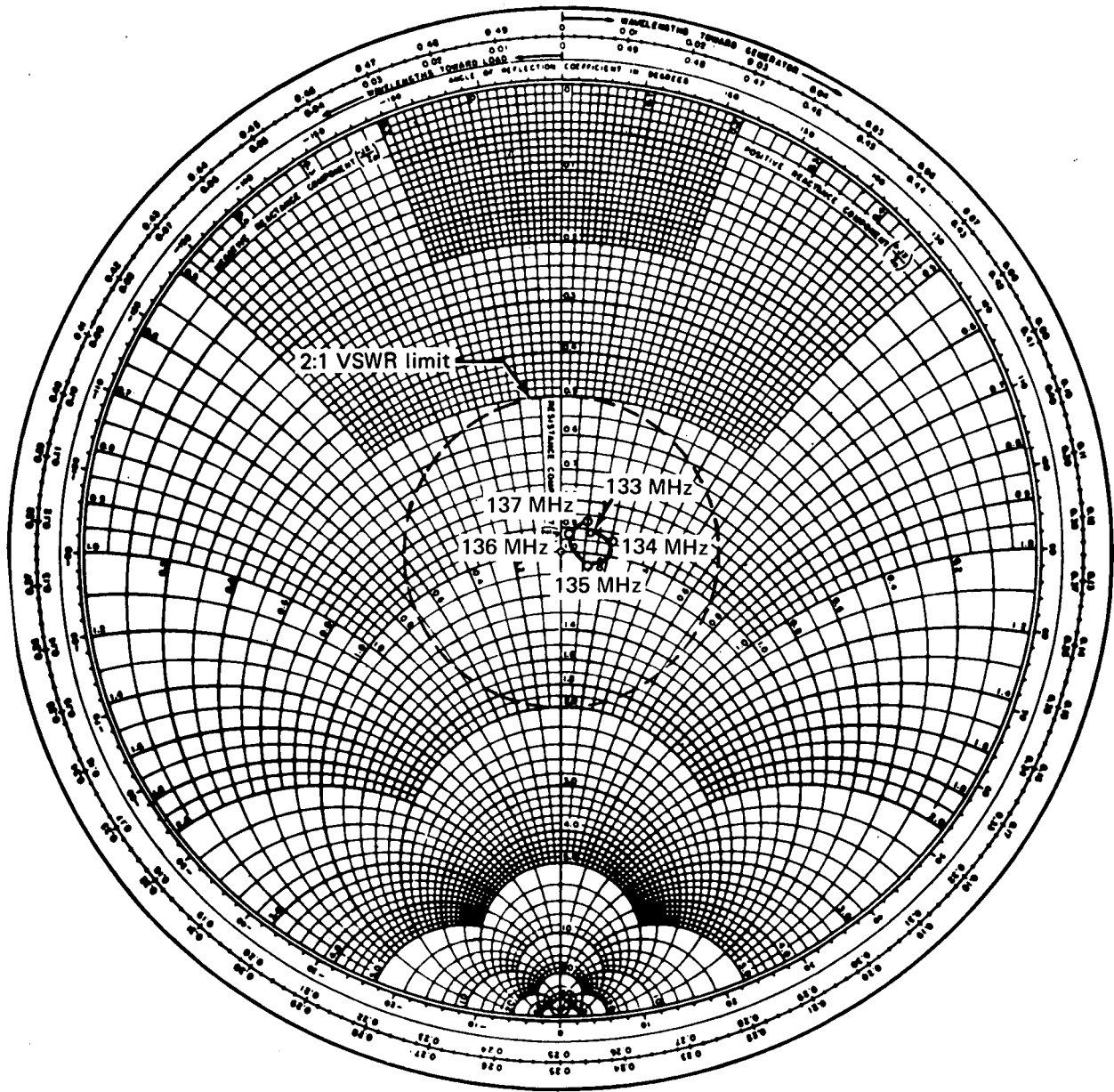Figure 69.—VHF Crossed-Loop Antenna Impedance Plot, Linear Polarization
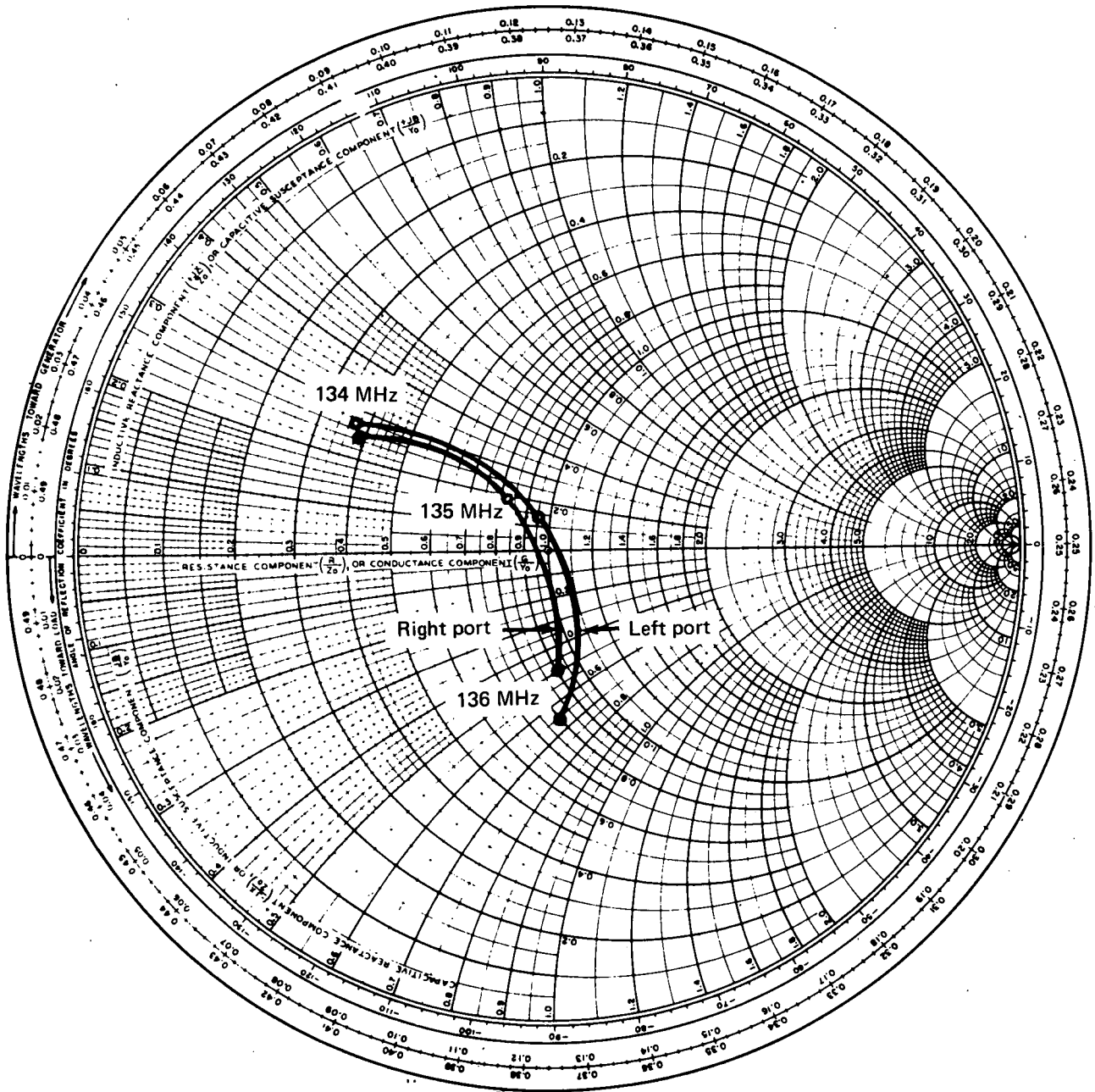
$Z_0 = 50$ ohms

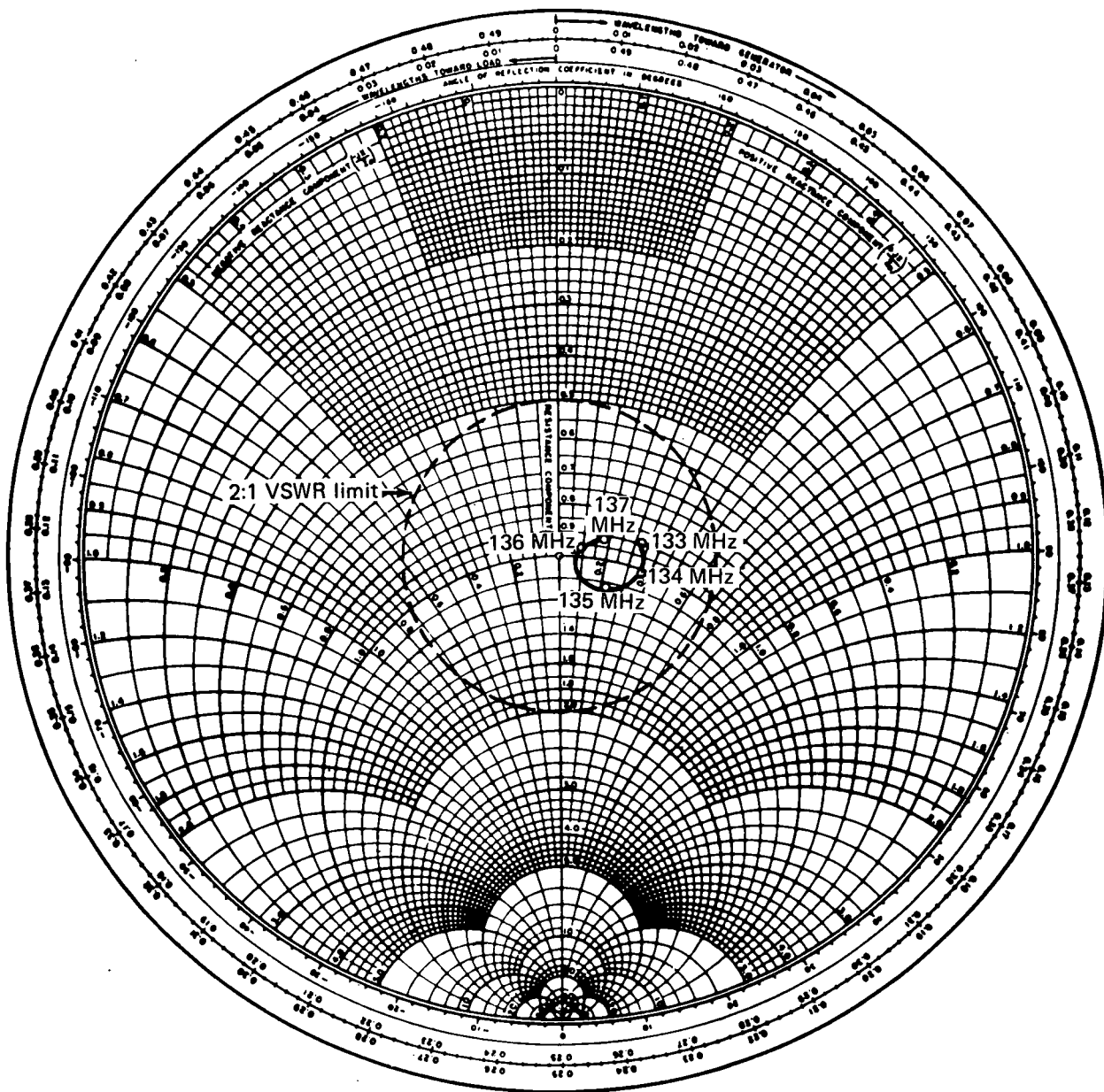*Figure 70.—VHF Crossed-Loop Antenna Impedance Plot, Right-Hand Circular Polarization*
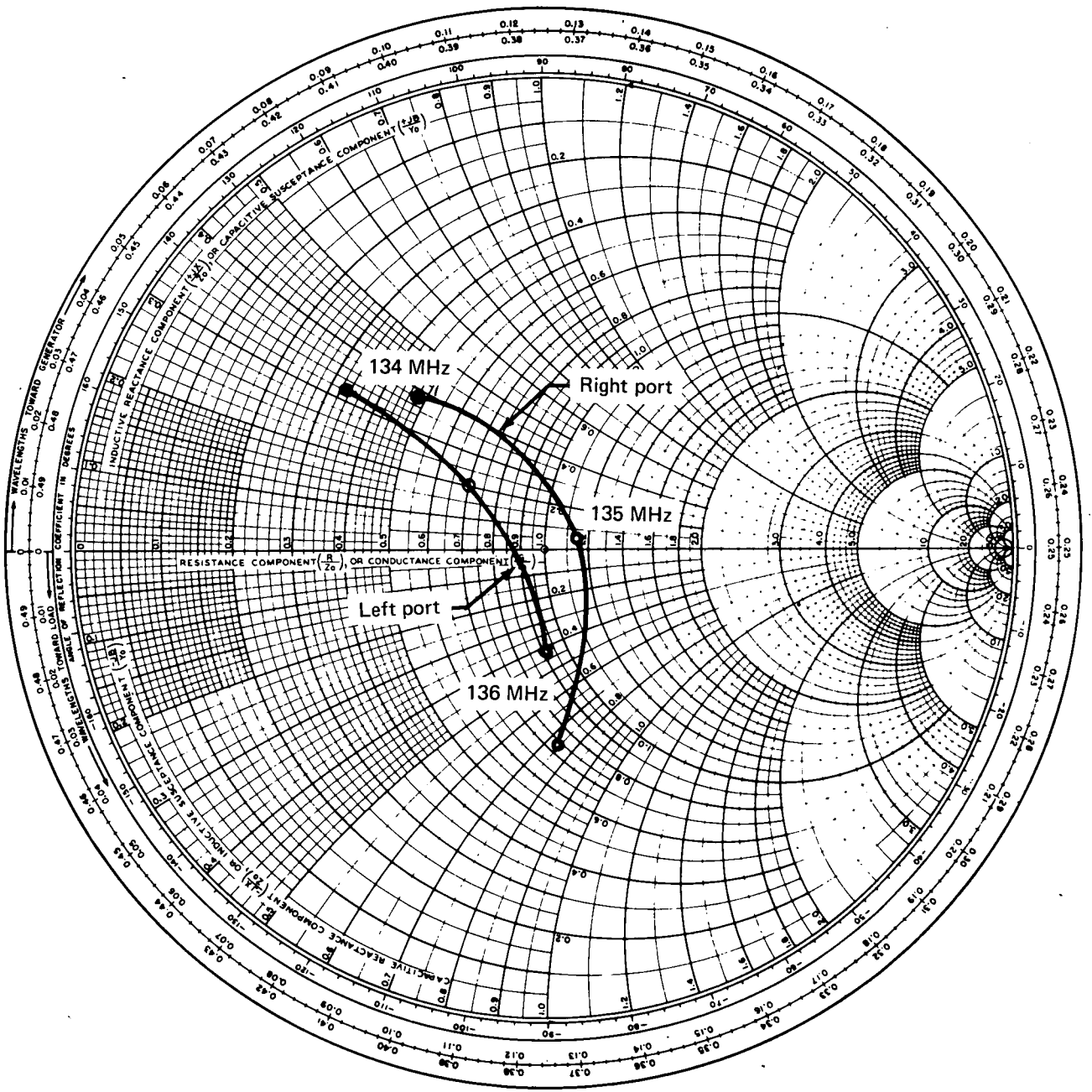
Figure 71.—VHF Crossed-Loop Antenna Impedance Plot, Left-Hand Circular Polarization

Z_0 = 50 ohms   Remarks: Impedance measured at
                                            port C on hybrid.

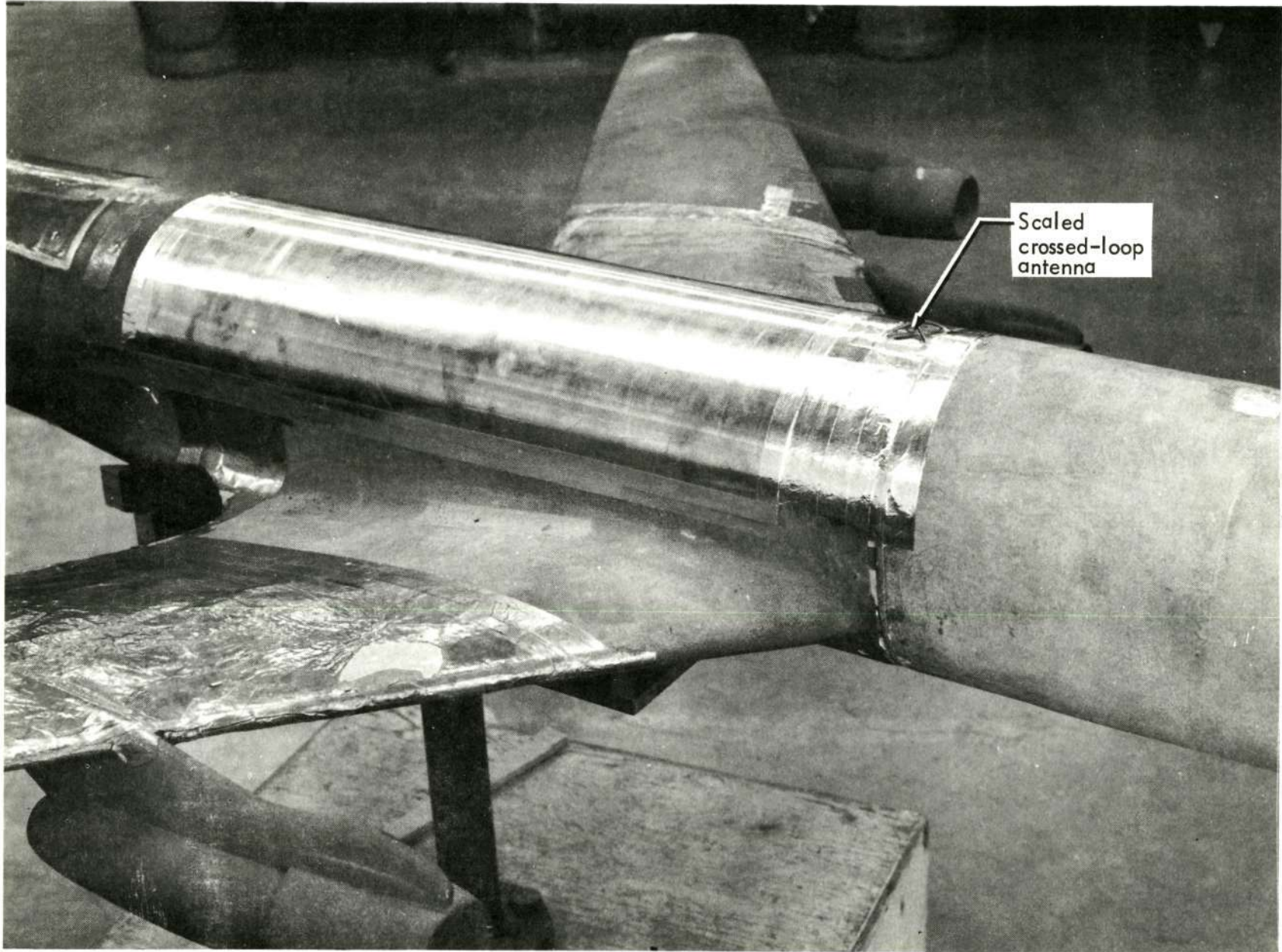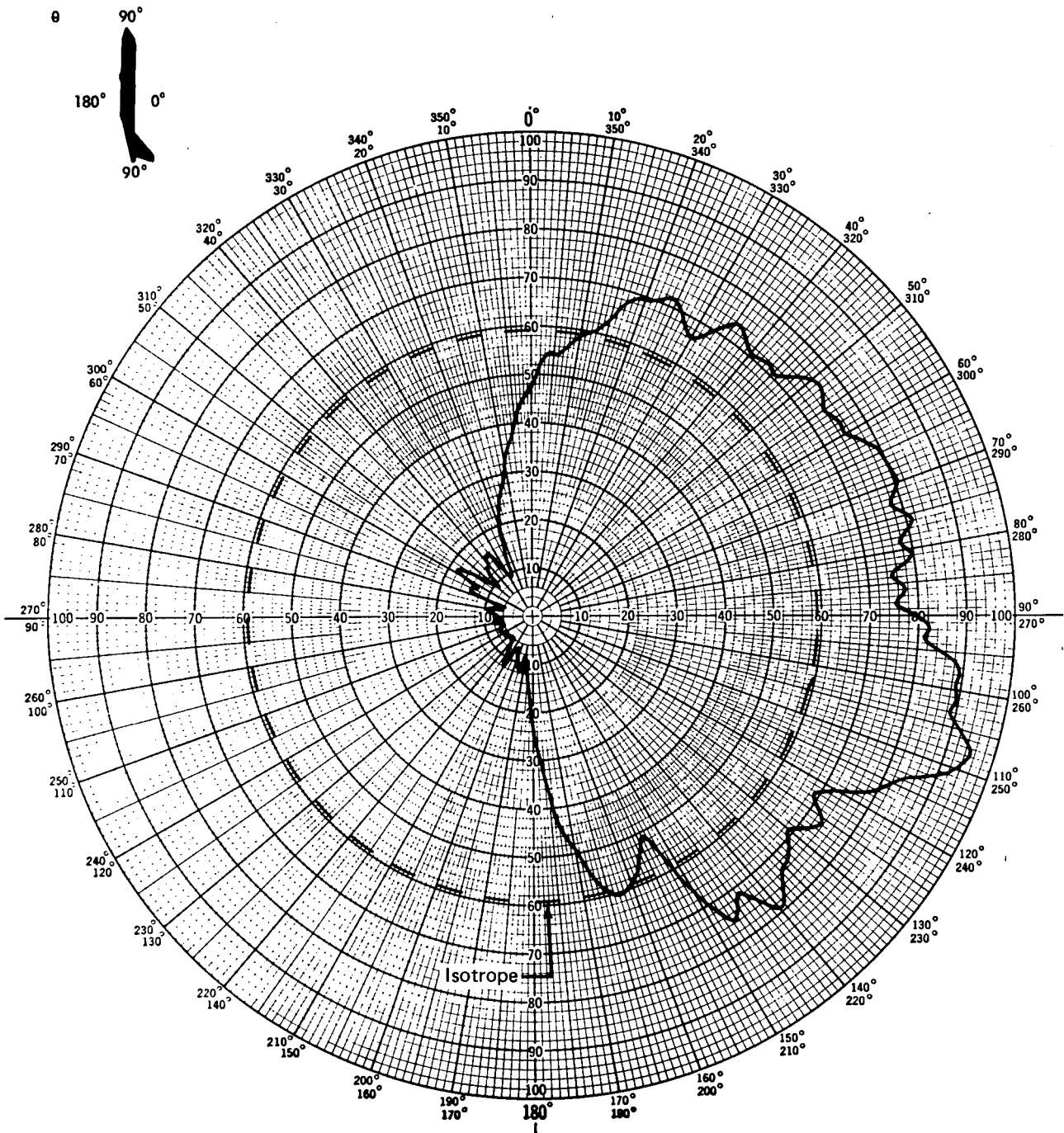*Figure 72.—Antenna Impedance Plot at Hybrid, Right-Hand Circular Polarization*

99

$Z_0 = 50$ ohms   Remarks: Impedance measured at
                              port D on hybrid.

Figure 73.—Antenna Impedance Plot at Hybrid, Left-Hand Circular Polarization

100

Scaled crossed-loop antenna

Figure 74.—707 Airplane Model—1/20-Scale

Maximum directivity: 4.5 dB Model scale: 1/20
Curve plotted in voltage Full-scale frequency: 135 MHz
Variable angle θ 707 airplane
Constant angle $\phi = 0°$ Antenna location: top centerline at STA 600

Figure 75.—VHF Crossed-Loop Antenna Pitch Plane Pattern, Circular Principal Polarization
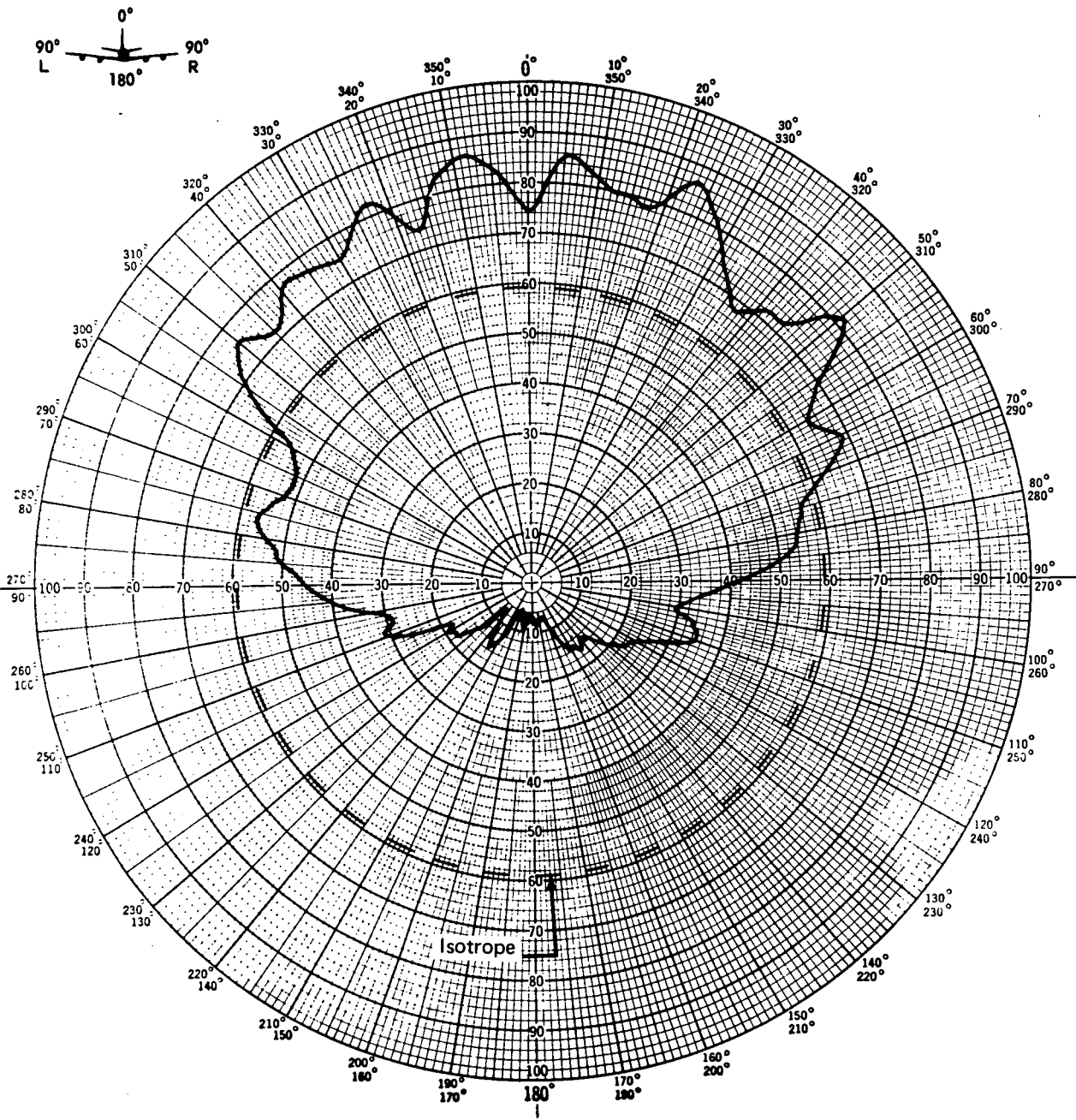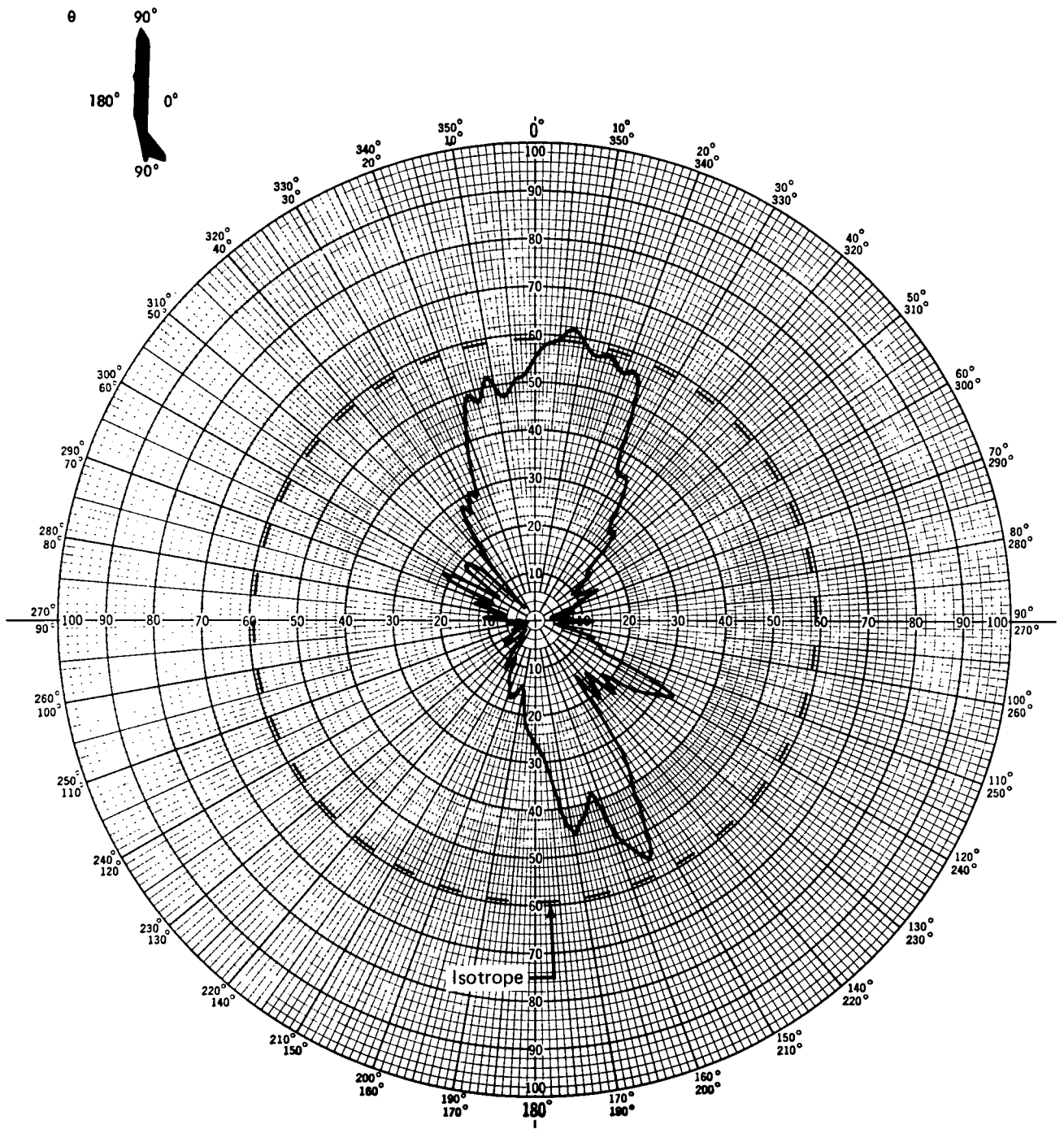
Maximum directivity: 4.5 dB
Curve plotted in voltage
Variable angle θ
Constant angle $\phi = 90°$

Model scale: 1/20
Full-scale frequency: 135 MHz
707 airplane
Antenna location: top centerline at STA 600

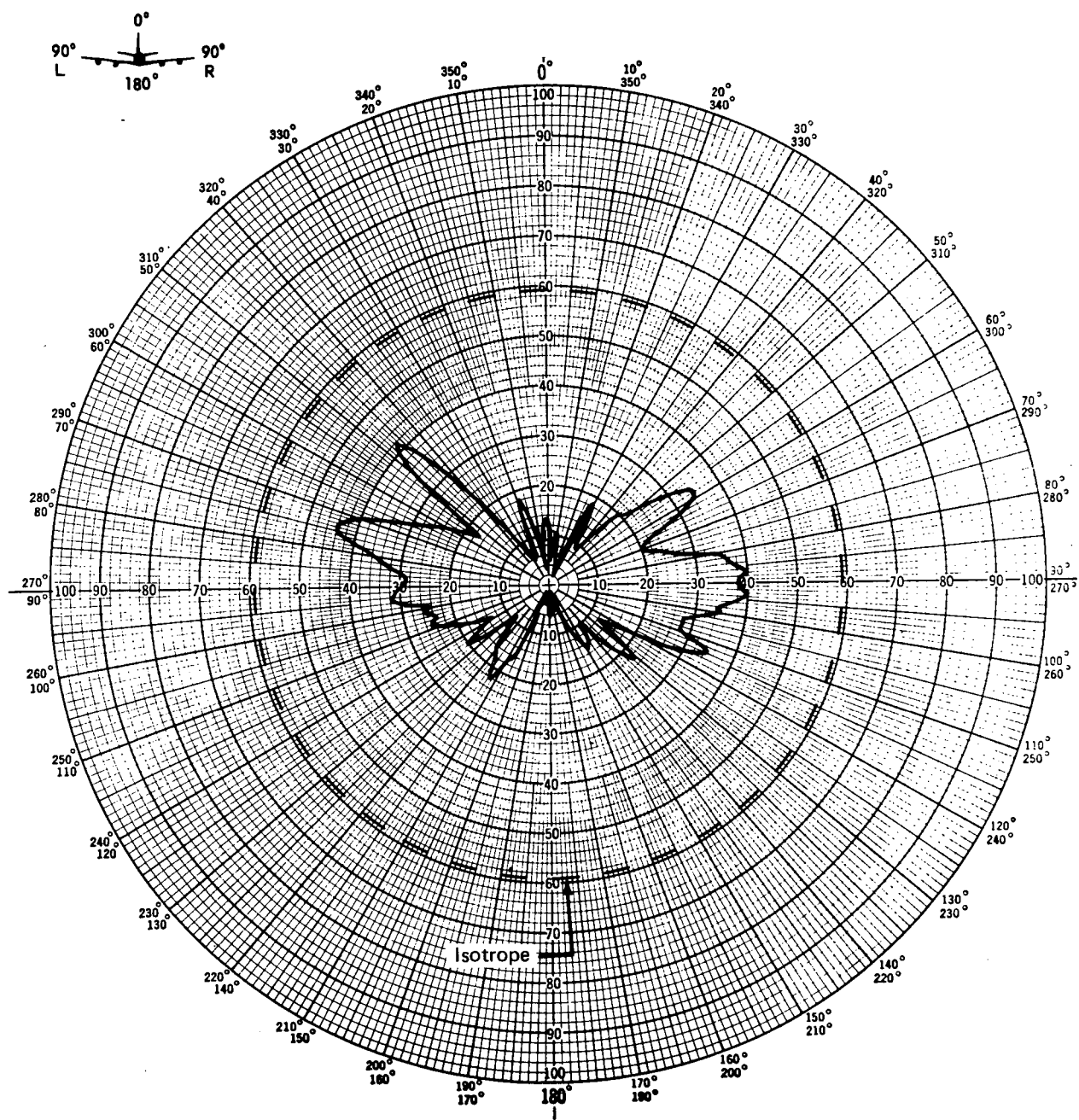*Figure 76.—VHF Crossed-Loop Antenna Roll Plane Pattern, Circular Principal Polarization*

103

Curve plotted in voltage
Variable angle θ
Constant angle $\phi = 0°$

Model scale: 1/20
Full-scale frequency: 135 MHz
707 airplane
Antenna location: top centerline at STA 600

Figure 77.—VHF Crossed-Loop Antenna Pitch Plane Pattern, Circular Cross Polarization

Curve plotted in voltage
Variable angle θ
Constant angle $\phi = 90°$

Model scale: 1/20
Full-scale frequency: 135 MHz
707 airplane
Antenna location: top centerline at STA 600

Figure 78.—VHF Crossed-Loop Antenna Roll Plane Pattern, Circular Cross Polarization
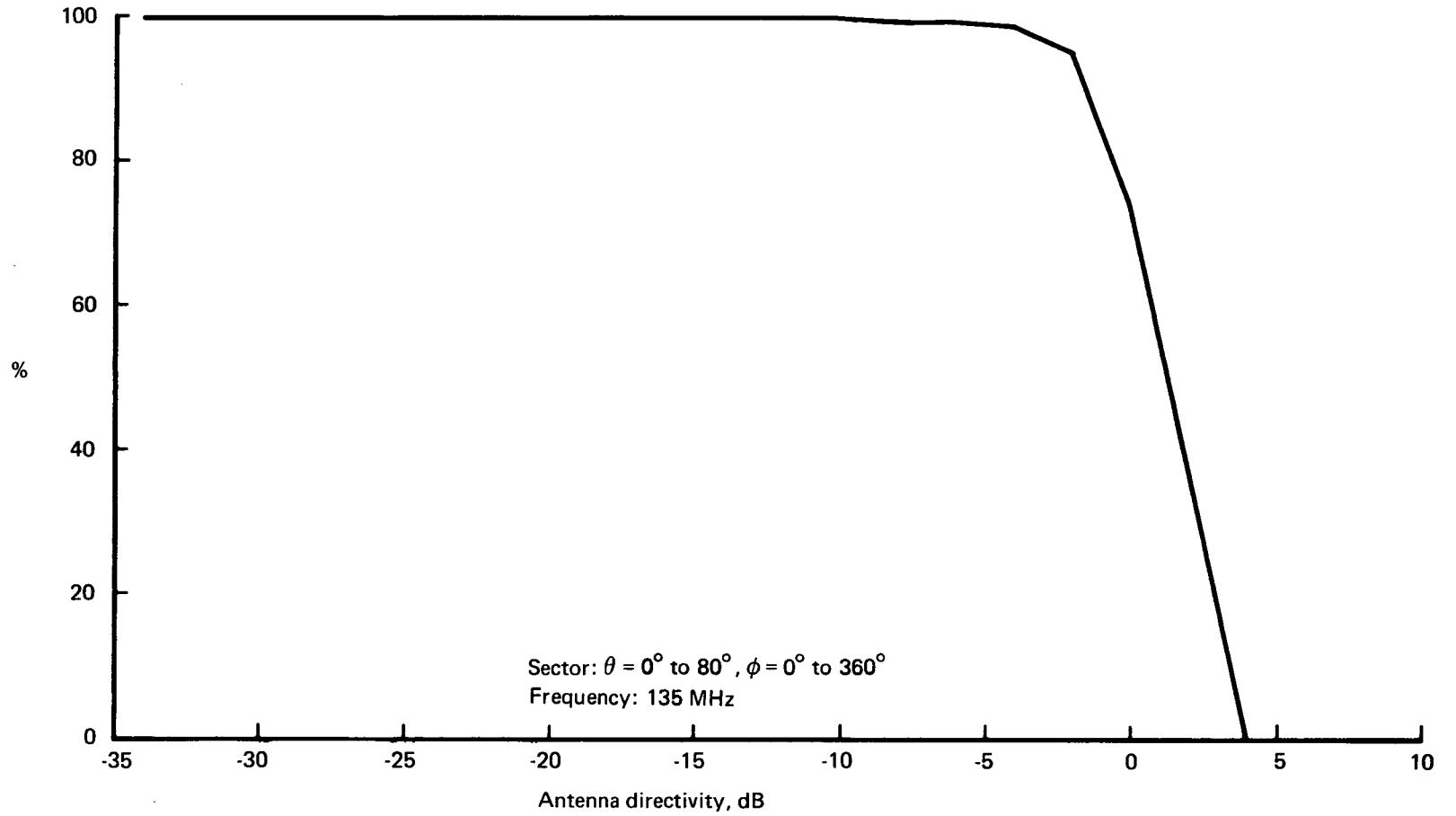
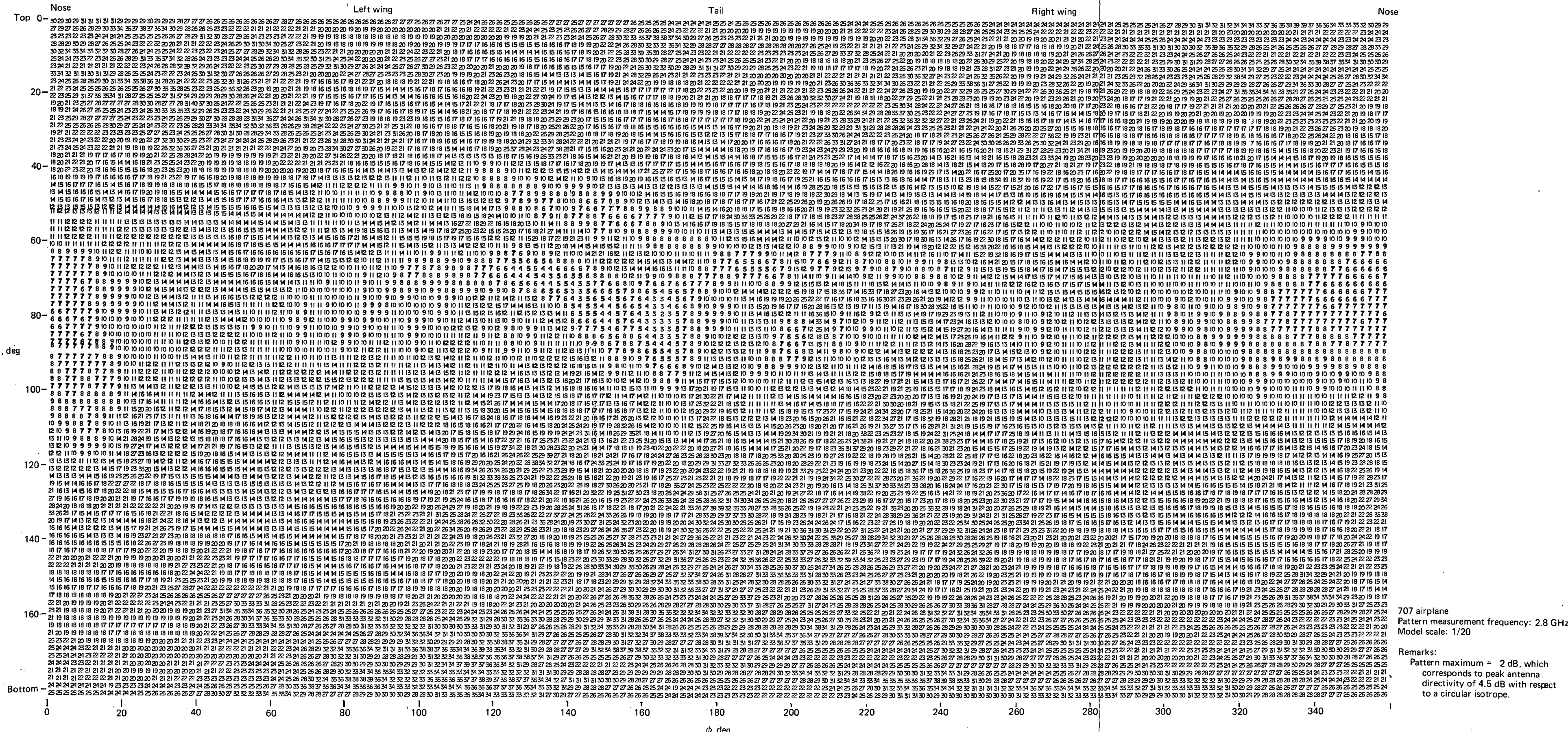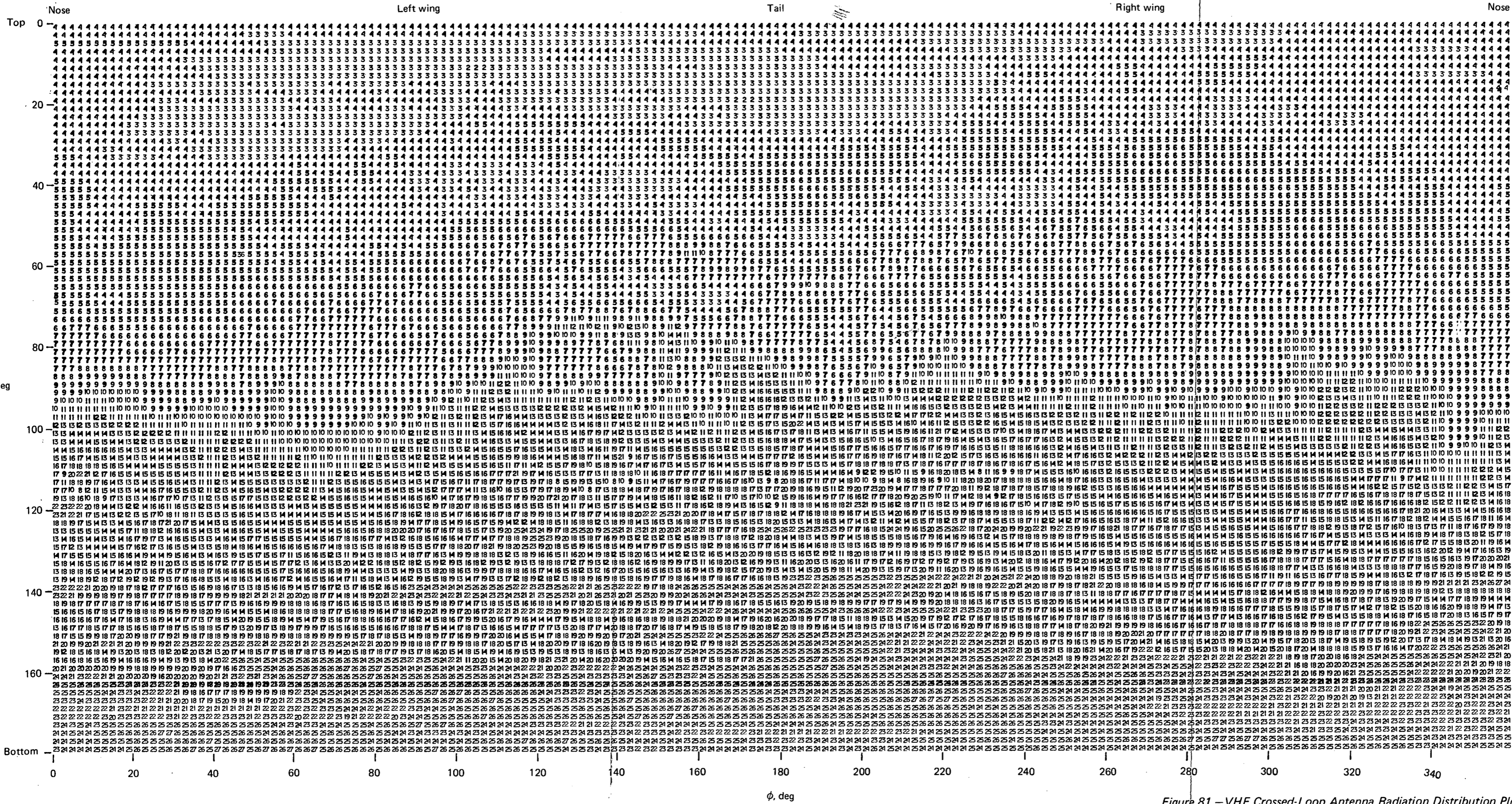Figure 79.—VHF Crossed-Loop Antenna Percent Coverage

Top 0—

Nose · Left wing · Tail · Right wing · Nose

θ, deg

20—
40—
60—
80—
100—
120—
140—
160—

Bottom—

0 20 40 60 80 100 120 140 160 180 200 220 240 260 280 300 320 340

ϕ, deg

707 airplane
Pattern measurement frequency: 2.8 GHz
Model scale: 1/20

Remarks:
Pattern maximum = 2 dB, which
corresponds to peak antenna
directivity of 4.5 dB with respect
to a circular isotrope.

Figure 80.—VHF Crossed-Loop Antenna Radiation Distribution Plot, Circular Cross Polarization   107

Figure 81.—VHF Crossed-Loop Antenna Radiation Distribution Plot, Circular Principal Polarization 109

REPORT OF INVENTIONS APPENDIX

After a diligent review of the work performed under this contract, no new innovation, discovery, improvement, or invention was made.

DATE:

In reply
refer to: AMT

SUBJECT: Distribution of Reports

FROM : AMT/Technical Conference and Publication Branch

TO   : Distribution:

In accordance with the memorandum of understanding,
enclosed are copies of the subject report described
below.

A. L. Waters
A. L. Waters
Technical Conference &
    Publication Branch

Enclosure (s) 20 copies

Title: L-Band Orthogonal-Mode Crossed-Slot
             Antenna and VAF Crossed-Loop Antenna
             DOT-TSC-NASA-72-2

Distribution
             Input Section, KSI
             National Aeornautic & Space Admin.
             Scientific & Technical Information Facility
             Collete Park, MD 20740

112